

Journal of the Nevada Water Resources Association

Fall 2006

A publication of the Nevada Water Resources Association, providing hydrologic information to the people of Nevada and adjacent States



Volume 3, Number 2

Nevada Water Resources Association

Executive Director

Donna Bloom
Nevada Water Resources Association

President

Michael Johnson
Virgin Valley Water District

Editor-in-Chief

Michael Strobel
USGS Nevada Water Science Center

Assistant Editors

Chris Benedict, Washoe Co. Department of Water Resources
David Berger, USGS Nevada Water Science Center
Terry Katzer, Cordilleran Hydrology, Inc.
Michael Widmer, Washoe Co. Department of Water Resources

Associate Editors (this edition)

Robert Burrows, USGS Nevada Water Science Center
John Enloe, ECO:LOGIC Engineering
Mark Forest, HDR Engineering, Inc.
Kimball Goddard, USGS Nevada Water Science Center
Jon Hutchings, Eureka Co. Department of Natural Resources
Laurel Saito, University of Nevada, Reno
Ralph Seiler, USGS Nevada Water Science Center
Victor Vasquez, University of Nevada, Reno

Correspondence: Manuscripts should be submitted to Dr. Michael Strobel, USGS, 2730 North Deer Run Road, Carson City, NV 89701. Inquires: (775) 887-7604, mstrobel@usgs.gov

Responsibility: The Nevada Water Resources Association and the organizations of any of the editors or the Board of Directors are not responsible for statements and opinions advanced in this publication.

Cover photo by Michael Strobel. Pictured are Spencer and Hunter Strobel.

Web design and layout by Shannon Watermolen, USGS

Copyright ©2006 NWRA



Table of Contents

Page

Editor's notes 1

Jon Hutchings, Guest editorial

Developing a Synthetic, Long-Term Flow Record for the Lower Virgin River Using Flow-Duration Curves 5

Stephanie L. Bache, Jeffrey Johnson, and Craig T. White

Where does the water go? Agreement Investigation 25

Robert D. Baggs, Jr., and D'Layne M. Reynolds

Trace Element and Radionuclide Concentrations in Walker River Bottom Sediment and Weber Reservoir Sediment Core, West-Central Nevada, 2005 31

Carl E. Thodal and Michael S. Lico

Technical Note: New method for calculating activity coefficients of surface ions in concentrated electrolytes 63

Anpalaki J. Ragavan

Editor's Notes

Central Nevada Regional Water Authority

Jon Hutchings, Ph.D., Executive Director, Central Nevada Regional Water Authority

It is with pleasure that I respond to the NWRA Journal Editorial Board's invitation to provide a guest editorial about the recently formed Central Nevada Regional Water Authority. As a co-founder and the Authority's first Executive Director, I have invested dearly in the organization's success. The local measure of that success will be predicated on the honesty, ambition and plain hard work we lay out here in central Nevada. More importantly, though, is that our activities one day be contemplated as a solid contribution to water resource management for Nevadans statewide. After all, rural and urban, north and south, our contribution today defines the Nevada of tomorrow. With that prelude, I offer your readers the following overview of the Central Nevada Regional Water Authority, its structure, its goals and its ambitions.

What is the Central Nevada Regional Water Authority?

The Central Nevada Regional Water Authority (CNRWA) is a unit of local government that collaboratively and proactively tackles water resource issues common to communities in Nevada's rural interior. CNRWA exists under Nevada's Interlocal Cooperation Act and performs its delegated authority separate and apart from the member counties. The organization was formally chartered in August of 2005 with six members. With the addition of Churchill County in September of this year, the members number seven. The members are Churchill, Elko, Esmeralda, Eureka, Lander, Nye and White Pine Counties.

CNRWA's Mission

The CNRWA mission is to prepare communities in central and eastern Nevada for sound water-resource decisions that promote prosperous economies and strong civic institutions in a healthy natural environment. Under the interlocal agreement, member counties work toward water resource solutions that

1. Support their local and regional economies by
 - *developing and maintaining cost-effective water infrastructure, and*
 - *maximizing economic benefit from regional water resources.*
2. Meet the needs of their citizens by
 - *providing access to clean, inexpensive water supplies, and*
 - *sponsoring water-resource education aimed at local governments and the public.*

3. Build their capacity for making sound water-resource decisions by
 - *assisting member counties to predict long-term water needs,*
 - *identifying gaps in water resource data and information,*
 - *developing a uniform and accessible base of knowledge about regional water resources,*
 - *creating a regional water plan based on common aspects of county plans, and*
 - *assessing impacts of regional water resource development proposals.*
4. Maintain their natural environment in a healthy condition by
 - *assessing impacts of development on the region's ecosystems, and*
 - *protecting against the irreversible impacts of over-development.*

What is the Central Region?

The Central Hydrographic Region consists of 78 ground water basins in 11 Nevada counties (figure 1). The region is the largest of our State's 14 Hydrographic Regions, encompassing much of central, eastern and southern Nevada. The Central Region is distinguished by 1) its arid environment, 2) absence of regional surface water flows, 3) productive alluvial aquifers and 4) deeper, largely uncharacterized bedrock aquifers. Ground water basins in the Central Region receive little contemporary recharge, are often interconnected by subsurface flows and depend largely on ground water discharge to supply present and future natural and human uses.

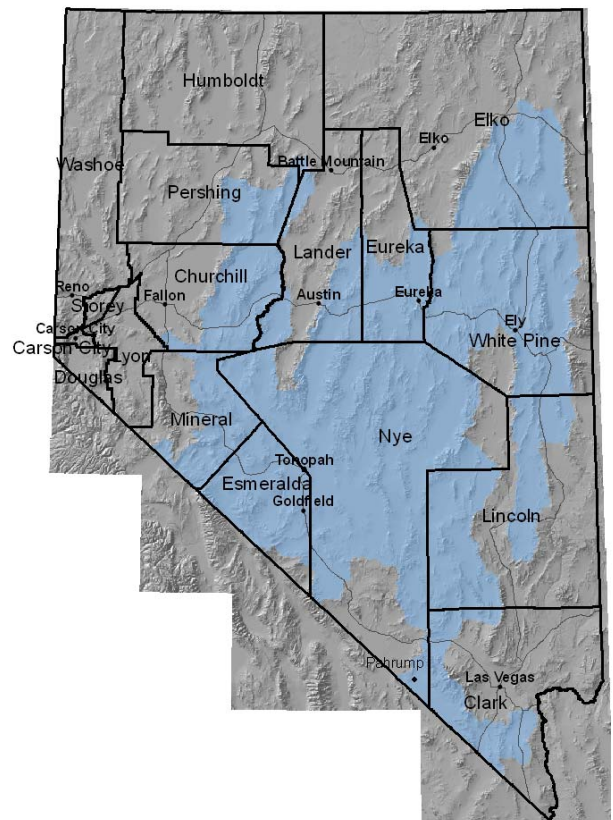


Figure 1. The Central Hydrographic Region as defined by the Division of Water Resources

What does a county's involvement in CNRWA mean for its citizens?

The physical distance of these ground water basins from population centers and the absence of perennial streams to readily transport water have protected the Central Region from past development pressures; however, their near pristine condition renders them a valuable future resource. The hydrologic, geographic and political hurdles to effective management of these resources for local benefit are shared among the Authority's members and is the common thread underlying CNRWA activities. CNRWA is a forum for finding solutions to these hurdles and leveraging those solutions through coordinated project funding, resource planning and policy making.

Current activities

CNRWA Members judge the primary hurdles to sound water resource decision-making to be 1) insufficient hydrologic information at the local government level, 2) inadequate local and regional water resource planning and 3) an ineffective voice in State and Federal actions. To overcome these hurdles CNWRA is presently collaborating with the Division of Water Resources and the U.S. Geological Survey to develop an information management system that will efficiently avail all existing water-level information in the Central Region to local government decision-makers and the capable public. CNRWA is preparing a comparative analysis of Member water resource plans and continues to engage the Interim Legislative Committee on Use, Management and Allocation of Water Resources on water resource issues that affect its members.

What's the cost?

Member Counties are committed to contributing \$7,500 per annum (the amount is determined each new fiscal year) to the daily operation of the Authority. Staff commitments are modest, requiring quarterly meetings, periodic consultations, document review, etc... The most important contribution, that most essential to the Authority's legitimacy, is that at least one County Commissioner is truly committed to the effort, regularly attend meetings and transmit the benefits of the Authority's work to the to the public at home. The overall fiscal impact to each Member is estimated to be less than \$10,000 per year.

For more information contact:

Jon Hutchings, Executive Director
PO Box 475
Eureka, NV 89316
Phone: (775) 237-6010
jhutchings@eurekanv.org

Jon Hutchings is the Natural Resources Manager for Eureka County. By virtue of his position, Jon is deeply involved in natural resource and public land concerns across the state. He is focused on balanced results for Nevada's rural communities in the areas of energy development, water resource development, land tenure changes, mine permitting, livestock grazing, range management and general quality-of-life concerns. Before coming to Nevada, Jon headed up the geochemistry component of a regional ground water flow system analysis in southwestern Idaho for the Idaho Water Resources Institute. Jon is a soil scientist and hydrologist by training. He received his Ph.D. in Soil Science and M.S. in Hydrology from the University of Idaho in Moscow. Jon, his wife and their three children presently reside in Eureka.

This page left blank intentionally

Developing a Synthetic, Long-Term Flow Record for the Lower Virgin River Using Flow-Duration Curves

STEPHANIE L. BACHE, Parsons Water and Infrastructure, 110 West A St., Suite 1050, San Diego, CA 92101 (Stephanie.Bache@parsons.com)

JEFFREY JOHNSON, Southern Nevada Water Authority, 1900 E. Flamingo Rd., Suite 170, Las Vegas, NV 89119 (Jeff.Johnson@snwa.com)

CRAIG T. WHITE, Parsons Water and Infrastructure, 110 West A St., Suite 1050, San Diego, CA 92101 (Craig.White@parsons.com)

ABSTRACT

The Virgin River is a key component of the water resource portfolios of Nevada and Utah. Arizona has also developed water rights in its 26-mile section of the river between Utah and Nevada. The Virgin River has a 6,000-mi² (square mile) watershed, which originates in Utah and discharges into Lake Mead approximately 60 miles upstream from the Hoover Dam. The flow in the Virgin River is highly variable, both on a daily and annual basis. Streamflow gage records for the Lower Virgin River in Nevada are limited. Establishment of reliable estimates of daily and annual flows in the Lower Virgin River is of interest to those seeking to understand the river ecosystem, evaluate potential resources for development, and assess associated environmental effects.

The most extensive flow data set for the lower Virgin River is the U.S. Geological Survey (USGS) Littlefield Gage (1929 to present), which is cooperatively funded by the Southern Nevada Water Authority (SNWA). A shorter data set is also available for the Virgin River at the USGS Halfway Wash Gage, which was operated from 1978 to 1985 (excluding water year 1984). These data do not adequately reflect long-term variations in river flows as observed at the Littlefield Gage. The purpose of this analysis was to develop a synthetic, daily long-term flow record for the Halfway Wash Gage based on historic flows at both the Littlefield and Halfway Wash Gages.

The synthesized flow record for the Halfway Wash Gage is based on the use of flow-duration curves, a statistical method of evaluating the variability of river flows. Flow-duration curves were developed for both the Littlefield and Halfway Wash Gages for the 7 concurrent years of streamflow records, and a flow-duration curve was developed for the Littlefield Gage for its 74-year period of record. Based on the relationships between the 7-year and 74-year flow-duration curves for the Littlefield Gage at corresponding probabilities, the 7-year Halfway Wash flow-duration curve was proportionally adjusted to produce a synthetic flow-duration curve for the Virgin River at Halfway Wash corresponding to the 74-year record. Based on this methodology, a synthetic 74-year daily flow record was developed for the Virgin River at Halfway Wash, which correlates extremely well to recorded flow data at the Halfway Wash Gage and at the downstream Overton Gage. An advantage of this methodology is that it provides reasonable estimates of flow on both a daily and annual basis throughout the entire flow range, enabling the flow record to be used for a variety of analyses.

INTRODUCTION

Background and Hydrologic Setting

The Virgin River occupies a 6,000-mi² watershed situated between the Colorado Plateau, the Great Basin, and the Mojave Desert, within the states of Nevada, Arizona, and Utah. As shown on Figure 1, the Virgin River is a tributary to the Colorado River and discharges to Lake Mead approximately 60 miles upstream of Hoover Dam. The river has long been an important water resource. The Anasazi Indians built villages on the banks of the Virgin River in the first century A.D. and were followed by the Puebloans and Paiute Indians. The Virgin River was a vital re-watering point on the Mormon and Spanish Trails in the 19th Century. Today, the Virgin River is a key component of the water resource portfolios of Nevada and Utah. Arizona has also developed some of its rights on the river in the small section of the state through which the river flows. There are several diversions on the river that currently supply water for municipal and agricultural purposes.

The Virgin River begins in Washington County, Utah, at an elevation of approximately 10,000 ft above mean sea level (MSL), some 150 miles from its mouth at Lake Mead. After flowing past the city of St. George, Utah, where Virgin River flows are extracted for municipal and agricultural purposes, the river begins a steep descent through the Virgin River Gorge at approximately 2,300 ft MSL.

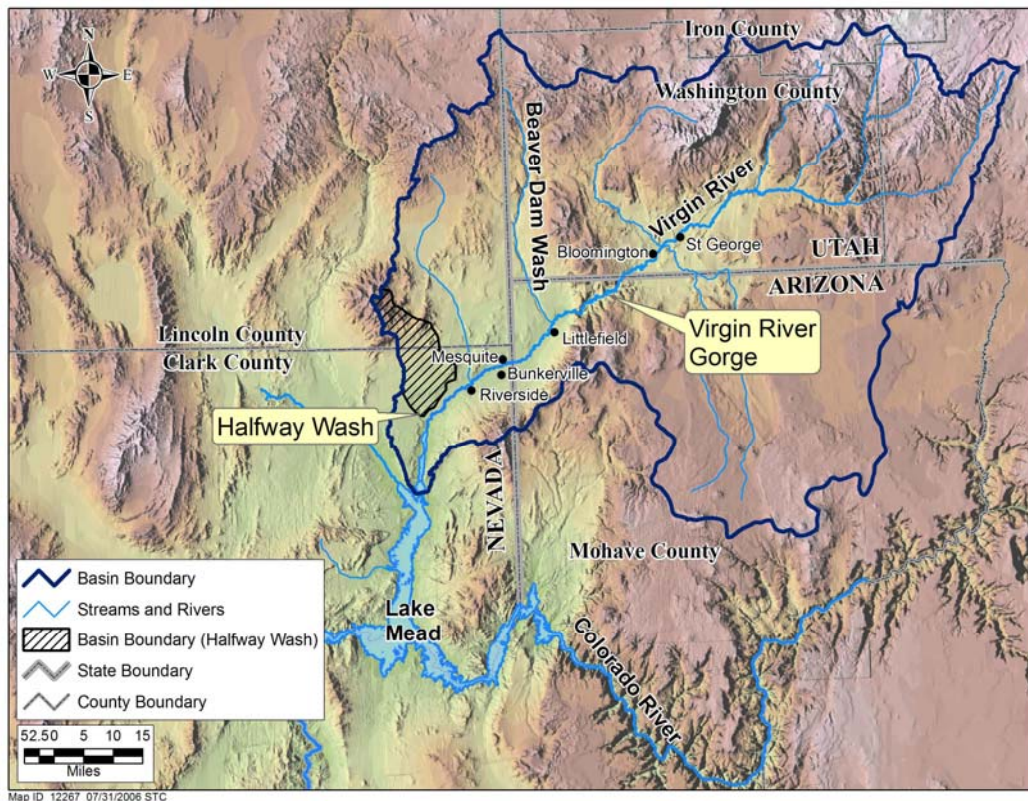


Figure 1. Virgin River Watershed

Although no major dams have been built within the watershed, existing water diversions on the river include Quail Creek Reservoir in Utah, domestic water-supply diversions primarily at Mesquite, Nevada and St. George, Utah, and agricultural diversions on the lower Virgin River. Populated areas along the Virgin River include St. George and Bloomington, Utah; Littlefield, Arizona; and Mesquite, Bunkerville, and Riverside, Nevada. Flows in the Virgin River are principally influenced by snowmelt in the mountains in southwestern Utah and flooding from summer monsoonal storms.

Purpose and Scope

The purpose of this analysis is to establish baseline flow conditions for the lower Virgin River downstream of existing diversions before its discharge into Lake Mead. Baseline flow refers to the flow regime that existed from water year 1930 to present. The objective is to capture the variation of flows in this lower reach of the Virgin River by producing a long-term record. An additional objective of the study is to develop accurate estimates of daily flows, particularly in the low-flow range that is important in measurements of the river ecology and morphology. Once completed, the flow record can be used to assess changes in river conditions, plan for feasible development of the river, and estimate the effects of development. For instance, estimated daily flows could be used to estimate the effects of evapotranspiration (ET) rates or sediment movement due to a proposed diversion that would change minimum or maximum daily flows during certain months. The change in pattern and variation of flows might be more important than the change in monthly or annual volume.

This report reviews the available hydrologic data, discusses previous hydrologic studies for the river, describes the methodology used to establish a baseline flow estimate for the lower Virgin River, and presents a validation of the methodology.

HISTORICAL FLOW DATA

Four gages have operated on the lower Virgin River between Littlefield and Lake Mead. These gages are shown on Figure 2 and identified in Table 1.

Table 1. Lower Virgin River Gaging Stations

	Gaging Station			
	At Littlefield	At Riverside	Above Halfway Wash Near Riverside	Near Overton
USGS Station Number	9415000	9415190	9415230	9415240
Drainage Area (mi ²)	5,090	5,890	5,980	N/A
Elevation (ft MSL)	1,764	1,410	1,320	1,230
Period of Streamflow Records	1929–2005	1970–74; and 1992–1995	1977–83; and 1985	2003
Years of Record	76	6	7	1

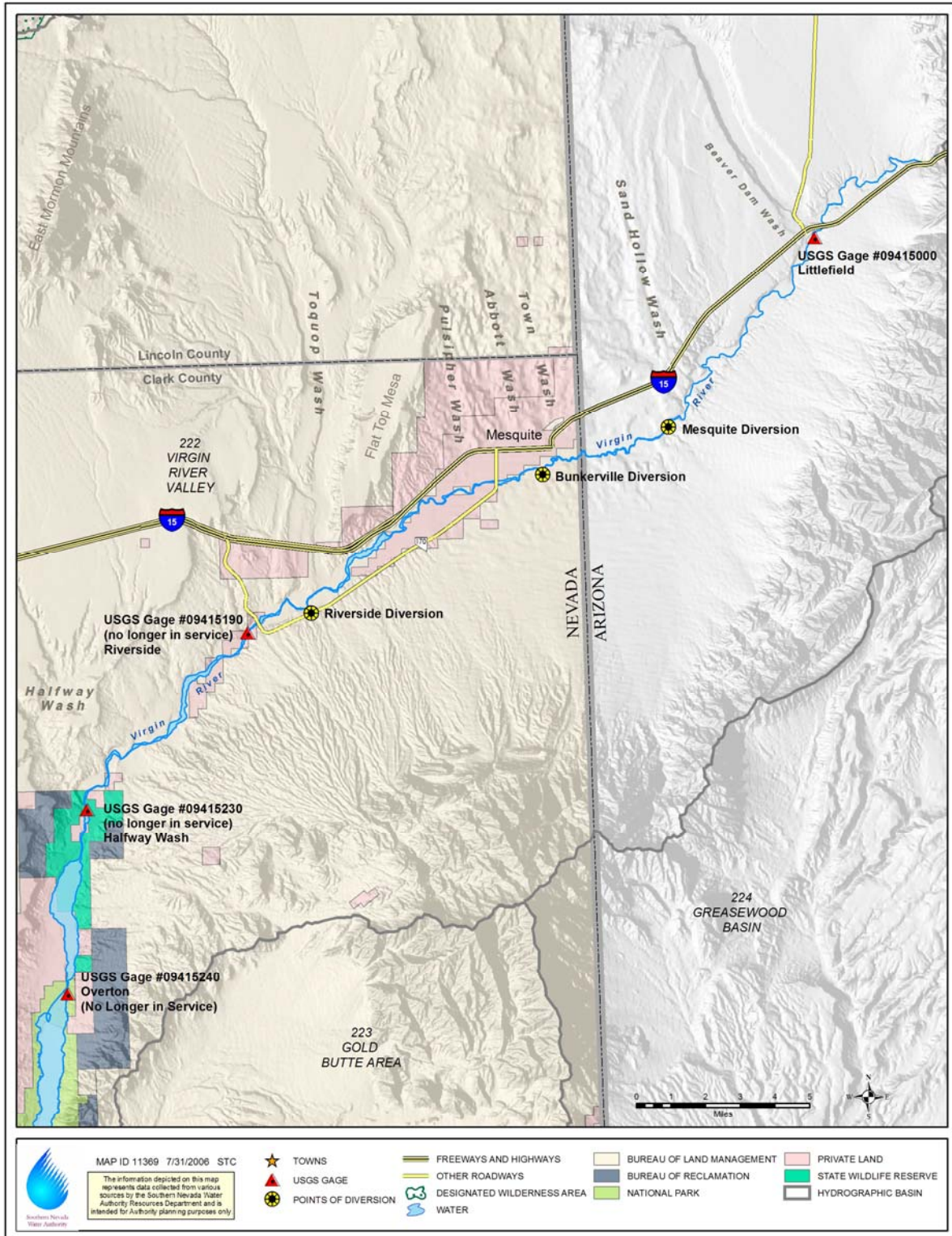


Figure 2. Lower Virgin River Gages and Diversions

The most extensive streamflow data set for the Virgin River is for the Littlefield Gage (1929 to present). The variability of flows at the Littlefield Gage is evident in the hydrograph in Figure 3. Agricultural diversions, evaporation, and inflows from tributaries occur in the river downstream from Littlefield, so the Littlefield Gage record does not necessarily provide an accurate representation of downstream flows. The Littlefield Gage is approximately 26 miles upstream from the Halfway Wash Gage and there are three major diversions within that reach of the river. The Mesquite and Bunkerville Canals divert approximately 50 and 20 cfs (cubic feet per second) on average, respectively, and the Riverside Canal diverts up to 9 cfs (LVVWD, 1992). Although various studies have estimated groundwater recharge and evapotranspiration (ET) consumptive use for portions of the river at particular periods in time, there are no known long-term estimates of ET consumptive use or groundwater recharge for the reach of the Virgin River between Mesquite and Halfway Wash.

The Virgin River Basin experiences highly variable precipitation; therefore, the relatively short data sets for the three gages downstream of the Littlefield gage may not adequately reflect long-term trends. The Overton Gage is the closest to Lake Mead; however, data at this gage are limited (Table 1) and contribute little to understanding long-term variability. Simultaneous records at both the Littlefield and Halfway Wash Gages are available for a period of 7 years (water years 1978–83 and 1985) and at Littlefield and Riverside for a period of 6 years (water years 1972–74 and 1993–95). The Virgin River streamflow gage at Halfway Wash is downstream from agricultural diversions and return flows, and there are no major tributaries between Halfway Wash and Lake Mead. Consequently, these data, used in conjunction with the long-term record at Littlefield, provide a good basis for synthesizing a representative long-term record.

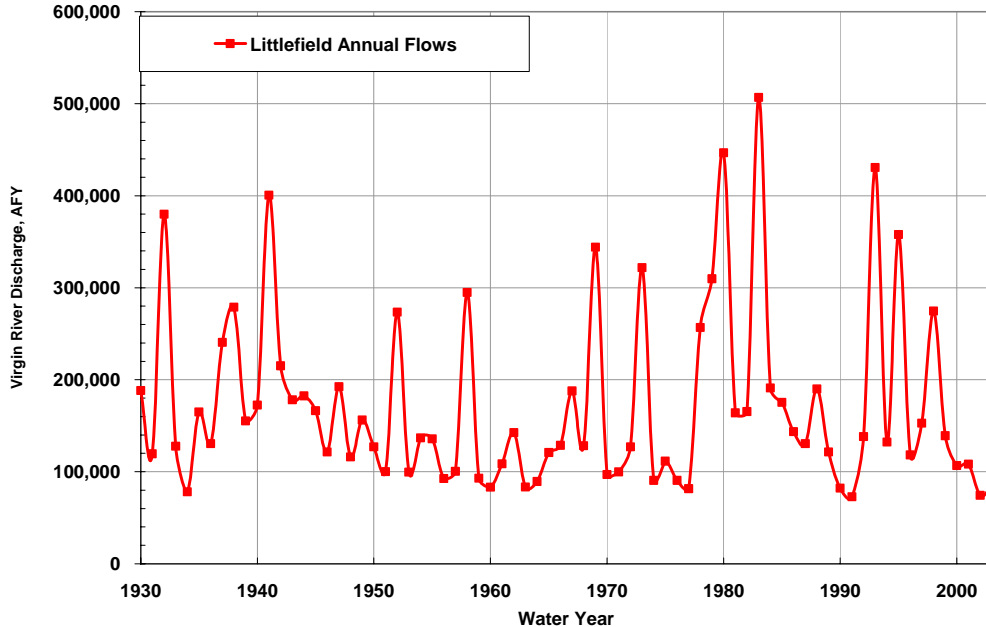


Figure 3. Virgin River Annual Flows¹ at the Littlefield Gage

¹ Estimated by USGS based on the stage-discharge relationship

Flow-duration curves can be statistically analyzed to evaluate the variability of river flows. Figure 4 presents a flow duration curve for the annual volumes (in acre-feet per year, or afy) at Littlefield. The graph represents a cumulative frequency curve for river flows in an average year, and shows the percentage of the time that a particular streamflow is equaled or exceeded. Also plotted is the flow-duration curve for Littlefield in water years 1978–85 (excluding water year 1984) and the period of record for the Halfway Wash and Riverside gages.

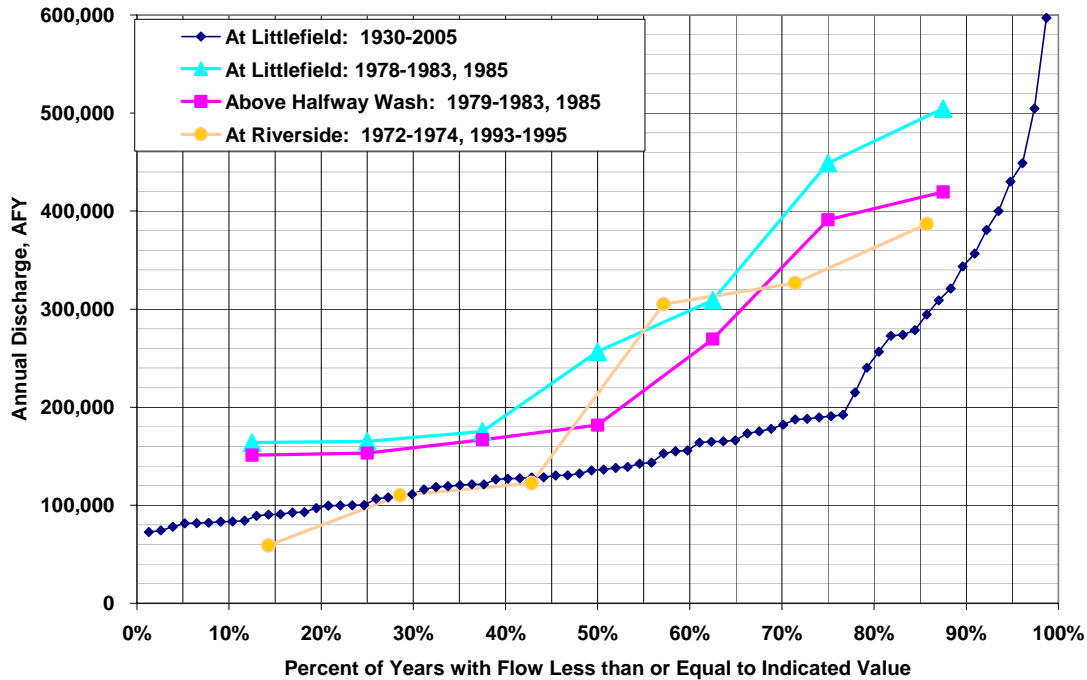


Figure 4. Flow-Duration Curves for Selected Gages on the Lower Virgin River (based on annual flow)

Comparing the Littlefield long-term curve (1930–2005 in dark blue) to the 7-year curve (1978 to 1983, 1985 in light blue) demonstrates that the annual flow volume in the river during these 7 years was substantially higher than average. Therefore, use of only the recorded gage data from Halfway Wash during the 7 years of record would not provide a reliable estimate of either long-term annual or seasonal flow rates.

PREVIOUS STUDIES

Several studies have been conducted that are based on different methods for developing synthetic, long-term flow records for the Virgin River at Halfway Wash. Three of these studies are described below:

- *“Hydrology and Interactive Computer Modeling of Ground and Surface-Water in the Lower Virgin River Valley, Primarily in Clark County, Nevada”*, Las Vegas Valley Water District (LVVWD, 1992). A hydrologic basin model was used to estimate average annual streamflow in the Virgin River at Halfway Wash. The model estimated an average annual streamflow of 141,000 af (acre-feet). The model was based on 1989

conditions and used an inflow of 174,000 af at Littlefield, which was the average annual at the Littlefield gage for water years 1930–89. The hydrologic basin model predicts only the long-term average annual flow, and does not predict daily flow rates.

- The addendum to the 1992 LVVWD report, published by LVVWD in 1993, used a least-squares linear regression of concurrent monthly streamflow data at Halfway Wash and the upstream gage at Littlefield to estimate the flow at Halfway Wash from 1929 to 1993. The estimated average annual streamflow at Halfway Wash was 154,000 afy. The regression formula was:

$$Y = 0.81X + 21.14 \quad (1)$$

where:

Y = monthly streamflow at Halfway Wash (cfs)

X = monthly streamflow at Littlefield (cfs)

The correlation coefficient for the above equation is $R=0.98$, suggesting that the LVVWD methodology may provide a reliable estimate. However, because it is based on monthly streamflow data and a linear relationship between flows at Littlefield and Halfway Wash, it does not necessarily reflect the variations in the relationship between the gages that might occur over shorter time periods. Figure 5 illustrates the daily flows up to 500 cfs at Littlefield and Halfway Wash for the 7-year record and the regression line developed by LVVWD. As noted in the study, “the equation tends to overpredict very low flows mostly in the less than 100 cfs range and underpredict very large flows.” The study goes on to say that the equation manages to balance the underpredictions and overpredictions reasonably well, except for in extremely dry years when low flows predominate and the method appears to significantly overpredict the flow in the Virgin River at Halfway Wash.

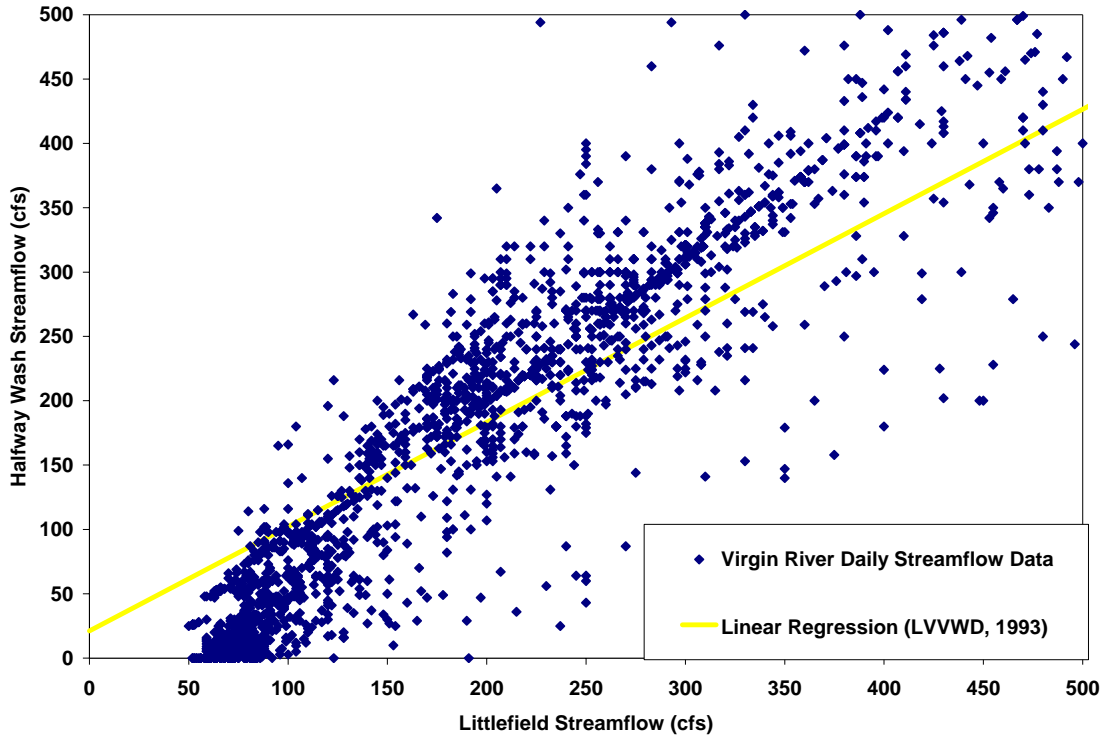


Figure 5. Virgin River Daily Flow Data Less than 500 cfs and LVVWD Regression Line

- “*Lower Virgin River – Boron Total Maximum Daily Loads,*” Bureau of Water Quality Planning, Nevada Division of Environmental Protection (NDEP), 2002. As part of the study, a least-squares linear regression analysis was performed between the average annual flows for the Halfway Wash Gage station and the historic average annual flows for the Littlefield Gage station. The regression formula was determined to be:

$$Y = 0.813X - 11,600 \quad (2)$$

where:

Y = annual flow at Halfway Wash (afy)

X = annual flow at Littlefield (afy)

The correlation coefficient for the above equation is R=0.98. This methodology appears to be appropriate for predicting annual flow volumes but is less suitable for assessing daily flows.

Table 2 summarizes the findings of these studies and the average annual flow predicted for the Virgin River at Halfway Wash.

Table 2. Summary of Previous Studies on Virgin River Flows at Halfway Wash

Previous Study	Estimated Average Streamflow at Halfway Wash (afy)	Analytical Method	Correlation Coefficient (R)
LVVWD (1992)	141,000	Hydrologic basin model	N/A
LVVWD (1993)	154,000	Linear regression of Littlefield and Halfway Wash data	0.98
NDEP (2002)	134,200	Linear regression based on annual flow volumes	0.98

METHODOLOGY

A synthetic, daily long-term Virgin River flow record at Halfway Wash was developed using a method based on flow-duration curves. When river streamflow data for a particular site are limited, the available data can be extended by using streamflow data for a nearby station that has both a longer period of record and is subject to similar hydrological conditions. This methodology, described by Wisler and Brater (1959), Chow (1964), and the Bureau of Reclamation (USBR, 1973), was used to extend the record of Virgin River flows at Halfway Wash based on the longer term records available for river flows at Littlefield.

Flow-duration curves were developed using daily flow data for both the Littlefield and Halfway Wash Gages for the 7 years of concurrent flow records as illustrated on Figure 6.

Next, a flow-duration curve was developed for the Littlefield Gage using daily streamflow data for the entire 74-year period of record. Based on the relationships between the 7-year and 74-year flow-duration curves for the Littlefield Gage at corresponding probabilities, the 7-year Halfway Wash flow-duration curve was proportionally adjusted using the formula below. At any given probability:

$$Q_{\text{Halfway (74 yrs)}} = Q_{\text{Halfway (7 yrs)}} \times \frac{Q_{\text{Littlefield (74 yrs)}}}{Q_{\text{Littlefield (7 yrs)}}} \quad (3)$$

where: Q = Average Daily Flow (cfs)

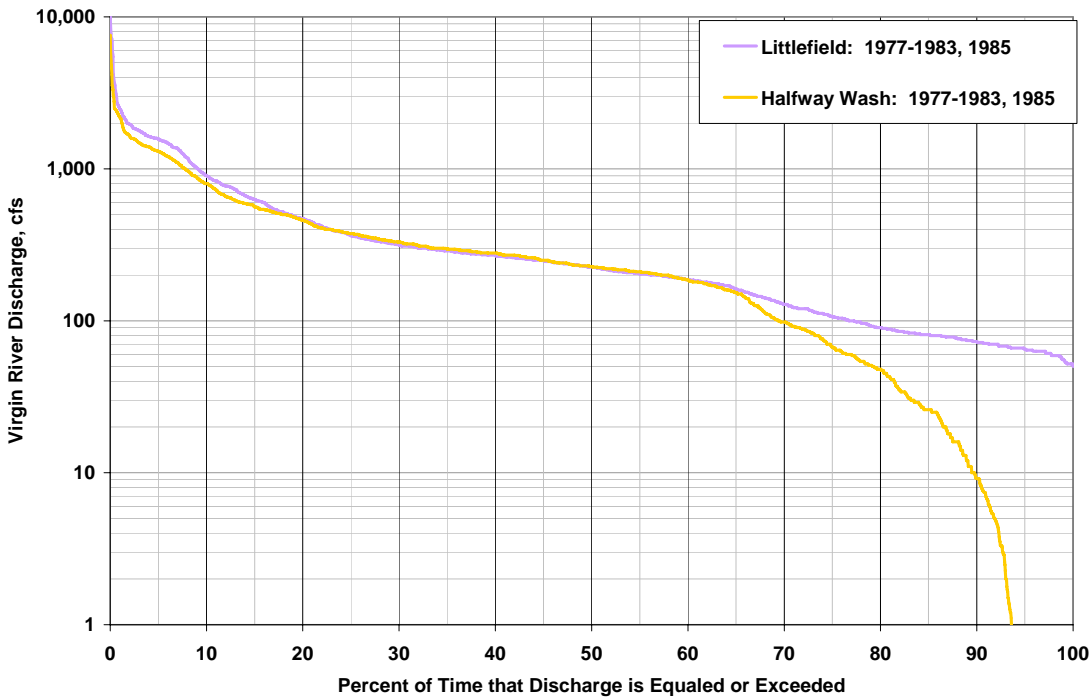


Figure 6. Flow-Duration Curves for 7 Years of Concurrent Gage Records at the Littlefield and Halfway Wash Gages (based on daily average flows)

As an example, for the 7 years of available data at the Halfway Wash gage, there was an 80% probability that the daily flow in the river would be greater than 48 cfs. This is because during the 7-year period of record, the flow in the river was greater than 48 cfs 80% of the time, and less than or equal to 48 cfs 20% of the time. At the Littlefield gage, the flow with 80% probability of exceedance was 90 cfs for the same 7-year period of record, but only 69 cfs for the entire 74-year gage record. Using these values in equation 3, it is predicted that there would be an 80% probability of exceedance that the flow at Halfway Wash would be greater than 37 cfs during the 74-year period from water years 1930 through 2003. This methodology was used to produce a synthetic, long-term flow-duration curve for the Virgin River at Halfway Wash. Figure 7 presents the flow-duration curves.

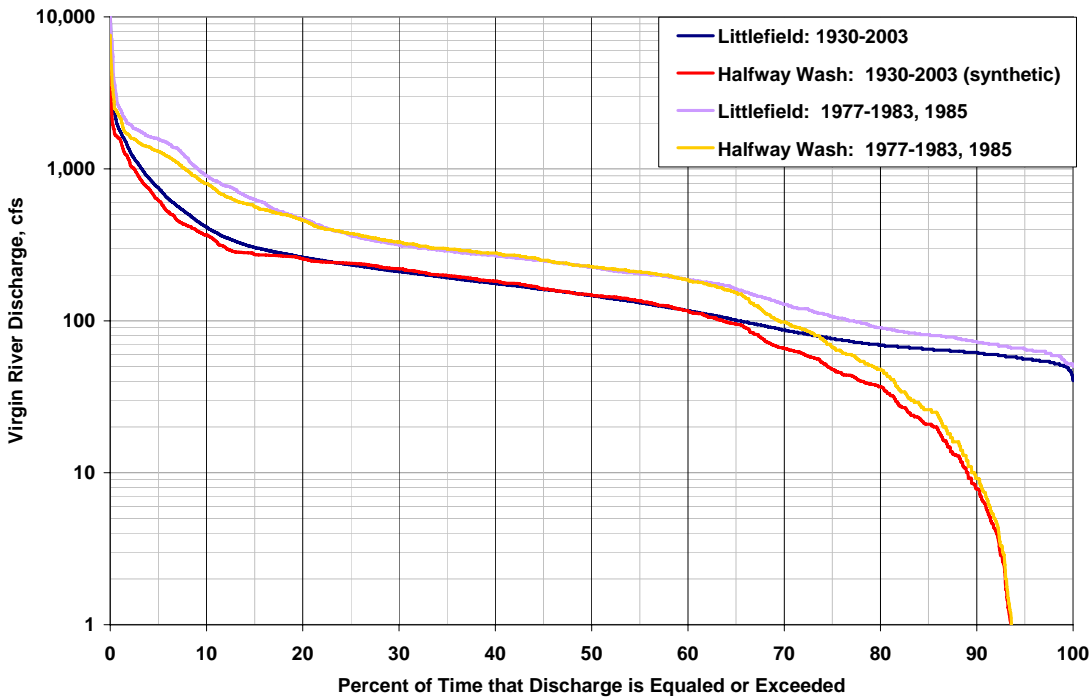


Figure 7. Flow-Duration Curves for the Littlefield and Halfway Wash Gages (based on daily average flows)

An estimated, daily flow record for the Virgin River at Halfway Wash, starting in water year 1930, was then developed for the 74-year period based on

- the measured daily average flows at Littlefield,
- the probability corresponding to each daily flow at Littlefield based on the 74-year Littlefield flow-duration curve, and
- the daily flow from the estimated, 74-year flow-duration curve for Halfway Wash corresponding to the identical probability from the 74-year flow-duration curve at Littlefield.

For example, on October 7, 1954, the average daily flow as measured at the Littlefield gage was 69 cfs, which corresponds to an 80% probability of exceedance. The 80% probability of exceedance on the Halfway Wash synthetic curve is 37 cfs, and is thus assigned as the synthetic flow rate for October 7, 1954. Figure 8 illustrates the resulting flow-duration curve generated from the methodology described above.

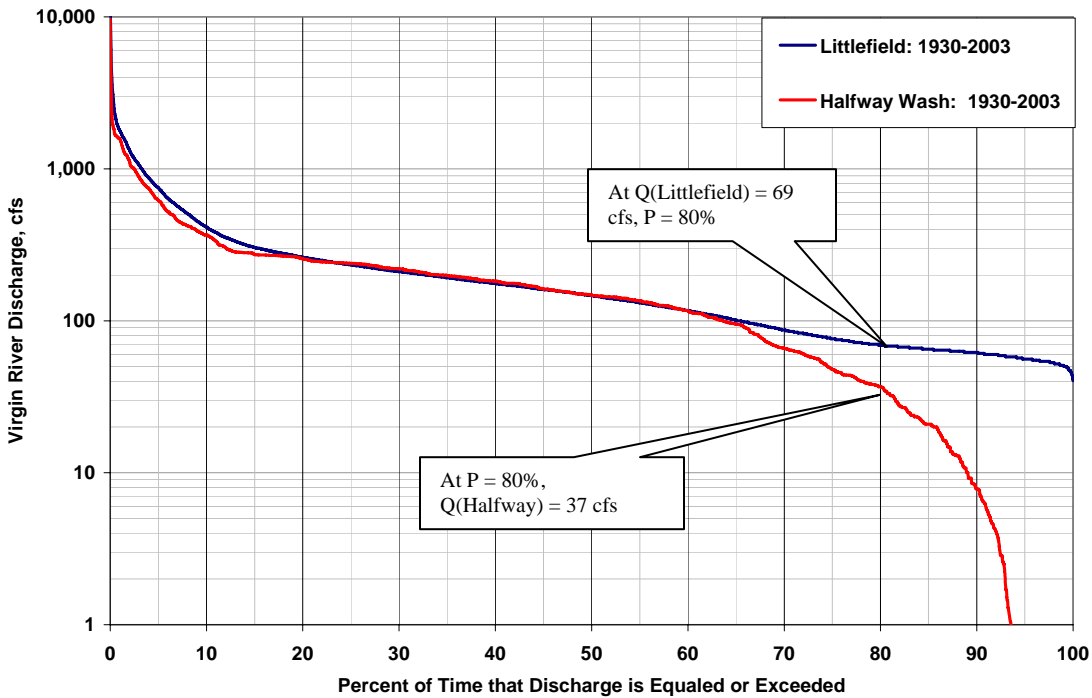


Figure 8. Flow-Duration Curves for the 74-year Littlefield and Halfway Wash Gages (based on daily average flows)

Table 3 presents the observed Littlefield flows from October 7–11, 1954, and the estimated Halfway Wash flows for the same time period.

Table 3. Virgin River Flows Observed at the Littlefield Gage and Estimated Flows for Halfway Wash

Date	Littlefield Flow (cfs)	Probability of Exceedance (%)	Halfway Wash Estimated Flow (cfs)
10/7/1954	69	80	37
10/8/1954	209	30	219
10/9/1954	904	4	761
10/10/1954	235	25	240

Based on this methodology, a day-by-day estimate of the flow of the Virgin River at Halfway Wash was developed. The resulting minimum and average annual flows at Halfway Wash, presented on a water year basis over the period of record, are approximately 57,000 and 145,000 afy, respectively. Table 4 presents the Virgin River flow volumes observed at the Littlefield Gage, and the synthetic volumes for the Virgin River at Halfway Wash.

Table 4. Virgin River Annual Flows

Water Year	Recorded Flow at Littlefield ¹	Synthetic Flow at Halfway Wash	Recorded Flow at Halfway Wash ¹	Water Year	Recorded Flow at Littlefield ¹	Synthetic Flow at Halfway Wash	Recorded Flow at Halfway Wash ¹
	(afy)	(afy)	(afy)		(afy)	(afy)	(afy)
1930	188,100	151,300		1969	343,600	282,800	
1931	119,400	101,100		1970	97,000	82,400	
1932	381,900	290,500		1971	99,800	84,200	
1933	127,400	116,300		1972	126,900	97,700	
1934	78,000	56,600		1973	321,000	264,500	
1935	164,800	143,200		1974	90,500	75,200	
1936	131,000	111,200		1975	111,200	95,600	
1937	240,300	204,500		1976	91,200	75,100	
1938	278,600	218,900		1977	81,400	61,400	
1939	154,900	131,000		1978	256,600	185,000	181,800
1940	173,700	141,200		1979	308,900	260,900	269,700
1941	400,000	315,600		1980	450,200	351,600	392,300
1942	215,000	185,400		1981	163,900	152,200	151,200
1943	178,100	153,700		1982	165,200	154,600	153,100
1944	182,700	158,800		1983	504,600	422,900	419,500
1945	166,300	147,400		1984	191,400	175,800	
1946	121,200	110,700		1985	175,300	156,600	
1947	192,200	164,100		1986	143,300	135,200	
1948	116,400	105,400		1987	130,400	122,400	
1949	155,900	137,200		1988	190,200	176,400	
1950	127,100	115,300		1989	121,300	95,300	
1951	99,900	83,200		1990	82,100	65,800	
1952	273,500	227,900		1991	72,600	59,300	
1953	99,500	87,500		1992	138,400	124,500	
1954	136,500	120,300		1993	430,100	347,600	
1955	135,500	117,400		1994	132,200	122,300	
1956	92,800	76,700		1995	356,700	289,000	
1957	100,200	84,300		1996	118,900	108,900	
1958	294,600	249,400		1997	152,700	138,900	
1959	92,900	76,600		1998	273,900	242,900	
1960	83,400	65,800		1999	139,000	133,100	
1961	108,500	88,300		2000	106,900	96,300	
1962	142,400	117,000		2001	108,100	100,800	
1963	83,300	64,800		2002	74,300	60,100	
1964	89,500	71,700		2003	84,200	68,500	
1965	120,400	98,600		Mean	171,900	144,800	260,300
1966	128,500	107,100		Median	136,000	121,300	269,700
1967	187,600	142,400		Minimum	72,600	56,600	151,200
1968	128,700	114,400		Maximum	504,600	422,900	419,500

¹ Source: United States Geological Survey (2005)

Note: include water year 1979.

VALIDATION OF EXTENDED FLOW RECORD

Figures 9 and 10 present the daily flow data for the 7 years of gage record at the Virgin River at Halfway Wash, the function derived from the flow-duration method previously described, and the LVVWD and NDEP regression formulas. As seen in Figure 9, the flow-duration method most accurately represents flows less than 500 cfs because the LVVWD regression tends to overpredict flows less than 100 cfs, and the NDEP regression tends to underpredict flows greater than 75 cfs.

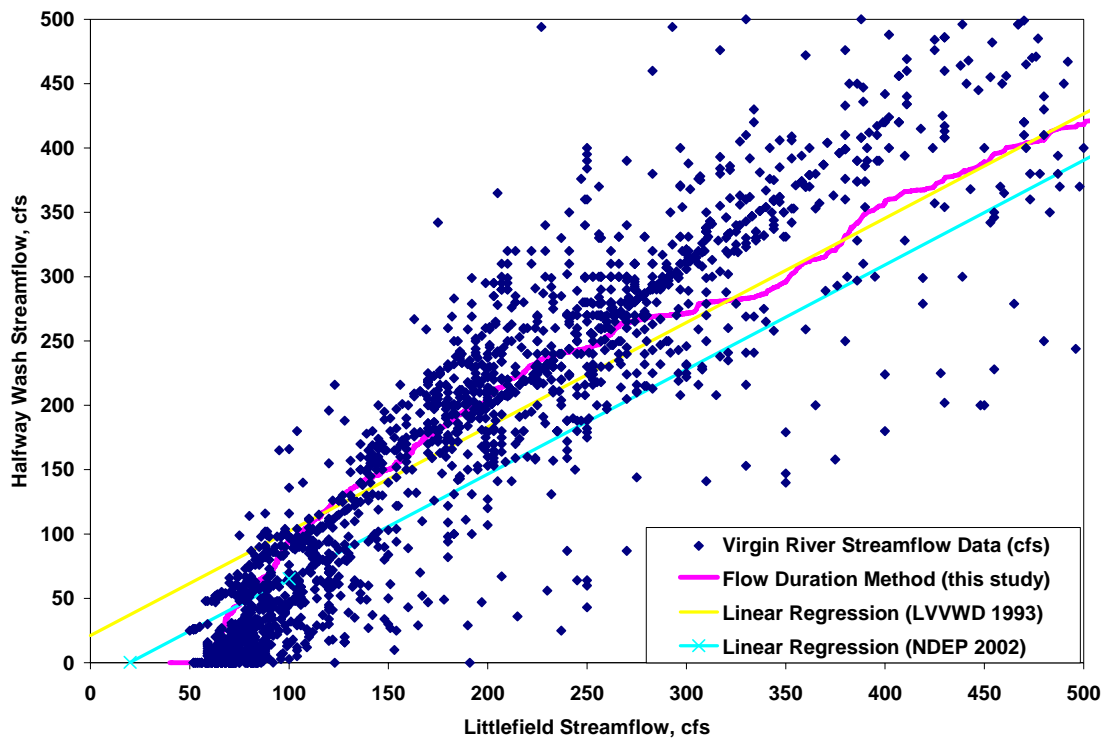


Figure 9. Virgin River Daily Streamflow Data Less than 500 cfs

Figure 10 presents the results of the analyses over the whole range of data. The flow-duration method produces conservative results in the high-flow range. For flows greater than about 2,000 cfs, it would be expected that the flow at Halfway Wash would generally be equal or greater than the flow at Littlefield because the watershed increases downstream and diversions, because of their relatively small size, would have little affect on the flow in those ranges. There would be some losses expected from ET consumption, bank storage, and recharge of the alluvial aquifer. Regardless of the influence from these individual factors, all three methods predict lower flows at Halfway Wash than at Littlefield because this is what is reflected in the 7-year gage record. This could be because of losses described above, however, it is more likely that the stage discharge relationship that was developed for Halfway Wash Gage does not adequately reflect flows in the higher flow ranges. In any case, it is expected that use of any of the three methods for estimating flows at Halfway Wash yields results that may be lower than the actual flows in the high-flow ranges.

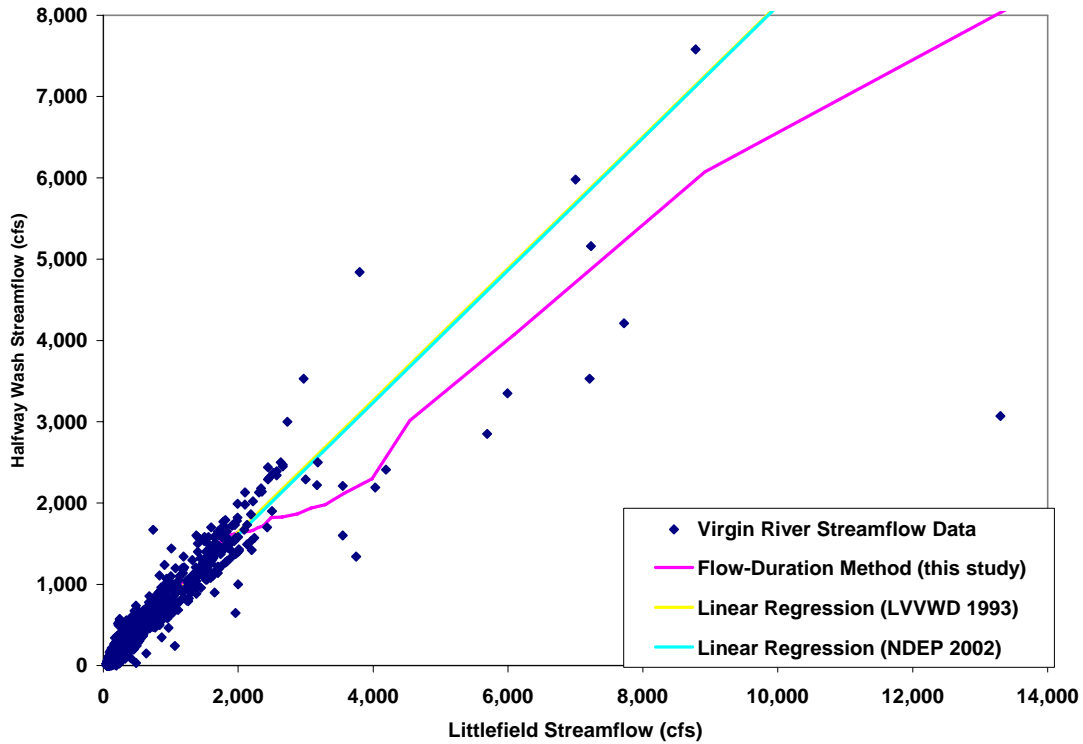


Figure 10. Virgin River Daily Streamflow Data

Figure 11 shows the recorded versus synthetic data for Halfway Wash for the 7-year period of record (water years 1978–83 and 1985). Figure 12 presents a comparison of recent flow data measured at the USGS gages at Littlefield and Overton with the flows for Halfway Wash that were synthesized using the methodology of flow-duration curves described. Figures 11 and 12 indicate that the synthetic flow record shows a strong correlation to the observed flow data at the Halfway Gage during water years 1978–85 and at the Overton Gage during water year 2003. This also implies that the factors influencing changes in flows between the Littlefield Gage and Halfway Wash Gage have remained the same from 1978 to present.

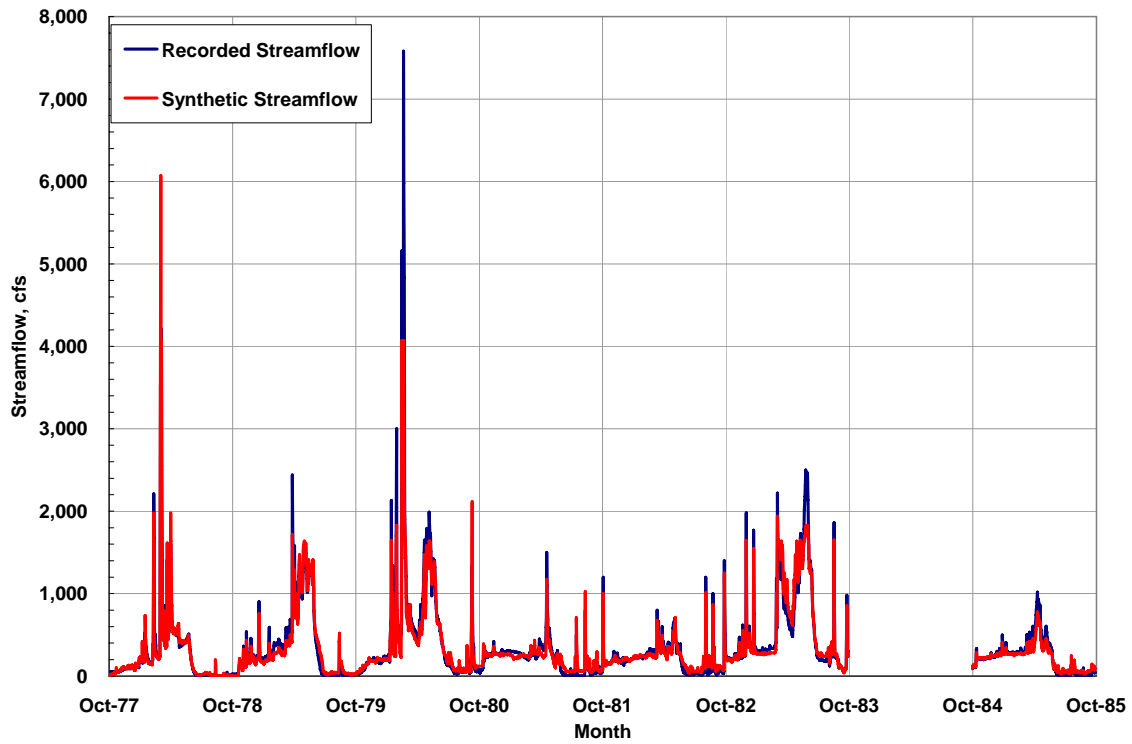


Figure 11. Comparison of Observed and Estimated Flow for the Virgin River at Halfway Wash

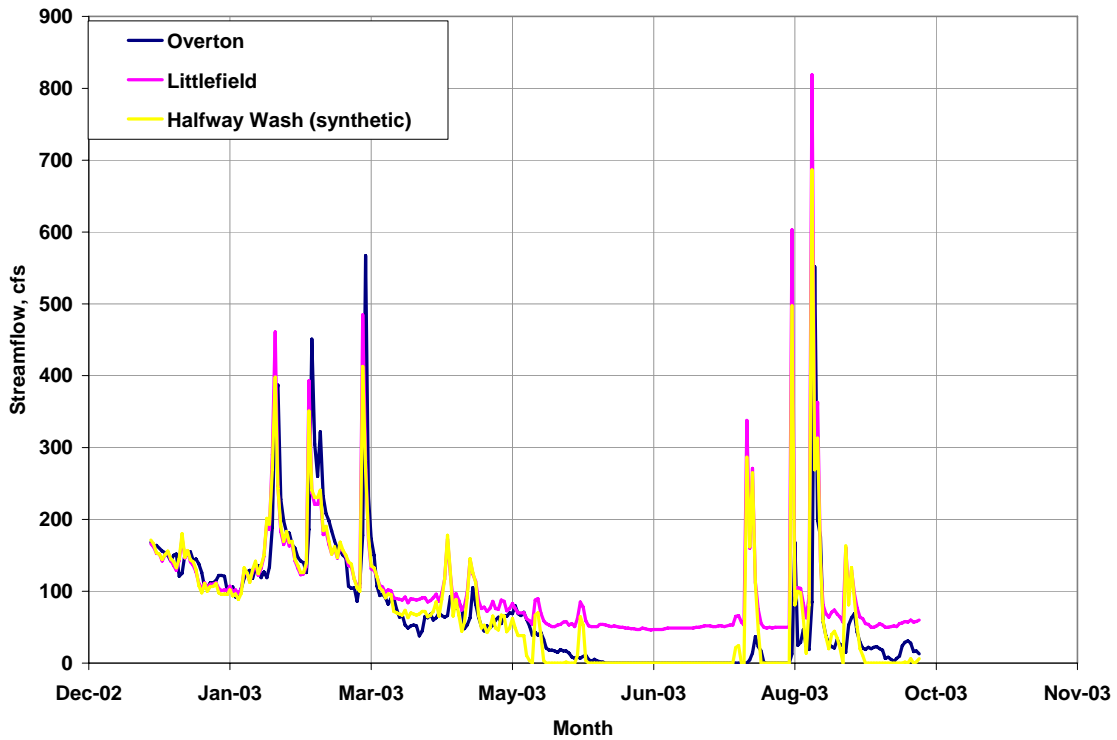


Figure 12. Virgin River Flow at Littlefield, Halfway Wash and Overton

Figure 13 presents a double-mass curve. A double-mass curve plots the accumulation of an element over time at a reference station versus the corresponding accumulation of the same element over time at a test station. Double-mass curves are typically used to compare data sets and to detect changes in data as revealed by changes in the slope of the curve. In this case, the x-axis presents the cumulative streamflow volume as recorded during the 7 years of gage record at Halfway Wash (the reference station), and the y-axis presents the streamflow volume predicted for each of the methods (the test stations). A perfect correlation would yield a line at 45 degrees above horizontal. Both the flow-duration method and LVVWD regression method show good results, with the LVVWD regression slightly over-predicting flows and the flow-duration method slightly under-predicting flows. The NDEP regression is farthest from the 45 degree angle.

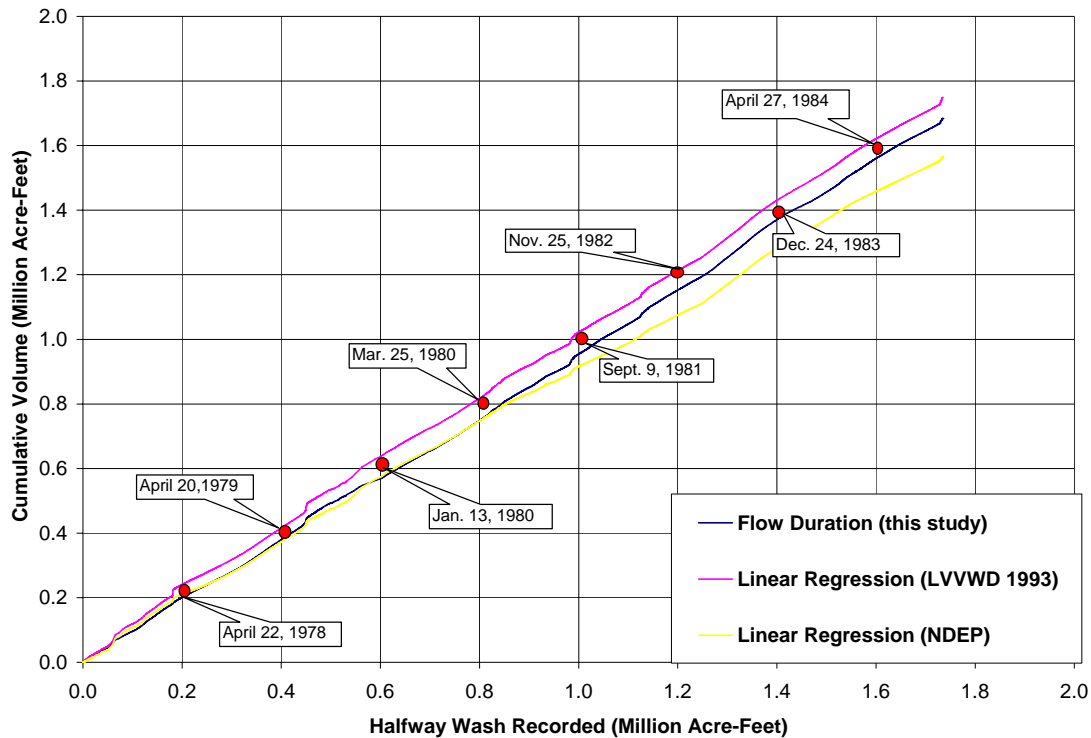


Figure 13. Double-Mass Curves for Virgin River at Halfway Wash Recorded Flows and Virgin River at Halfway Wash Synthetic Flows

The synthetic flow record is based on the variation of flows as observed at the Littlefield Gage from 1929 to 2003. Although it presents a good baseline of Virgin River flows, it is possible that annual streamflow volumes could occur on the Virgin River that are higher or lower than those predicted. Also, if the factors influencing the relationship between the two gages were to change, the model would require revisions to reflect these changes.

CONCLUSION

Short-term gage records are available for the lower Virgin River downstream of the Littlefield Gage, but a consistent, long-term gage record is not available. Previous studies used linear regressions to estimate the long-term flow record at the Halfway Wash Gage based on the long-term data at the Littlefield Gage. Although the linear regressions appear to be reasonable in predicting annual streamflow volumes, they appear to be less accurate in prediction of daily average flows, particularly in the low-flow range. The objective of this study was to establish a long-term daily flow record for the lower Virgin River that is reliable even in the low-flow range. This study presents a method of estimating flows that uses flow-duration curves to extend the short-term records. It was demonstrated that the methodology returns reasonable predictions of flow in the low-flow range, and overall predictions that are somewhat conservative (lower than may actually occur). The flows derived using this method can and should be used as a baseline flow record for the lower Virgin River, particularly in the low-flow regime, to assess the impacts of possible water resources developments. The synthesized flow record for the Virgin River above Halfway Wash may be obtained from the authors.

REFERENCES

- Brothers, K., Tracy, J.V., Katzer, T.L., Stock, M., Bentley, C., Zdon, A., Kepper, J. 1992, Hydrology and Interactive Computer Modeling of Ground and Surface-Water in the Lower Virgin River Valley, Primarily in Clark County, Nevada: Cooperative Water Project, Report Number 1, 90 p.
- Brothers, K., Katzer, T.L., Mojib, R.M., Grinnell, G., Bernholtz, A., Johnson, M. 1993, Addendum to Hydrology and Interactive Computer Modeling of Ground and Surface-Water in Lower Virgin River Valley, Primarily in Clark County, Nevada: Cooperative Water Project, Report Number 1-A, 35 p..
- Chow, V.T. (editor), 1964, Handbook of Applied Hydrology: A Compendium of Water-resources Technology, McGraw-Hill, New York.
- Hilmes, M.M., and Vaill, J.E., 1997, Estimates of Bridge Scour at Two Sites on the Virgin River, Southeastern Nevada, Using a Sediment Transport Model and Historical Geomorphic Data: U.S. Geological Survey Water-Resources Investigations Report 97-4073, 72 p.
- Las Vegas Valley Water District, 1992, The Mark Group, Hydrology and Interactive Computer Modeling of Ground and Surface-Water in the Lower Virgin River Valley, Primarily in Clark County, Nevada.
- National Oceanic and Atmospheric Administration National Weather Service Hydrology Lab, 2006, Recent Developments in Data Analysis Quality Control and Data Browsing at the National Weather Service Office of Hydrology: Available at <http://www.weather.gov/oh/hrl/papers/ams/ams98-4.htm>
- Nevada Division of Environmental Protection, Bureau of Water Quality Planning, 2002, Lower Virgin River – Boron Total Maximum Daily Loads

- Southern Nevada Water Authority, 2004, 2005 Water Resource Plan: Available at http://www.snwa.com/html/news_pubs_wr_plan.html
- U.S. Bureau of Reclamation, 1973, Design of Small Dams: A Water Resources Technical Publication, Second Edition.
- U.S. Geological Survey, 1979, Water Resources Data for Nevada, Water Year 1978: U.S. Geological Survey Water Data Report NV-78-1.
- U.S. Geological Survey, 1980, Water Resources Data for Nevada, Water Year 1979: U.S. Geological Survey Water Data Report NV-79-1.
- U.S. Geological Survey, 1981, Water Resources Data for Nevada, Water Year 1980: U.S. Geological Survey Water Data Report NV-80-1.
- U.S. Geological Survey, 1982, Water Resources Data for Nevada, Water Year 1981: U.S. Geological Survey Water Data Report NV-81-1.
- U.S. Geological Survey, 1983, Water Resources Data for Nevada, Water Year 1982: U.S. Geological Survey Water Data Report NV-82-1.
- U.S. Geological Survey, 1984, Water Resources Data for Nevada, Water Year 1983: U.S. Geological Survey Water Data Report NV-83-1.
- U.S. Geological Survey 1987, Water Resources Data for Nevada, Water Year 1985: U.S. Geological Survey Water Data Report NV-85-1.
- U.S. Geological Survey, 2005, Surface-Water Data for the Nation: Available at <http://waterdata.usgs.gov/nwis/sw>
- Wisler, C.O., and Brater, E.F., 1959, Hydrology, Second Edition: John Wiley & Sons, Inc, New York.

This page left blank intentionally

Where Does the Water Go? Agreement Investigation

ROBERT D. BAGGS, JR. Las Vegas Valley Water District, 1001 S. Valley View Boulevard, Las Vegas, Nevada 89153 (robert.baggs@lvvwd.com)

D'LAYNE M. REYNOLDS Las Vegas Valley Water District, 1001 S. Valley View Boulevard, Las Vegas, Nevada 89154 (dlayne.reynolds@lvvwd.com)

ABSTRACT

A development project – subdivision, shopping center, or irrigation system – requires the installation of a water meter to account for consumption by a developer or the retail customer. Once installed, it should begin measuring water flow and producing cash flow. Agreement Investigation (AI) is a post-development process that examines the timeliness of these flows. As with so many single-focus processes in a highly complex field and administrative system, investigating one problem often leads to opportunities in other functional areas.

INTRODUCTION

Problem

Water meters are installed by a contractor and accepted by the Las Vegas Valley Water District (LVVWD) for operation and maintenance following inspection and acceptance. The meters need to be activated (turned on, an administrative action) as quickly as possible. This activation does two things. One, it ensures that water is accounted for. Two, activation ensures that billing begins as soon as possible.

The AI project is a process for accounting for water and the resultant revenues from appropriate billing. The project did not include system design, projected demands of new services, effects on customer service or billing operations, or inspection of installed services. However, the latter item led to further ideas about examining the process of accounting for water in a more efficient manner.

Purpose

The purpose of this paper is to review the Agreement Investigation (AI) process as implemented by the LVVWD Development Services Office (DSO). AI is a post-development (after facility installation) process to account for the consumption of water through LVVWD meters. The objective of AI is to ensure that the water that flows through the meter is accurately logged into the resource and billing systems, that it is the correct size, and that revenue is generated as quickly as possible. Asking where the water goes taught us lessons that are leading us into future processes designed to reduce costs and increase operating efficiencies for the LVVWD.

Methodology

The process evolved based on previous efforts to improve water accountability and a review of available and appropriate staff resources.

BILL OF SALE:

- A document provided by the developer that transfers the water facilities (mains, meters, backflow assemblies, but not water lines between structures or parcels, or on-site plumbing) to the LVVWD for its operation and maintenance.

AI STAFF:

- DSO compares the Bill of Sale to as built drawings to ensure all services proposed to be installed were installed and accepted by the LVVWD.
- DSO develops work orders for Meter Services staff for field reviews of inactive meter locations.
- Meter Services investigates installation and activation, logs meter numbers, performs meter change outs, or reports status of meters for change out by developer (e.g., smashed lens, incorrect size) if project under warranty.
- Meter Services staff reports daily results to DSO for internal processes.
- DSO activates accounts, logs meter numbers and any consumption readings, prepares bills for consumption to either developers, who may have used water during construction, or to retail customer, who failed to sign for service. Once activated, Meter Readers have site added to database for monthly reading. Also, Billing Services' database is updated with these accounts.

Background

In late 2001, DSO received a phone call from a homeowner questioning his water bill. He was questioning whether he was paying for the common area irrigation service in addition to his domestic residential consumption.

We discovered four irrigation services that had never been activated by a developer for the purpose of monthly billing. The services were accepted by the LVVWD a year earlier and the meters were delivering water for irrigation.

Field checks of the four services led to \$149,538.00 in uncollected revenue. More importantly, this action placed the accounts in the billing system for regular monthly reading and billing.

This discovery and several other instances around that time caused our office to question the effectiveness of Agreement Investigation (AI). The rapid growth of the LVVWD (over 22,000 accounts yearly for the last four years) had changed priorities from post-development follow-up to sustaining the basic field functions of meter reading and maintenance. A data query showed 600 services still in an inactive (I) status which should be investigated for possible activation for billing.

A plan was developed with Meter Services to have all services on the report field checked to obtain meter numbers, meter readings and use type (residential, non-residential, irrigation). Work orders were created for each service. Copies of the work orders were printed, along with maps and other location information that would help locate services efficiently.

Over the course of about two weeks, two or three Meter Services personnel processed the orders, returning the hard copies with the information to Billing Services. Billing attached the meters to the accounts. Billing then sent any 'turn-on' information to Customer Services to prepare for any customer calls. We estimated that 90% of these services should have been activated for billing long before this special coordinated activity.

The total billing led to another \$2,000,000 of past-due revenues and the creation of new revenue streams from the activated meters. Customer Services was notified that write-offs were not to be considered until all other means to collect had been exhausted. Nearly all of those monies were collected through standard billing; special, interest-bearing payment arrangements; or through the established credit and collections process in Customer Services.

After the special field investigation, DSO initiated meetings to develop business processes that would restart the AI process among Billing, Meter Services, Customer Services, and Development Services. This included several work items. One, Billing would resume reviewing the large service (greater than 2-inch meter sizes) report to determine if these services were ready for activation and billing. Two, Meter Services would change the status of commercial and irrigation services from Inactive to Active following meter routing. The outcome was not what DSO expected. Billing continued to send Meter Services to investigate services for possible turn-on when the services had not been installed. Since we could not mediate this communication issue, DSO immediately cancelled the AI process.

In early 2003, following another data query, we researched 874 services, sending 48 work orders to have services checked by Meter Services. All were ready for billing, totaling \$90,916.28 in past-due revenues. The work established those accounts for regular billing.

At this time, DSO reviewed the process with all involved as if it were in charge of it from discovery through billing. Several approaches were developed. For example, as planning maps were reviewed, we checked irrigation and commercial services for a backflow (BF) device. If the device was attached to the account, the status of the service was changed to "A" from "I". We also tried to ascertain the possible meter number and place that number, along with the BF serial number, in the comments of the account. The date that the BF device was accepted served as the basis for activating the account for billing.

Despite these incremental improvements, there still was no consistency in the investigation process. If the DSO reviewed a plan map, the review would only capture what was on that map. The priority schedule for field investigations was unknown. Sometimes, field personnel, working on other priorities during their shift, had a hard time locating the services. This led to the work being sent to the lead technician or supervisor, creating another delay in capturing the information. For example, it took two months to find and read four of seven services. Development Services tried another approach.

In early 2004, Development Services requested a different kind of assistance from Meter Services. We asked for, and received, a meter reader on a weekly, part-time basis. We developed a daily list of accounts for field investigation. The reader provided the results each afternoon. The reader also noted field conditions while reading. These field conditions revealed how other divisions' processes were working in a way that would assist in accurate, timely water accountability.

Based on this initial success, the DSO negotiated a service agreement with Meter Services. All administrative work (data entry, research, work assignments, directions, unique information, and billing) connected with the AI process would be the responsibility of DSO. The reader and the truck were provided by Meter Services on a part-time basis. Further, DSO requested, and Billing agreed, to take the results of AI meter reading information and complete the billing process. This meant accepting AI meter reads and not sending Meter staff to the field to confirm a reading less than five days old.

The Managers of Meter Services and Financial Services agreed to the staffing and administrative procedures. This process change led to an added \$609,000 generated in developer and/or customer billings. Over 95% of these accounts will become permanent service billings, improving cash flow and accountability for water. Since this time, DSO has directed the AI process and has provided consistent reporting on and billing of new services.

RESULTS AND DISCUSSION

Some of the issues uncovered are best addressed through training and evaluation of field personnel; other issues require attention to administrative details, such as developers not calling for inspection of model home services, not calling to activate model home accounts, or not calling to schedule inspections of services with backflow assemblies prior to starting the use of services (irrigation, building occupancy, etc.). This information is reported to the inspection and water quality divisions to encourage added site visits to monitor development.

Another example is services are given LVVWD approvals for use or projects are accepted at 100% status with the wrong size meters in boxes, illegal services, idlers in meter boxes, non-LVVWD meters in boxes, no meters in boxes, meters installed backwards, stuck meters, backflow assemblies not installed or tested, wrong size backflow assembly. These events are recorded by service and distributed monthly for field training purposes.

Occasionally, the billing system drops a developer charge for consumption on the developer bill or meter change out fee. Because DSO is doing the billing for these accounts, we are an added review of these processes.

Meter readers may skip reading meters at locations that were under construction for a long time, but are now occupied, because the database used was not updated for new, active accounts. This is being addressed through the AI process activating accounts, thus ensuring that they are on the readers' route database.

CONCLUSIONS

With the ability to research service location and installation status and to activate services and bill for consumption, Development Services appears to be a logical location to manage AI.

However, the AI process is a component in post-development account auditing. The field investigations revealed information on quality of LVVWD staff work, developer responsibility, billing accuracy, and meter reading performance, all of which contribute to accounting for water. Furthermore, the volume of the AI work is really at a full-time level, not the part-time schedule that can be affected by illness, vacation, or higher priorities in either of the division providing the staff support.

What about the future? A test will be conducted in the near future that will co-locate the Billing and Meter Services functions into a Water Accountability Team. This test will provide lessons learned in inter-staff, face-to-face communication in one room, using a night shift to review meter reads. This pilot will examine the ability to make real time decisions based on added software, and the development of a level of communication and trust between historically separated staffs. The results of this experiment will provide the basis for further development of efficient and effective processes across organizational borders.

Another approach recently suggested is to have LVVWD staff install all meters. It is believed that this will reduce the post-development transaction time consumed by inspections, billing, DSO, and Meter Services. It will also eliminate issuing meter receipts to contractors and the quality control over the inventory once it leaves the LVVWD warehouse. Once a meter is installed by the LVVWD staff, all appropriate information as to size, location, meter number, reading, and activation is done at the time of installation, and distributed to affected divisions. This process is a prospect for a live pilot project in the near future.

This page left blank intentionally

Trace Element and Radionuclide Concentrations in Walker River Bottom Sediment and Weber Reservoir Sediment Core, West-Central Nevada, 2005

CARL E. THODAL, U.S. Geological Survey, 2730 N. Deer Run Road, Carson City, NV 89701 (cethodal@usgs.gov);

MICHAEL S. LICO, U.S. Geological Survey, 2730 N. Deer Run Road, Carson City, NV 89701 (mlico@usgs.gov)

ABSTRACT

The Walker River Paiute Tribe is concerned that operations at the Yerington copper mine in Lyon County, Nevada, have contaminated water resources on the Walker River Indian Reservation. Mining in the Walker River Basin, including at the Yerington site, began in the mid-1800s; large-scale open-pit mining began in 1952 and continued intermittently until closure of the mine in 2000 because of bankruptcy. Investigations authorized by the Comprehensive Environmental Response, Compensation, and Liability Act began in the late 1990s in response to reports that elevated concentrations of trace elements and radionuclides have been measured in ground water, tailings leachate, and leachate-contaminated soil samples. The U.S. Geological Survey, in cooperation with the Walker River Paiute Tribe, began an investigation in 2005 to establish a chronology of the sediment quality of Weber Reservoir. Bottom-sediment samples were collected from six river sites and one drain site tributary to Weber Reservoir and two sediment cores were collected from Weber Reservoir for determination of selected major and trace elements, and radionuclides. Construction of Weber Reservoir began in 1933, storage began in 1934, and construction of the dam was completed in 1935.

Mean concentrations and activities of constituents measured in bottom-sediment samples from river sites, both upstream and downstream of the mine, and from the drain site downstream of mine tailings, generally were lower than those measured in the reservoir sediment. Advisory concentrations for iron and manganese were exceeded in all the samples and the advisory concentration for arsenic was equaled in one riverbed sample collected downstream of the mine. The concentration of mercury in one reservoir sample collected from pre-reservoir sediment was near the advisory concentration, and all samples, except one river-bottom sample, exceeded a sediment effects threshold concentration that may adversely affect freshwater invertebrates. No other advisory concentration or activity in the sediment samples was exceeded.

Cesium-137 data from a sediment core collected from Weber Reservoir show a clearly defined peak in sediment from a depth of 2.2–2.5 feet below the sediment surface and initial detection was in the sample from a depth of 2.8–3.2 feet. Assuming a linear rate of sedimentation and neglecting density compaction, sediment accumulated in Weber Reservoir at a rate of 0.06 feet per year during the 70 years since construction of the reservoir was completed. Each 0.3-foot length of sediment core represents about 5.5 years.

Maximum concentrations of aluminum, arsenic, beryllium, cadmium, copper, iron, lead, manganese, thorium, and zinc measured in the core were from the subsample that represents sedimentation during 1957–62. Of the 37 other analytes measured, 17 also had maximum

concentrations in this subsample. Maximum concentrations of chromium and nickel were from the subsample deposited during 1979–84 and maximum concentrations of uranium were from two adjacent subsamples deposited before the reservoir was constructed until 1944. Radium-226, radium-228, and gross alpha radioactivity had maximum activities in the subsamples from the interval deposited during 1968–73 and gross beta radioactivity had maximum activities in two adjacent subsamples deposited during 1940–51. Maximum concentrations of mercury and molybdenum were from the subsample deposited during 1935–40.

Contaminants from the Yerington copper mine site can be delivered to Weber Reservoir by direct fallout of windborne dust, fluvial transport of dust blown from the site to drainages, stormwater runoff from the site into the river, and contaminated ground water that discharges into Wabuska Drain. Concentrations and activities of constituents of concern in the sediment-core subsamples indicate varying rates of deposition; but, because each subsample represents sediment that accumulated over 5–6 years, episodic stormwater releases from the mine site would be diluted by normal sedimentation. The samples of river-bottom sediment generally had lower concentrations and activities than the reservoir-core samples, but the differences were small because both were derived from sources with a common geology owing to more than a century of mining in the Walker River Basin.

INTRODUCTION

The Walker River Paiute Tribe is concerned that discharges from the Yerington copper mine site, located in the Singatse Range, near Yerington in Lyon County, Nevada (Fig. 1) have contaminated water resources on the Walker River Indian Reservation (WRIR). Mining at the site began in 1952, and operations stopped in 1978 because of low copper prices and depletion of copper oxide reserves. In 1985, an Administrative Order was issued by the Nevada Division of Environmental Protection that alleged illegal discharge of pollutants from former mine tailings ponds (Nevada Division of Environmental Protection, 2002, accessed March 6, 2006). The mine was sold in 1989, and a solvent extraction and electrowinning plant was constructed to recover cathode copper from low-grade stockpiles and tailings with anticipation of expanding mining operations to include the nearby MacArthur copper deposits. In the late 1990s, the U.S. Environmental Protection Agency began preliminary investigations at the Yerington Mine following allegations of unlawfully discharged pollutants into waters of Nevada and pursuant to the Comprehensive Environmental Response, Compensation, and Liability Act (CERCLA). In November 1998, the State of Nevada ordered operations at the Yerington Mine to cease because of bankruptcy and subsequent invalidation of the corporate guaranteed environmental bond (Nevada Division of Environmental Protection, 2003, accessed March 6, 2006). However, copper leaching operations continued until January 2000. Concentrations of trace elements (aluminum, arsenic, beryllium, boron, cadmium, chromium, copper, iron, lead, manganese, mercury, molybdenum, nickel, selenium, thorium, uranium, and zinc), sulfate, and radionuclides have been reported in dust, sediment, and ground-water samples at levels that are greater concentrations than background (Seitz and others, 1982; James Sickles, U.S. Environmental Protection Agency Remedial Project Manager, written comm., May 2006). In 2005, the U.S. Geological Survey (USGS) began a paleolimnologic investigation at Weber Reservoir to establish a chronology of the sediment quality of the reservoir.

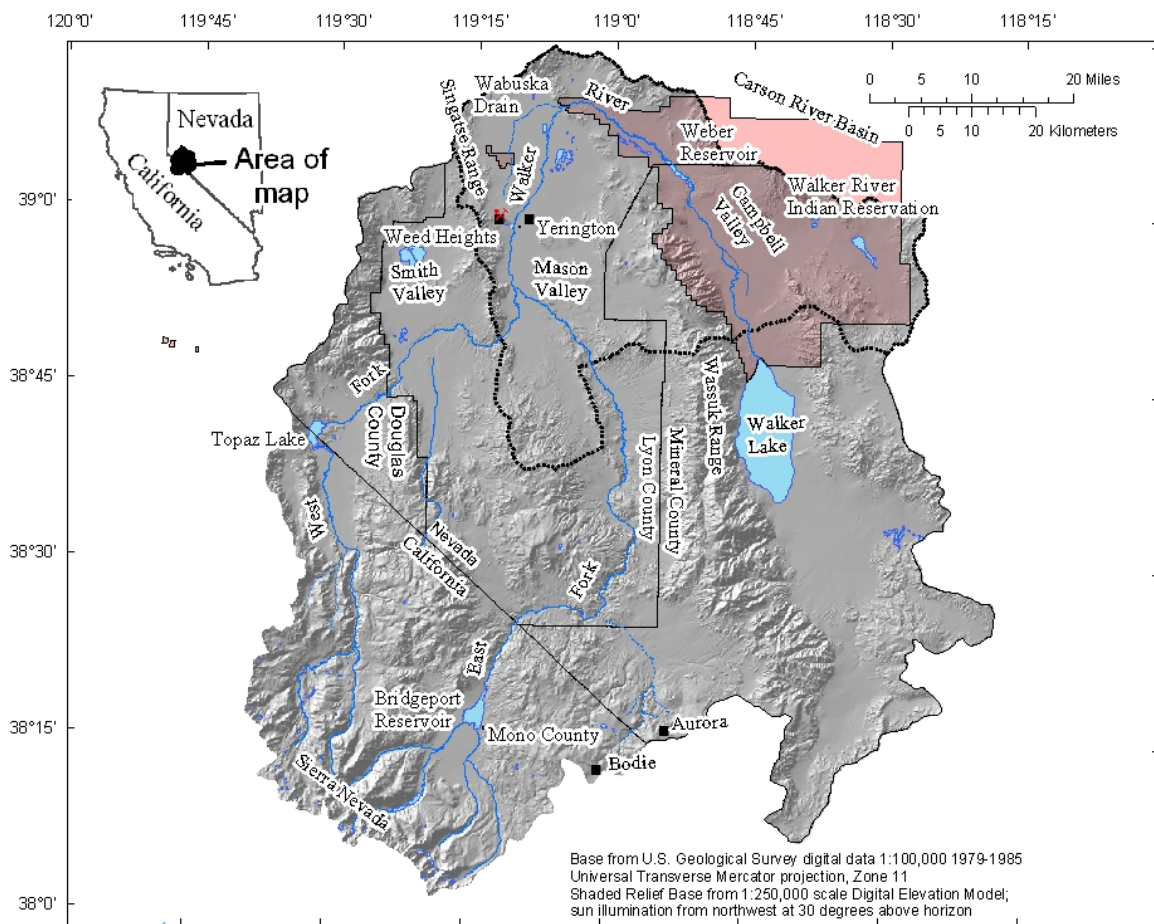


Figure 1. Location and selected geographic features of the Walker River Basin, Nevada and California, generalized extent of study area (outlined in black) and location of Yerington copper mine site (x).

Purpose and Scope

The purpose of this report is to describe concentrations of trace elements in bottom sediment from Wabuska Drain, Weber Reservoir, and the Walker River upstream of and downstream from the defunct copper mine, and to evaluate if changes occur in concentrations of trace elements in the sediment profile of Weber Reservoir that coincide in time with the operation of the copper mine. The scope of this report emphasizes data collected from six river sites, one drain site, and Weber Reservoir by the USGS in 2005. Previously published data from other investigations were used for comparison.

DESCRIPTION OF STUDY AREA

Physical Setting

Walker River Basin is a 4,050-mi² (square mile) closed hydrologic basin with headwaters in the eastern Sierra Nevada, in Mono County, California, and includes parts of Lyon, Mineral, and Douglas Counties in western Nevada. The Walker River Basin is in a transitional zone between the Sierra Nevada section of the Pacific Mountain System physiographic region and the Great Basin section of the Intermontane Plateaus physiographic region, with several mountain ranges 2,000–7,000 ft above adjacent valley floors.

The study area for this investigation is in Mason Valley and Campbell Valley in the northern part of the Walker River Basin (Fig. 2). This part of the basin is an arid, high desert with cold winters and warm summers. Average annual precipitation was 5.31 in. at the National Weather Service station at Yerington during 1971-2000 (Western Regional Climate Center, accessed March 27, 2006). Yerington is the largest community in this area with 2,883 inhabitants reported in the 2000 Census (Nevada State Library and Archives, 2000, accessed April 18, 2006). The population of WRIR was 853 in 2000, with most (721) residing in Schurz. The town of Yerington is a ranching and farming center, as well as a mining town (University of Nevada, Reno, accessed March 17, 2006). WRIR covers about 500 mi² in the northeastern part of the basin and extends into the southwestern part of the Carson River Basin (Fig. 1).

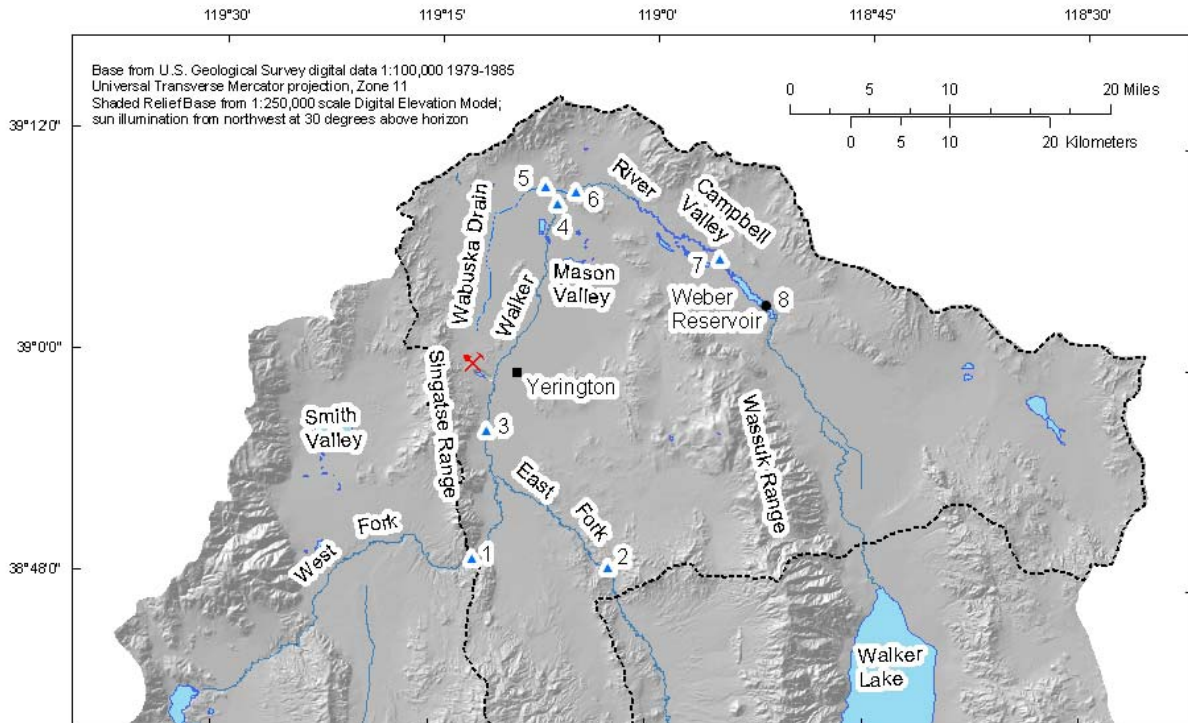


Figure 2. Location of sample-collection sites, site number (table 1; bottom-sediment site: ▲2; Weber Reservoir core site: ●8), and of Yerington copper mine site (×), northern Walker River Basin, west-central Nevada.

Geologic Setting

Consolidated rocks in the Walker River basin range in age from Triassic to Quaternary and primarily consist of quartz monzonite, granodiorite, basalt, rhyolite, and andesite. The Singatse and Wassuk Ranges are Cenozoic fault-block structures, indicating continuity with the Sierra Nevada (Moore and Archbold, 1969, p. 3). Basin-fill deposits are unconsolidated Tertiary and Quaternary alluvial sediments that underlie the valley floors and alluvial fans near the base of mountain ranges. Valley-floor sediments are fine sand, silt, and clay alluvium and playa clay and sand, and fan sediments are primarily gravel, coarse sand, and silt with some talus material (Huxel, 1969, p. 6 and 7; plate 1). Lacustrine clay deposits at least 200-ft thick are exposed near Weber Reservoir and may extend from Walker Lake to the high-water stage of Pleistocene Lake Lahontan in Mason Valley as far south as Yerington (Moore and Archbold, 1969, p. 15; Reheis, 1999). The distribution of these geologic units is generalized in figure 3 (modified from Ludington and others, 2005) to show basin fill and upland alluvium, volcanic rocks, sandstone, granitic rocks and metamorphic rocks.

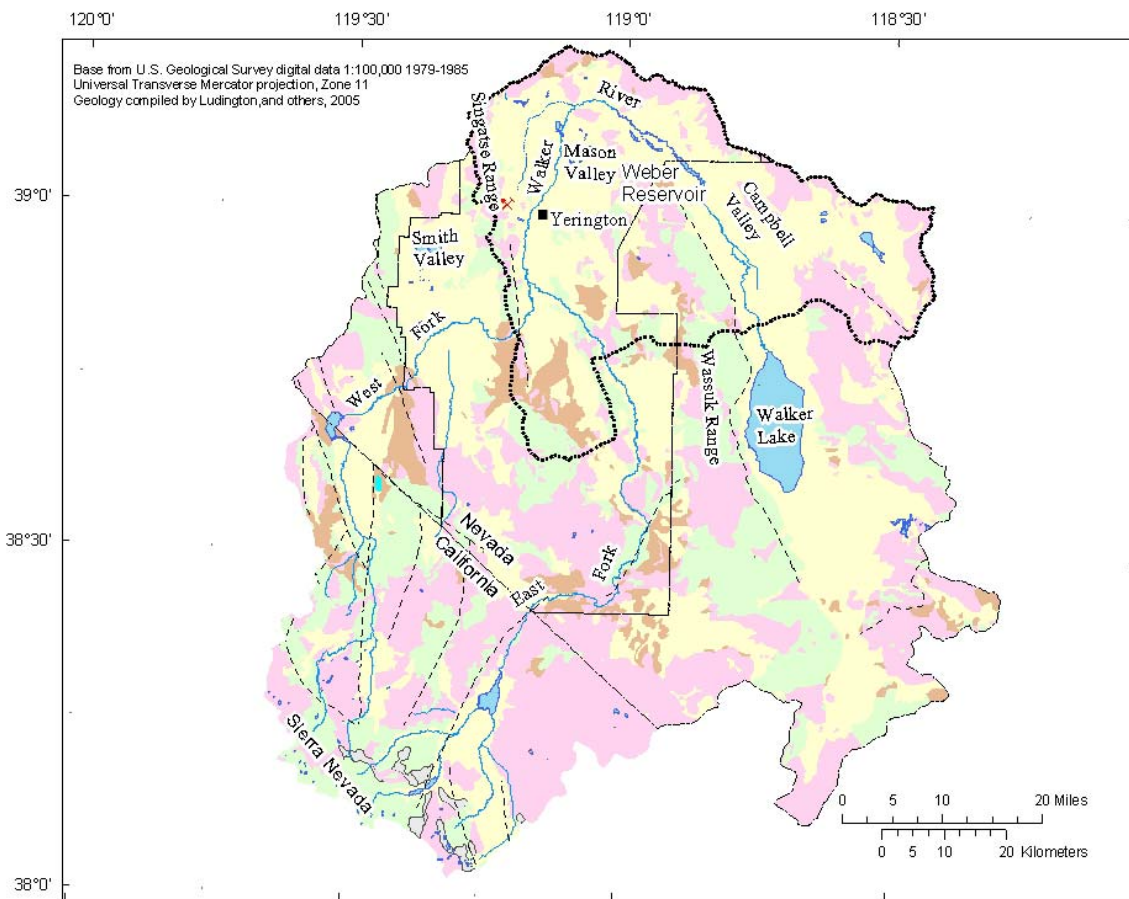


Figure 3. Generalized geologic units (basin fill and upland alluvium of Tertiary and Quaternary age, yellow; volcanic rocks of Triassic through Quaternary age, pink; sandstone of Tertiary age, orange; granitic rocks of Jurassic and Cretaceous age, green; metamorphic rocks of Ordovician through Triassic age, grey), faults (dashed black), and location of Yerington copper mine site (x), Walker River Basin, Nevada and California. (Modified from Ludington and others, 2005)

Mining Activities in the Walker River Basin

Prospecting and mining in the Walker River Basin began in the mid-1800s by individuals seeking gold and silver deposits similar to those found at the Mother Lode in California that triggered the gold rush in 1849, and later to those found at the Comstock Lode in Virginia City, Nevada (Moore and Archbold, 1969, p. 22). After 1859, numerous mining districts formed in areas surrounding the Comstock Lode, including in the Walker River Basin. Major mining districts active in the Walker River Basin during the late 1800s include Aurora (gold), Bodie (gold), and Yerington (copper), and at least nine smaller districts that mined mineral commodities including barite, coal, gypsum, iron, lead, molybdenum, nickel, silver, tin, turquoise, tungsten, uranium, and zinc (Tingley, 1992).

The Yerington mining district includes most of the Singatse Range, the northwestern Wassuk Range, and buttes protruding above Mason Valley just east of Yerington (Fig. 1; Moore and Archbold, 1969, p. 26). The district was formed in 1865, after oxidized copper ore was found in Triassic-age andesites, soda rhyolite-felsites, and limestone that had been metamorphosed by granodiorite and porphyritic quartz monzonite intrusions. Skarn and porphyry copper deposits in the district were first mined in the Singatse Range. However, the most important mineral commodity before 1900 was natural bluestone mined for copper sulfate used in the early amalgamation of silver ore from the Comstock Lode (Knopf, 1918, p. 11). By 1940, the district had earned more than \$17 million, chiefly in copper (Moore and Archbold, 1969, p.26).

The Anaconda Minerals Company began exploring the granitic rock of the Singatse Range around 1942 and began mining operations at the site 10 years later. Copper oxide ore was processed at its mill in the town of Weed Heights (Fig. 1), and, between 1953 and 1965, the mine produced more than 800 million pounds of copper worth more than \$255 million (Moore and Archbold, 1969, p. 28). About 360 million tons of ore and waste rock were removed from more than 350 acres, creating an open pit that by 1978 was 800 ft deep (Seitz and others, 1982, p. 2). Arimetco Inc. purchased the mine site in 1989 to mill low-grade copper ore stockpiles and tailings until 1996. Arimetco Inc. received permits from the State of Nevada in 1994 to develop other copper deposits, which outcrop northeast of Yerington and have an estimated copper oxide reserve of 97 million tons containing 21 percent copper (Price, 1995, p. 19).

Hydrologic Setting

The East and West Forks of the Walker River flow in a northeasterly direction into Mason Valley; there they converge into the main stem of the Walker River, which flows northward into Campbell Valley and then turns south to ultimately flow into Walker Lake (Fig. 1). During 1939–93, annual runoff averaged 133,000 acre-ft from the West Walker River (site 1); 105,000 acre-ft from the East Walker River (site 2); and 128,000 acre-ft from the main stem Walker River at Wabuska (site 6; Thomas, 1995). The 110,000 acre-ft difference between combined inflow to the main stem Walker River and the station at Wabuska (Fig. 2, site 6) represents streamflow that had evaporated, was transpired by riparian vegetation and agricultural crops, and had infiltrated to recharge ground water beneath the riverbed (Thomas, 1995).

The principal use of water in the Walker River Basin is for irrigation of crops and pastures. Extensive networks of mostly unlined canals, ditches, and drains have been constructed to convey water from the river to irrigate crops and to return excess water from fields back to the river. Several reservoirs, including Bridgeport and Weber Reservoirs, and Topaz Lake were constructed to store snowmelt runoff for release during the drier growing season. Wabuska Drain originates at the base of tailings from the Yerington copper mine and intermittently discharges to the Walker River (Brown and Caldwell, 2003). Weber Reservoir is the only reservoir on the main stem of the Walker River. The reservoir was constructed in 1934; it has a maximum storage capacity of 10,700 acre-ft and surface area of 900 acres (Stockton and others, 2004, p. 172).

The arid valley floors and semiarid mountains are the result of the rain shadow effects of the Sierra Nevada, which intercept moisture in wet storms. However, runoff in ephemeral channels in northern Mason Valley occasionally results in flash floods (Huxel, 1969, p. 21-22).

Ground water in Mason Valley is withdrawn primarily from the basin-fill deposits, which contain more than 1 million acre-ft of water in the uppermost 50 ft of saturated sediments (Huxel, 1969, p. 5). Ground water is often less than 5 ft below land surface near the river and increases with distance from the river to more than 100 ft below land surface beneath alluvial-fan deposits (Huxel, 1969, p. 13–15). Near the river, ground water can both discharge to the river and receive recharge from the river, depending on the river stage and water-table altitude.

METHODS

Selection of Sampling Sites

Bottom-sediment samples were collected from six sites along the Walker River, one site on the Wabuska Drain, and one site in Weber Reservoir. The sites and the rationale for their selection are listed in table 1, and their locations are shown in figure 2. Sites 1 through 3 were selected to characterize the chemical quality of bottom sediment in the river upstream of the Yerington mine site and sites 4 through 7 were selected to characterize the quality of sediment downstream from the mine site. Site 5 is on Wabuska Drain, an agricultural drain that intercepts shallow ground water downgradient from mine tailings, waste rock, heap leach pads, and lined and unlined process-fluid and evaporation ponds. Site 8 is in Weber Reservoir and was selected for collection of sediment cores to reconstruct the history of the chemical quality of sediment. The preferred coring location was near the dam on the thalweg of the reservoir, where sediment typically is homogeneous, fine-grained lacustrine sediment.

Table 1. Sampling sites for collection of bottom sediment and sediment cores, Walker River Basin, west-central Nevada, 2005.

[Sampling sites are assigned unique identification numbers on basis of geographic location. Eight-digit numbers are station numbers that follow "downstream order system": First two digits, or part number, refer to drainage basin, and the following six digits are downstream-order number, which is assigned according to geographic location of site in drainage basin. Stations with higher numbers are downstream from stations with lower numbers.]

Site number (fig. 2)	U.S. Geological Survey site identification	Site description	Rationale for sampling
1	10300000	West Fork Walker River near Hudson, Nev.	Background site upstream of mine
2	10293500	East Fork Walker River above Strosnider Ditch, near Mason, Nev.	Background site upstream of mine
3	10300600	Walker River near Mason, Nev.	Background site upstream of mine
4	10301497	Walker River above confluence of Perk and Joggle Slough, Nev.	Site is downstream from the mine and upstream of Wabuska Drain
5	10301495	Wabuska Drain upstream from Walker River, Nev.	Site is on drain carrying water from mine area to the Walker River
6	10301500	Walker River near Wabuska, Nev.	Site is downstream from mine and Wabuska Drain
7	10301600	Walker River above Weber Reservoir near Schurz, Nev.	Site is upstream of Weber Reservoir on tribal land
8	10301700	Weber Reservoir near Schurz, Nev. (near dam)	Cores collected to document accumulation of sediment and trace elements since reservoir storage in 1934

Collection of Bottom-Sediment Samples

Bottom-sediment samples were collected from sites 1 through 7 (Fig. 2; table 1) following protocols described by Shelton and Capel (1994). Representative samples were obtained by compositing samples from the upper 0.5 to 1 in. of sediment from 5 to 10 depositional areas at each site. Samples were collected using a Teflon spatula to transfer the sediment into a glass bowl. Composite samples were sieved through a pre-cleaned 62.5- μm (micron) nylon mesh and the resulting fine-grained fraction placed in an acid-cleaned jar.

Collection of Reservoir-Sediment Core

Two sediment cores were collected from Weber Reservoir using a boat equipped with a gravity coring system. The coring system has a polycarbonate barrel designed to avoid contamination by metals. The first core was collected on January 13, 2005, when the reservoir had an ice layer that restricted access to the preferred sampling location. This core was collected less than 500 ft from the southeastern shore of the reservoir and 2,000 ft from the dam. A 2.1-ft length of core was retrieved, packed in dry ice, and returned to the USGS laboratory in Carson City, Nev., where 38 subsamples (0.6–0.8 in. long) were extruded into individual sample jars for laboratory analysis.

The second core was collected on June 23, 2005, using the coring system described previously and a boat equipped with a depth sounder and a Global Positioning System. In addition, two sediment samples were collected from an adjacent location using a Russian peat borer-type sampler attached to rigid aluminum rods hand driven to a sediment depth that was deeper than the depth penetrated by the gravity coring apparatus. The second core was collected near Weber Dam, at the deepest point of a transect parallel to the dam. A 4.0-ft length of core was retrieved using the gravity coring device and two additional samples were collected using a Russian peat borer-type sampler from an adjacent location from depths 4.2 to 4.6 ft beneath the sediment surface. The core was taken to shore where it was suspended vertically using a tripod, and 13 subsamples (3–4 in. long) were extruded into polyethylene sample bags. The sediment collected with the Russian peat borer was divided into two 10-in. long samples and placed in separate polyethylene bags.

Laboratory Analyses

Sediment samples from the Walker River, Wabuska Drain, and Weber Reservoir were analyzed for trace elements, total and organic carbon, and selected major ions at the USGS Geologic Division laboratory in Lakewood, Colorado, using methods described by Arbogast (1996) and Taggart (2002). Radium-226 (^{226}Ra) and radium-228 (^{228}Ra) activities were determined by gamma spectrometry and gross alpha (gross α) and gross beta (gross β) radioactivities were determined by gas-flow proportional counting (Melissa Mannion, Eberline Analytical Services, written commun., 2005). Table 2 lists the constituents analyzed and their laboratory reporting levels. Cesium-137 (^{137}Cs) activity in selected sediment core subsamples collected from Weber Reservoir was measured using a high-resolution germanium well detector and a multichannel analyzer. The activity of ^{137}Cs was quantified using an energy-efficiency calibration curve from a suite of analytical-grade radioisotope standards that encompass gamma emission energies from 46 to 1,460 keV (103 electronvolts), which brackets energy emitted by ^{137}Cs (Daniel Engstrom, Science Museum of Minnesota, written commun., May 2005).

Table 2. Analytical reporting limits for constituents detected in bottom-sediment and reservoir-sediment core samples, northern Walker River Basin, west-central Nevada.

[µg/g, micrograms per gram; pct., percent; pCi/g, picocuries per gram]

Analyte	Laboratory reporting level (dry weight)	Analyte	Laboratory reporting level (dry weight)
Aluminum	8 µg/g	Molybdenum	0.50 µg/g
Antimony	0.02 µg/g	Nickel	2 µg/g
Arsenic	0.1 µg/g	Niobium	4 µg/g
Barium	0.5 µg/g	Phosphorus	0.005 pct
Beryllium	0.001 µg/g	Potassium	0.005 pct
Bismuth	0.005 µg/g	Rubidium	0.01
Cadmium	0.003 µg/g	Scandium	2 µg/g
Calcium	20 µg/g	Silver	0.1 µg/g
Carbon, total	0.01 pct.	Sodium	0.005 pct
Carbon, inorganic	0.01 pct.	Strontium	2 µg/g
Carbon, organic	0.01 pct.	Sulfur	0.05 pct
Cerium	1 µg/g	Tantalum	1 µg/g
Cesium	0.003 µg/g	Thallium	1 µg/g
Chromium	1 µg/g	Thorium	1 µg/g
Cobalt	1 µg/g	Titanium	0.005 pct
Copper	1 µg/g	Uranium	0.1 µg/g
Gallium	1 µg/g	Vanadium	2 µg/g
Iron	0.005 pct	Yttrium	1 µg/g
Lanthanum	1 µg/g	Zinc	2 µg/g
Lead	1 µg/g	Radium-226	0.8 pCi/g
Lithium	1 µg/g	Radium-228	0.8 pCi/g
Magnesium	0.005 pct	Gross alpha activity	6 pCi/g
Manganese	4 µg/g	Gross beta activity	3 pCi/g
Mercury	0.02 µg/g		

CONSTITUENTS OF CONCERN

Constituents of concern are identified by the U.S. Environmental Protection Agency to be hazardous substance(s) as defined by section 101(14) of CERCLA. Constituents of concern for the Yerington copper mine site (table 3) were measured in samples from the Yerington copper mine site at levels that are greater than concentrations measured in samples collected from locations unaffected by mining operations (James Sickles, U.S. Environmental Protection Agency Remedial Project Manager, written comm., May 2006) or were identified as being potentially toxic or carcinogenic. Gross alpha and gross beta radioactivities, which are measures of radiation emitted as alpha and beta particles, respectively, also are of concern. Published advisory concentrations and activities, that is concentrations and activities of constituents in bottom sediment that have been determined to be potentially toxic to aquatic life (Ingersoll and others, 2000; Persaud and others, 1993; S.D. Luftig and S.D. Page, U.S. Environmental Protection Agency, Directive no. 9200.4-35P, written commun., April 11, 2000) also are listed in table 3. Concentrations at or exceeding advisory levels were not detected for aluminum, beryllium, boron, molybdenum, sulfate, thorium, uranium, or gross alpha and gross beta radioactivity.

CHARACTERISTICS OF RIVER AND RESERVOIR SEDIMENT SAMPLES

Results of analyses of bottom-sediment and reservoir-sediment core samples are listed in tables 4 (concentrations) and 5 (radioactivities) and summarized statistically in table 6. The bottom-sediment data represent the chemical quality of sediment that was moving within the river system in 2005. Sediment core data represent a chronologic history of sediment quality deposited in Weber Reservoir. Cores of lake sediment have been used to determine historical deposition of contaminants in locations throughout the United States (for example, Van Metre and others, 2004), including Walker Lake, Nevada (Seiler and others, 2004).

Table 3. Advisory concentrations and activities for constituents of concern detected in sediment at Yerington copper mine, in the northern Walker Basin, west-central Nevada.

[Constituents were defined as hazardous substances on the basis of section 101(14) of Comprehensive Environmental Response, Compensation, and Liability Act (CERCLA), 42 United States Code § 9601(14). µg/g, micrograms per gram; –, no advisory available for constituent in sediment; pCi/g, picocuries per gram]

Constituent of concern	Advisory concentration or activity (dry weight, in µg/g, except as indicated)
Aluminum	–
Arsenic	¹ 33
Beryllium	–
Boron	–
Cadmium	¹ 4.98
Chromium	¹ 111
Copper	¹ 149
Iron	² 21,200
Lead	¹ 128
Manganese	² 460
Mercury	¹ 1.06
Molybdenum	–
Nickel	¹ 48.6
Radium-226	³ 5 pCi/g
Radium-228	³ 5 pCi/g
Sulfate	–
Thorium	–
Uranium	–
Zinc	¹ 459
Gross alpha radioactivity	–
Gross beta radioactivity	–

¹ Ingersoll and others, 2000.

² Persaud, and others, 1993.

³ S.D. Luftig and S.D. Page, U.S. Environmental Protection Agency, Directive no. 9200.4-35P, written commun., April 11, 2000. Advisory activity is additive (radium-226+radium-228) and is increased to 15 pCi/g for subsurface soil samples.

Table 4. Concentrations of constituents in bottom-sediment samples from Walker River, Wabuska Drain, and Weber Reservoir, northern Walker River Basin, Nevada, 2005

[ft, feet; μm , micron; <, actual value is less than value shown]

Site no. (fig. 2)	Sample date	Depth, (ft below sediment surface)	Estimated period of sedimentation	Fraction	Concentration, dry weight, in micrograms per gram, except as indicated							
					Aluminum	Antimony	Arsenic	Barium	Beryllium	Bismuth	Cadmium	Calcium
1	04/26/2005	0–.07	2004-2005	<63 μm	79,000	1.6	19	1,000	2.0	0.33	0.22	23,000
2	04/28/2005	0–.07	2004-2005	<63 μm	85,000	1.9	17	1,000	2.2	0.45	0.16	24,000
3	04/26/2005	0–.07	2004-2005	<63 μm	79,000	1.7	22	1,000	2.1	0.42	0.22	20,000
4	04/25/2005	0–.07	2004-2005	<63 μm	78,000	1.6	25	900	2.1	0.44	0.23	18,000
5	04/22/2005	0–.07	2004-2005	<63 μm	78,000	1.5	19	1,000	2.2	0.36	0.19	24,000
6	04/22/2005	0–.07	2004-2005	<63 μm	81,000	1.6	24	1,000	2.3	0.45	0.24	19,000
7	04/21/2005	0–.07	2004-2005	<63 μm	82,000	1.6	33	1,000	2.3	0.42	0.17	20,000
8	06/23/2005	0–.26	2001-2005	total	87,000	2.0	18	920	3.2	0.64	0.25	19,000
8	06/23/2005	.26–.59	1996-2001	total	95,000	2.2	28	1,000	3.3	0.58	0.22	41,000
8	06/23/2005	.59–.92	1990-1996	total	96,000	2.3	22	990	3.3	0.68	0.22	19,000
8	06/23/2005	.92–1.2	1984-1990	total	94,000	2.4	26	900	3.4	0.72	0.24	22,000
8	06/23/2005	1.2–1.6	1979-1984	total	86,000	1.9	23	800	2.8	0.57	0.20	22,000
8	06/23/2005	1.6–1.9	1973-1979	total	87,000	2.0	22	820	2.9	0.59	0.20	22,000
8	06/23/2005	1.9-2.2	1968-1973	total	96,000	2.3	25	890	3.0	0.66	0.22	24,000
8	06/23/2005	2.2–2.6	1962-1968	total	91,000	2.1	26	810	3.0	0.64	0.23	25,000
8	06/23/2005	2.6–2.9	1957-1962	total	110,000	2.5	32	1,000	3.9	0.77	0.27	36,000
8	06/23/2005	2.9–3.2	1951-1957	total	91,000	2.2	24	870	3.3	0.66	0.24	23,000
8	06/23/2005	3.2–3.5	1946-1951	total	99,000	2.2	23	1,000	3.3	0.60	0.26	25,000
8	06/23/2005	3.5–3.9	1940-1946	total	89,000	2.2	24	910	3.1	0.67	0.22	28,000
8	06/23/2005	3.9–4.2	1935-1940	total	90,000	3.5	25	990	3.4	0.72	0.25	24,000
8	06/23/2005	4.7–5.0	Pre-reservoir	total	82,000	2.2	24	850	3.3	0.61	0.22	25,000

Table 4. Concentrations of constituents in bottom-sediment samples from Walker River, Wabuska Drain, and Weber Reservoir, northern Walker River Basin, Nevada, 2005--Continued

Site no. (fig. 2)	Concentration, dry weight, in micrograms per gram, except as indicated												
	Depth, (ft below sediment surface)	Carbon, total (percent)	Carbon, inorganic (percent)	Carbon, organic (percent)	Cerium	Cesium	Chromium	Cobalt	Copper	Gallium	Iron	Lanthanum	Lead
1	0-.07	1.6	0.08	1.6	74	14	49	15	49	19	42,000	34	21
2	0-.07	1.1	0.09	1.0	83	9	44	15	43	20	42,000	39	21
3	0-.07	1.8	0.06	1.8	73	11	40	15	47	19	40,000	33	21
4	0-.07	2.1	0.03	2.1	73	12	38	14	55	20	42,000	33	21
5	0-.07	0.94	0.12	0.82	83	11	45	15	48	19	44,000	38	19
6	0-.07	2.0	0.05	2.0	73	12	40	14	53	20	42,000	34	21
7	0-.07	1.4	0.04	1.3	81	11	43	15	51	20	44,000	38	20
8	0-.26	1.3	0.05	1.2	86	16	39	19	66	24	54,000	44	27
8	.26-.59	1.4	0.52	0.90	86	15	41	20	61	25	52,000	43	28
8	.59-.92	0.90	0.04	0.86	94	18	44	20	71	25	58,000	48	28
8	.92-1.2	1.2	0.13	1.1	93	18	44	20	74	26	59,000	47	28
8	1.2-1.6	1.2	0.2	1.0	80	16	68	17	66	22	53,000	40	24
8	1.6-1.9	1.2	0.2	1.0	83	16	40	17	67	23	53,000	42	25
8	1.9-2.2	1.2	0.22	1.0	88	17	44	19	73	25	58,000	44	27
8	2.2-2.6	1.3	0.28	1.0	83	17	42	18	70	24	56,000	42	26
8	2.6-2.9	1.4	0.34	1.0	107	20	52	23	84	30	70,000	54	31
8	2.9-3.2	1.2	0.18	1.0	91	18	44	19	71	25	58,000	46	27
8	3.2-3.5	0.98	0.18	0.80	92	17	42	20	69	25	57,000	46	26
8	3.5-3.9	1.2	0.32	0.86	89	17	42	18	66	23	55,000	45	25
8	3.9-4.2	1.2	0.13	1.1	93	17	43	19	62	24	52,000	47	27
8	4.7-5.0	1.3	0.28	0.98	83	15	38	17	61	22	50,000	42	24

Table 4. Concentrations of constituents in bottom-sediment samples from Walker River, Wabuska Drain, and Weber Reservoir, northern Walker River Basin, Nevada, 2005--Continued

Site no. (fig. 2)	Concentration, dry weight, in micrograms per gram, except as indicated												
	Depth, (ft below sediment surface)	Lithium	Magnesium	Manganese	Mercury	Molybdenum	Nickel	Niobium	Phosphorus	Potassium	Rubidium	Scandium	Silver
1	0-.07	41	13,000	1,200	0.04	1.4	23	15	1,400	1,400	80	13	<3
2	0-.07	35	12,000	870	0.50	1.7	22	19	1,300	1,300	88	13	<3
3	0-.07	39	12,000	1,500	0.32	1.6	22	15	1,300	1,300	80	12	<3
4	0-.07	42	13,000	1,400	0.31	1.9	23	15	1,300	1,300	81	13	<3
5	0-.07	50	14,000	1,000	0.04	2.3	23	16	1,400	1,400	96	13	<3
6	0-.07	42	14,000	2,000	0.26	1.6	23	15	1,400	1,400	86	13	<3
7	0-.07	41	12,000	1,700	0.29	1.8	23	17	1,400	1,400	90	13	<3
8	0-.26	67	17,000	1,370	0.34	3.4	25	17	1,200	24,000	140	17	<3
8	.26-.59	63	16,000	1,300	0.30	5.4	25	17	1,200	25,000	130	17	<3
8	.59-.92	71	19,000	1,500	0.43	2.9	27	18	1,300	25,000	140	18	<3
8	.92-1.2	74	18,000	1,500	0.43	3.5	28	18	1,300	24,000	140	19	<3
8	1.2-1.6	66	17,000	1,400	0.33	3.0	38	16	1,200	21,000	120	17	<3
8	1.6-1.9	66	17,000	1,400	0.43	3.0	25	16	1,200	22,000	120	17	<3
8	1.9-2.2	69	19,000	1,400	0.50	3.7	27	18	1,400	23,000	130	19	<3
8	2.2-2.6	63	18,000	1,500	0.32	3.4	27	17	1,300	22,000	120	18	<3
8	2.6-2.9	83	22,000	1,900	0.30	4.6	33	20	1,600	27,000	160	23	<3
8	2.9-3.2	72	19,000	1,600	0.34	4.5	28	17	1,300	23,000	140	19	<3
8	3.2-3.5	68	20,000	1,600	0.28	3.3	26	18	1,300	26,000	150	19	<3
8	3.5-3.9	71	18,000	1,500	0.42	5.3	26	17	1,300	24,000	140	18	<3
8	3.9-4.2	71	16,000	1,400	1.0	7.7	25	17	1,200	25,000	140	17	<3
8	4.7-5.0	65	16,000	1,400	0.47	4.8	24	16	1,200	22,000	130	16	<3

Table 4. Concentrations of constituents in bottom-sediment samples from Walker River, Wabuska Drain, and Weber Reservoir, northern Walker River Basin, Nevada, 2005--Continued

Site no. (fig. 2)	Concentration, dry weight, in micrograms per gram, except as indicated											
	Depth, (ft below sediment surface)	Sodium	Strontium	Sulfur (percent)	Tantalum	Thallium	Thorium	Titanium	Uranium	Vanadium	Yttrium	Zinc
1	0-.07	17,000	540	0.07	1.1	0.60	16	6,600	6.5	120	20	100
2	0-.07	19,000	530	0.08	1.4	0.71	18	6,700	5.6	130	22	99
3	0-.07	16,000	500	0.11	1.1	0.66	14	6,000	5.6	110	18	95
4	0-.07	13,000	430	0.13	1	0.66	15	5,800	6.5	110	18	100
5	0-.07	18,000	560	0.08	1.1	0.70	17	6,700	6.1	120	21	110
6	0-.07	14,000	460	0.11	0.95	0.66	15	5,900	5.8	120	19	100
7	0-.07	16,000	500	0.08	1.2	0.70	17	6,600	6.2	130	21	100
8	0-.26	12,000	440	0.14	1.2	0.91	20	5,100	10	140	26	130
8	.26-.59	17,000	620	0.19	1.1	0.91	20	5,000	10	140	26	120
8	.59-.92	13,000	450	0.19	1.2	0.97	22	5,600	9.0	150	27	140
8	.92-1.2	12,000	450	0.26	1.3	0.96	22	5,400	10	150	27	140
8	1.2-1.6	10,000	400	0.25	1.1	0.82	19	4,900	8.0	140	24	130
8	1.6-1.9	11,000	410	0.20	1.1	0.84	19	4,900	9.0	140	24	130
8	1.9-2.2	11,000	430	0.23	1.3	0.91	22	5,300	9.0	150	26	140
8	2.2-2.6	10,000	410	0.24	1.3	0.86	20	5,000	9.0	140	25	130
8	2.6-2.9	13,000	550	0.28	1.4	1.0	26	6,300	11	180	32	170
8	2.9-3.2	11,000	440	0.22	1.2	0.91	22	5,400	11	150	27	140
8	3.2-3.5	14,000	480	0.19	1.2	0.94	22	5,600	9.0	150	28	140
8	3.5-3.9	12,000	460	0.21	1.2	0.90	21	5,200	12	150	26	130
8	3.9-4.2	14,000	510	0.29	1.2	0.98	22	5,100	12	140	26	130
8	4.7-5.0	12,000	450	0.23	1.1	0.87	20	4,800	11	130	26	120

Table 5. Activities of radioactive constituents in bottom-sediment samples from Walker River, Wabuska Drain, and Weber Reservoir, northern Walker River Basin, Nevada, 2005

Site no. (fig. 2)	Activity, dry weight, in picocuries per gram				
	Depth, (ft below sediment surface)	Gross alpha radioactivity	Gross beta radioactivity	Radium-226	Radium-228
1	0–.07	24	32	0.9	1.1
2	0–.07	27	33	1.5	2.0
3	0–.07	29	28	1.3	1.5
4	0–.07	21	32	1.3	1.7
5	0–.07	16	25	1.0	1.1
6	0–.07	26	30	1.0	1.3
7	0–.07	31	30	1.1	1.3
8	0–.26	24	32	1.4	2.0
8	.26–.59	26	38	1.7	2.1
8	.59–.92	21	40	1.4	2.1
8	.92–1.2	24	36	1.8	2.4
8	1.2–1.6	27	37	1.4	2.0
8	1.6–1.9	30	32	1.6	1.8
8	1.9–2.2	32	33	2.1	2.5
8	2.2–2.6	22	36	1.2	2.2
8	2.6–2.9	20	31	1.3	1.9
8	2.9–3.2	17	35	1.4	2.1
8	3.2–3.5	28	43	1.1	1.4
8	3.5–3.9	24	43	1.1	1.6
8	3.9–4.2	23	32	1.2	1.6
8	4.7–5.0	23	38	1.3	1.9

Table 6. Statistical summary of concentrations and activities of constituents in bottom sediment and Weber Reservoir sediment samples, northern Walker River Basin, Nevada, 2005

[Concentrations and activity values are rounded. pct., percent; pCi/g, picocuries per gram; <, actual value is less than value shown]

Constituent	Concentration (micrograms per gram, dry weight, except as indicated)							
	Stream-bottom sediment samples				Weber Reservoir sediment-core samples			
	<i>Maximum</i>	<i>Minimum</i>	<i>Median</i>	<i>Mean</i>	<i>Maximum</i>	<i>Minimum</i>	<i>Median</i>	<i>Mean</i>
Aluminum	85,000	78,000	79,000	80,000	110,000	82,000	91,000	92,000
Antimony	1.9	1.5	1.6	1.6	3.5	1.9	2.2	2.3
Arsenic	33	17	22	23	32	18	24	24
Barium	1,100	910	1,000	1,000	1,000	800	910	920
Beryllium	2.3	2.0	2.2	2.2	3.9	2.8	3.3	3.2
Bismuth	0.45	0.33	0.42	0.41	0.77	0.57	0.65	0.65
Cadmium	0.24	0.16	0.22	0.20	0.27	0.20	0.23	0.23
Calcium	24,000	18,000	20,000	21,000	41,000	19,000	24,000	25,000
Carbon, total (pct.)	2.1	0.94	1.6	1.6	1.4	0.90	1.2	1.2
Carbon, inorganic (pct.)	0.12	0.03	0.06	0.07	0.52	0.04	0.20	0.22
Carbon, organic (pct.)	2.1	0.94	1.6	1.6	1.2	0.8	1.0	0.99
Cerium	83	73	74	77	110	80	88	89
Cesium	14	8.6	11	11	20	14	17	17
Chromium	48	38	43	43	68	38	42	44
Cobalt	15	14	15	15	22	17	19	19
Copper	55	43	48	49	84	61	68	69
Gallium	20	19	20	20	30	22	24	25
Iron	44,000	40,000	42,000	42,000	70,000	50,000	55,000	56,000
Lanthanum	39	33	34	36	54	40	44	45
Lead	21	19	21	20	31	24	27	26
Lithium	50	35	41	41	83	63	68	69
Magnesium	14,000	12,000	13,000	13,000	22,000	16,000	18,000	18,000
Manganese	2,000	860	1,400	1,400	1,900	1,300	1,400	1,500
Mercury	0.50	0.04	0.29	0.25	1.0	0.28	0.38	0.42
Molybdenum	2.3	1.4	1.7	1.8	7.7	2.8	3.6	4.2
Nickel	23	22	23	23	38	24	27	27
Niobium	23	15	15	16	20	16	17	17
Phosphorus	1,400	1,300	1,400	1,400	1,600	1,200	1,300	1,300
Potassium	22,000	17,000	18,000	19,000	27,000	21,000	24,000	24,000
Rubidium	96	80	86	86	160	120	140	140
Scandium	13	12	13	13	22	16	18	18

Table 6. Statistical summary of concentrations and activities (rounded) of constituents in bottom sediment and Weber Reservoir sediment samples, northern Walker River Basin, Nevada, 2005--
Continued

[Concentrations and activity values are rounded. pct., percent; pCi/g, picocuries per gram; <, actual value is less than value shown]

Constituent	Concentration (micrograms per gram, dry weight, except as indicated)							
	Stream-bottom sediment samples				Weber Reservoir sediment-core samples			
	Maximum	Minimum	Median	Mean	Maximum	Minimum	Median	Mean
Silver	<3	<3	<3	<3	<3	<3	<3	<3
Sodium	19,000	13,000	16,000	16,000	17,000	10,000	12,000	12,000
Strontium	560	430	500	500	620	400	450	460
Sulfur (pct.)	0.13	0.07	0.08	0.09	0.29	0.14	0.23	0.22
Tantalum	1.4	0.95 ^e	1.1	1.1	1.4	1.0	1.2	1.2
Thallium	0.71 ^e	0.60 ^e	0.66 ^e	0.67 ^e	1.0	0.82 ^e	0.91 ^e	0.92 ^e
Thorium	18	14	16	16	26	14	21	17
Titanium	6,700	5,800	6,600	6,300	6,300	4,800	5,200	5,300
Uranium	6.5	5.6	6.1	6.0	12	8.5	10	10
Vanadium	130	110	120	120	180	130	140	150
Yttrium	22	18	20	20	32	24	26	26
Zinc	110	95	100	100	170	120	130	140
Radium-226 (pCi/g)	1.5	0.93	1.1	1.2	2.1	1.1	1.4	1.4
Radium-228 (pCi/g)	2.0	1.1	1.3	1.4	2.5	1.4	2.0	2.0
Gross alpha activity (pCi/g)	31	16	26	25	32	17	24	24
Gross beta activity (pCi/g)	33	25	30	30	43	31	36	36

^e estimated

Concentrations and activities of constituents in bottom-sediment samples collected upstream of the Yerington mine site (sites 1–3) were similar to concentrations in samples collected downstream from the mine site (sites 4–7). Average concentrations of arsenic, beryllium, copper, manganese, molybdenum, uranium, and zinc were higher in samples collected downstream from the mine site than in samples collected upstream, whereas average concentrations of aluminum, chromium, mercury, ^{226}Ra , ^{228}Ra , gross alpha and gross beta were higher in samples collected upstream of the mine (tables 4-5). But such small differences are not significant given the few samples of bottom sediment that were collected. The general similarity in the chemistry of the sediment samples is due to the distribution of minerals in source rock (Fig. 3) and the fluvial processes transporting sediment through the drainage basin.

Mean concentrations and activities of constituents in bottom-sediment samples generally were lower than those measured in reservoir-sediment subsamples, except for barium, organic and total carbon, phosphorus, sodium, and titanium. Strontium and gross alpha radioactivity averaged slightly higher in the bottom-sediment samples than in the reservoir-sediment samples, but the maximum radioactivities were slightly higher in the reservoir-bottom samples for both constituents (table 5). Advisory concentrations (table 3) for iron (21,200 $\mu\text{g/g}$ (micrograms per gram)) and manganese (460 $\mu\text{g/g}$) were exceeded in all bottom-sediment samples from both the river and the drain and from the reservoir-sediment cores (table 4). The advisory concentration for arsenic (33 $\mu\text{g/g}$) was equaled in one bottom-sediment sample collected at site 7 (Fig. 2; table 4). The concentration of mercury in one reservoir sample (1.00 $\mu\text{g/g}$) collected from pre-reservoir sediment is near the advisory concentration (1.06 $\mu\text{g/g}$; table 3). Concentrations of mercury in all samples, except two bottom-sediment samples (Fig. 2; sites 1 and 2) exceeded the concentration of mercury in sediment that may begin to adversely affect freshwater invertebrates (Ontario, Canada, sediment effects threshold concentration for freshwater invertebrates, 0.2 $\mu\text{g/g}$; Persaud and others, 1993). Elevated concentrations of mercury that have been documented in sediment, water, and biota samples from the East Fork and the main stem of the Walker River are attributed to 19th century mining of gold and silver from the Bodie and Aurora mining districts (Seiler and others, 2004, p. 14). Concentrations for the remaining constituents listed in table 3 did not equal or exceed the advisory concentration or activity.

Cesium-137 was measured in selected subsamples from the reservoir-sediment cores to determine the rate of sediment accumulation in Weber Reservoir and to estimate the timing of changes in sediment chemistry. Above-ground weapons testing first introduced ^{137}Cs to the atmosphere around 1950, and releases peaked in 1963. Thus, the earliest (deepest) detection of ^{137}Cs in a sediment profile corresponds with 1950, and the maximum ^{137}Cs activity corresponds with 1963. Identification of the pre-reservoir surface is an independent marker for 1934 because accumulation of sediment in Weber Reservoir began with its construction in 1934.

The ^{137}Cs data from the core collected from Weber Reservoir in January 2005 indicate that the core did not include the entire sediment profile and also that sediment may have been redistributed by near-shore wave action (Fig. 4). The core collected in June shows a clearly defined peak in ^{137}Cs (1963) in the subsample collected from 2.2 to 2.5 ft below the reservoir-sediment surface and an initial detection of ^{137}Cs (1950) in the subsample from 2.8 to 3.2 ft below the sediment surface (Fig. 4). One of the two sediment samples collected using the Russian peat borer-type sampler is believed to have been contaminated during retrieval. A slide hammer was used to drive the sampler into stiff pre-reservoir sediment, and the hinged cover designed to isolate the sediment sample during retrieval could not be closed completely. Assuming a linear rate of sedimentation and neglecting density compaction, sediment accumulated in Weber Reservoir at 0.07 ft/yr (foot per year) during 1934–50, 0.04 ft/yr during 1950–63, and 0.06 ft/yr during 1963–2005. An average sedimentation rate of 0.06 ft/yr was assumed for the 71-year period 1934–2005.

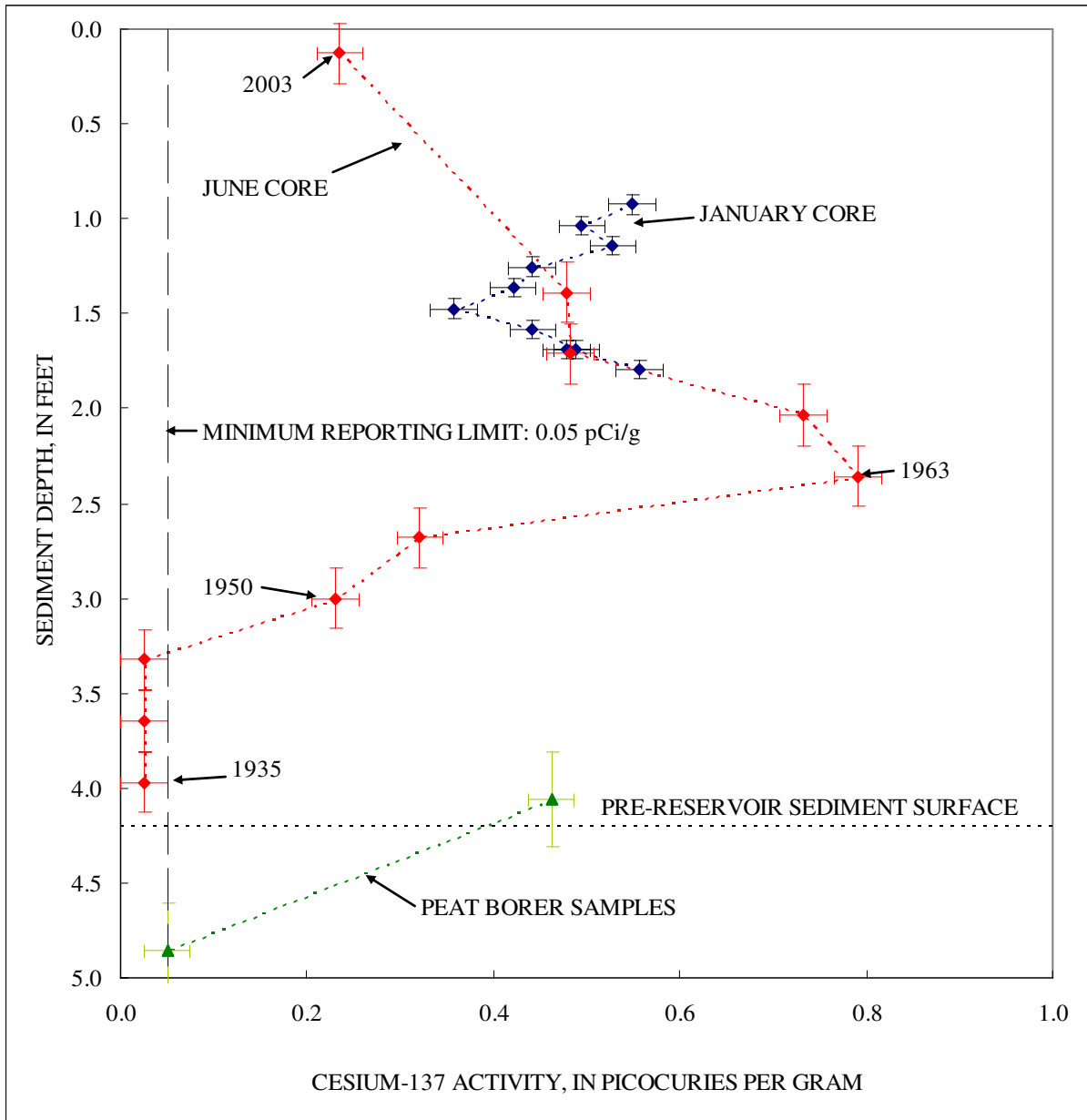


Figure 4. Distribution of cesium-137 in sediment cores collected from Weber Reservoir in the northern Walker River Basin, west-central Nevada, on January 13 and June 23, 2005.

Profiles of concentrations and activities of the 19 constituents of concern detected in the sediment core collected from Weber Reservoir are shown in figure 5. Also shown in figure 5 are estimated years of sediment deposition determined assuming a linear sedimentation rate of 0.06 ft/yr. Age estimates are plus or minus 2 to 3 years because each subsample was 0.2–0.3 ft in length. The estimated age of the subsample collected using the peat borer (4.7–5.0 ft beneath the sediment surface) is not reliable because pre-reservoir sediments were subject to the variable fluvial actions of the Walker River.

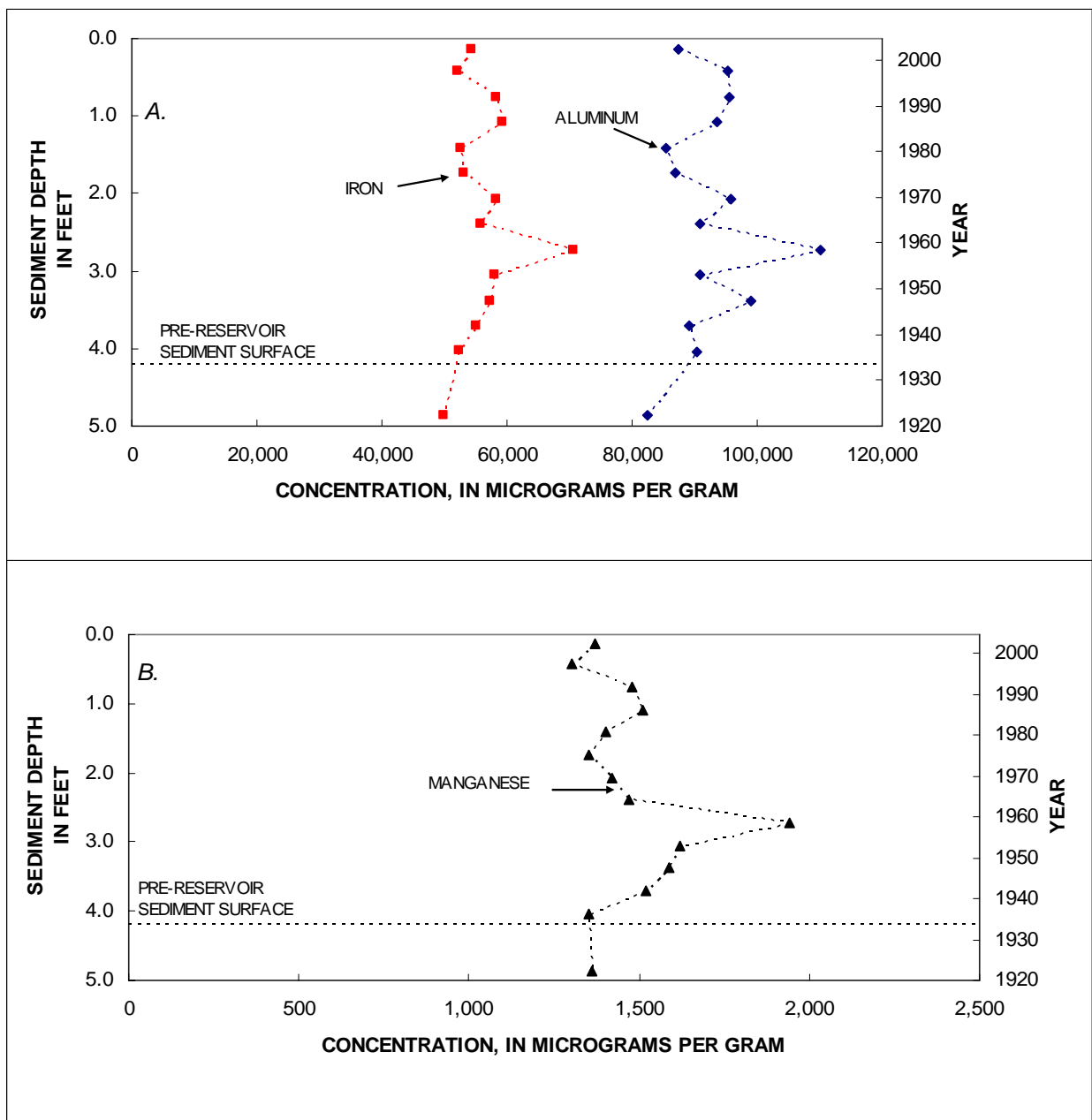


Figure 5. Concentrations or activities of constituents of concern in sediment, as a function of depth and time in Weber Reservoir, in the northern Walker River Basin, Nevada, on June 23, 2005. The year of deposition was estimated assuming a deposition rate of 0.06 foot per year and no sediment compaction. *A*, aluminum and iron. *B*, manganese. *C*, copper, lead, and zinc. *D*, arsenic, nickel, and chromium. *E*, thorium and uranium. *F*, beryllium and molybdenum. *G*, cadmium and mercury. *H*, radium-226 and radium-228. *I*, gross alpha and gross beta.

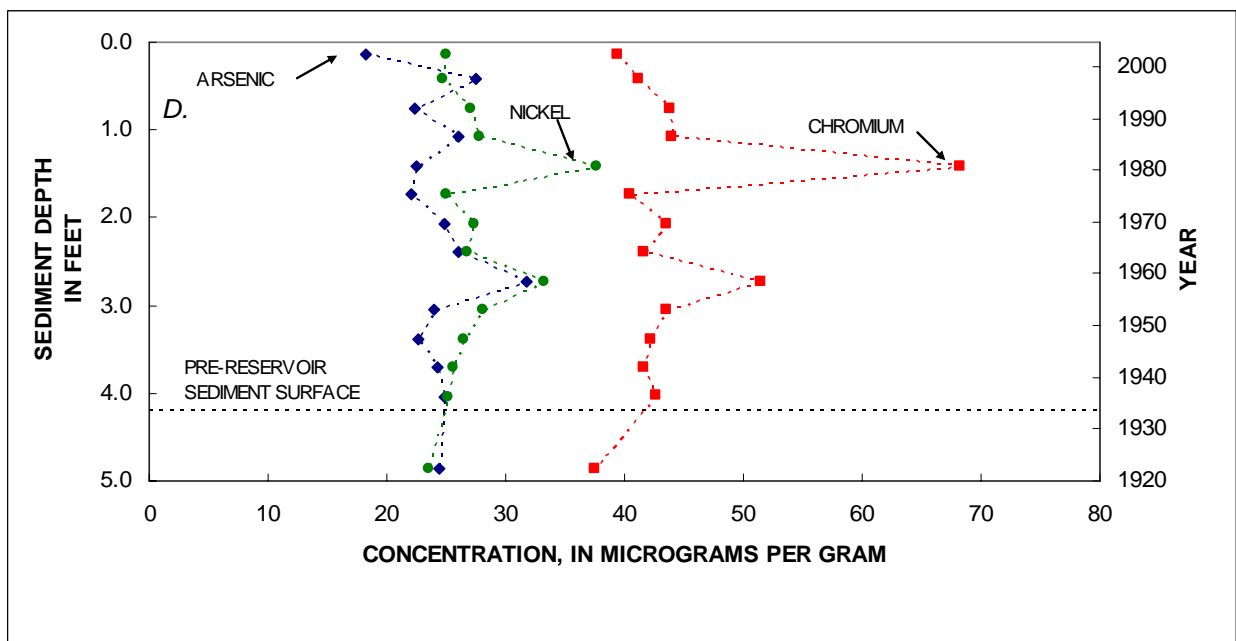
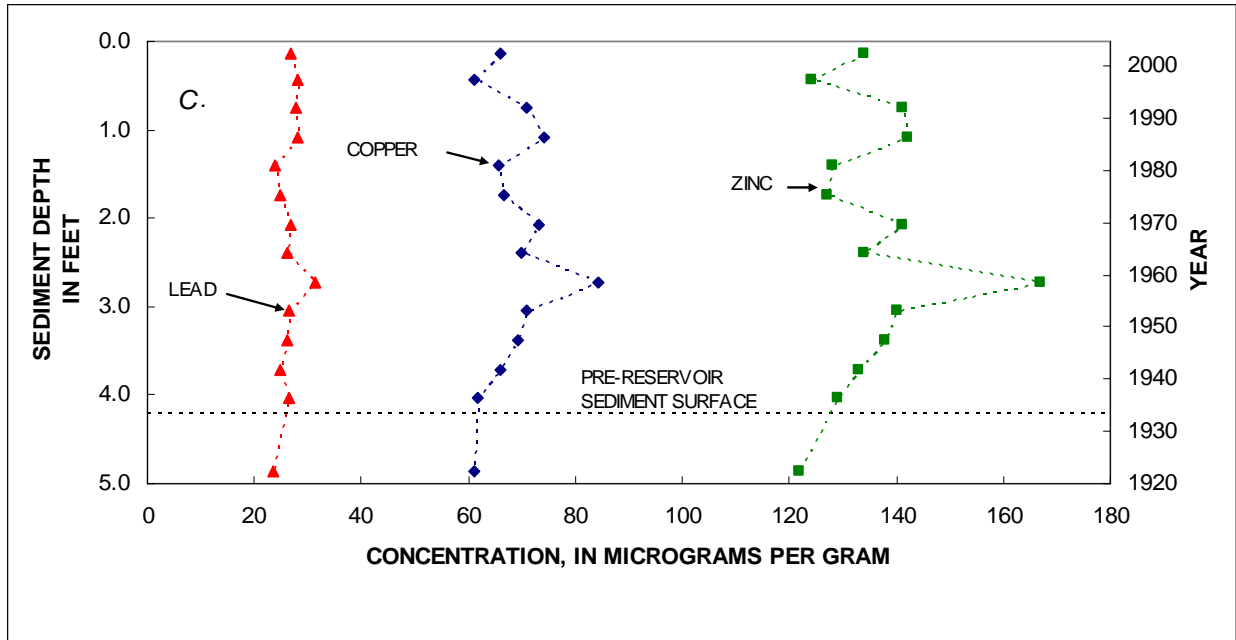


Figure 5. Concentrations or activities of constituents of concern in sediment, as a function of depth and time in Weber Reservoir, in the northern Walker River Basin, Nevada, on June 23, 2005. The year of deposition was estimated assuming a deposition rate of 0.06 foot per year and no sediment compaction--Continued.

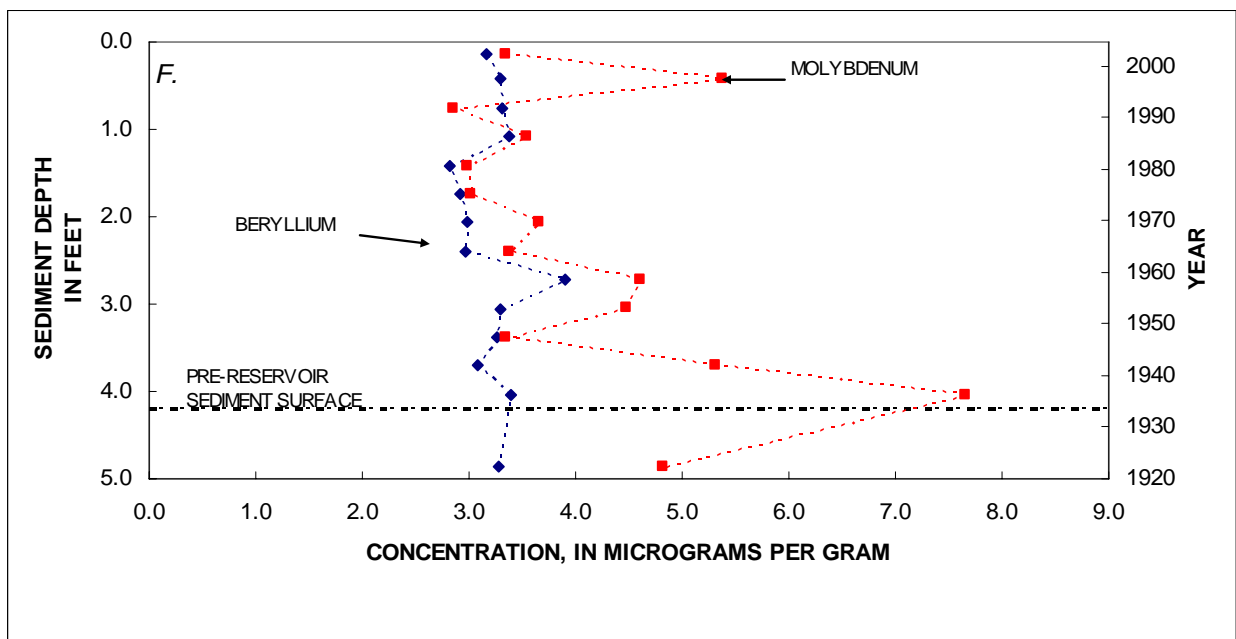
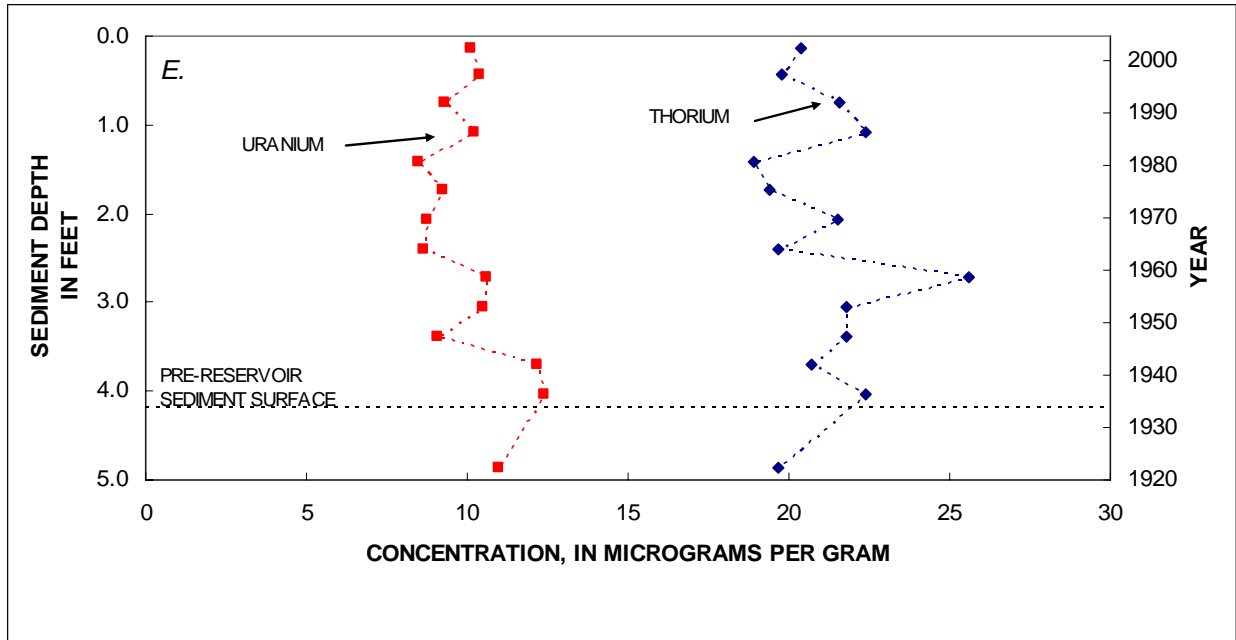


Figure 5. Concentrations or activities of constituents of concern in sediment, as a function of depth and time in Weber Reservoir, in the northern Walker River Basin, Nevada, on June 23, 2005. The year of deposition was estimated assuming a deposition rate of 0.06 foot per year and no sediment compaction--Continued.

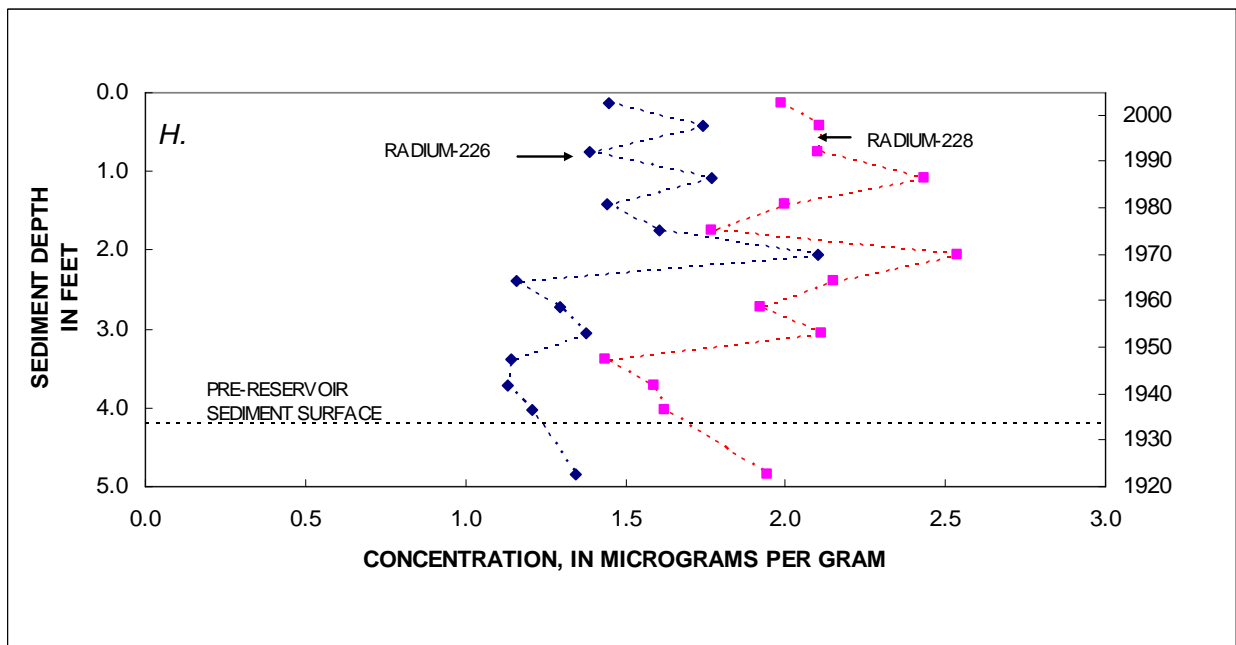
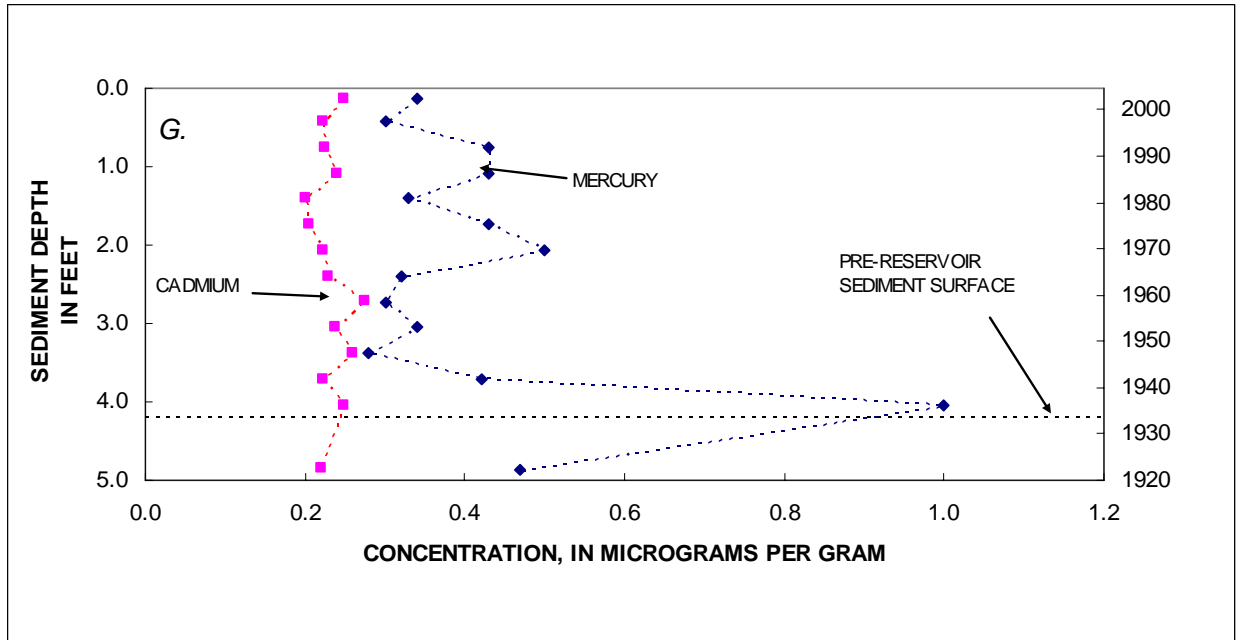


Figure 5. Concentrations or activities of constituents of concern in sediment, as a function of depth and time in Weber Reservoir, in the northern Walker River Basin, Nevada, on June 23, 2005. The year of deposition was estimated assuming a deposition rate of 0.06 foot per year and no sediment compaction--Continued

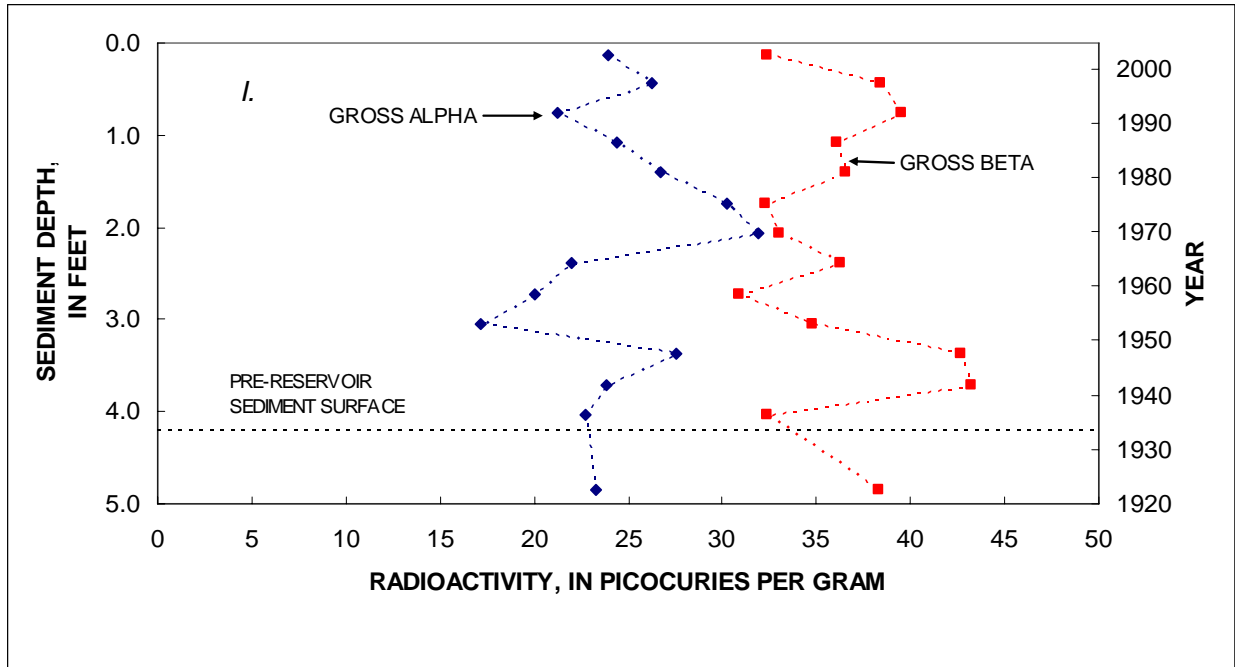


Figure 5. Concentrations or activities of constituents of concern in sediment, as a function of depth and time in Weber Reservoir, in the northern Walker River Basin, Nevada, on June 23, 2005. The year of deposition was estimated assuming a deposition rate of 0.06 foot per year and no sediment compaction--Continued.

Maximum concentrations and activities of constituents of concern in the reservoir-bottom core samples, the location in the sediment profile, and the estimated period of sedimentation for each maximum are listed in table 7. Maximum concentrations of 10 of the constituents of concern listed in table 3 (aluminum, arsenic, beryllium, cadmium, copper, iron, lead, manganese, thorium, and zinc) are from the sub-sample 2.6–2.9 ft below the sediment surface, which represents sedimentation during 1957–62 (Fig. 5). Seventeen of the 37 other analytes listed in table 2 also have maximum concentrations in this depth interval (table 4). Maximum concentrations of chromium and nickel are from the 1.2- to 1.6-ft interval that represents deposition during 1979–84 and secondary peaks were from the sub-samples representing deposition during 1957–62 (2.6–2.9 ft). Maximum concentrations of uranium are from two adjacent samples from the 3.5- to 4.2-ft interval, which represents 1935–46 deposition. Isotopes of radium (^{226}Ra and ^{228}Ra) and gross alpha radioactivity have maximum activities from the 1.9- to 2.2-ft interval representing deposition during 1968–73. The maximum gross beta radioactivity was detected in two adjacent samples from the 3.2- to 3.9-ft interval that represents deposition during 1940–51. Maximum concentrations of mercury and molybdenum were from the sub-sample deposited during 1935–40.

Table 7. Maximum concentration or activity of constituents of concern, depth of subsamples from sediment core, Weber Reservoir, northern Walker River Basin, Nevada, 2005.

[Concentrations and activity values are rounded ft, feet; µg/g, micrograms per gram; pCi/g, picocuries per gram]

Constituent	Maximum Concentration	Depth (ft)	Sedimentation period
Aluminum	110,000 µg/g	2.6-2.9	1957-1962
Arsenic	32 µg/g	2.6-2.9	1957-1962
Beryllium	3.9 µg/g	2.6-2.9	1957-1962
Cadmium	0.27 µg/g	2.6-2.9	1957-1962
Chromium	68 µg/g	1.2-1.6	1979-1984
Copper	84 µg/g	2.6-2.9	1957-1962
Iron	70,000 µg/g	2.6-2.9	1957-1962
Lead	31 µg/g	2.6-2.9	1957-1962
Manganese	1,900 µg/g	2.6-2.9	1957-1962
Mercury	1.00 µg/g	3.9-4.2	1935-1940
Molybdenum	7.7 µg/g	3.9-4.2	1935-1940
Nickel	38 µg/g	1.2-1.6	1979-1984
Thorium	26 µg/g	2.6-2.9	1957-1962
¹ Uranium	12 µg/g	3.5-4.2	1935-1942
Zinc	170 µg/g	2.6-2.9	1957-1962
Radium-226	2.1 pCi/g	1.9-2.2	1968-1973
Radium-228	2.5 pCi/g	1.9-2.2	1968-1973
Gross alpha radioactivity	32 pCi/g	1.9-2.2	1968-1973
¹ Gross beta radioactivity	43 pCi/g	3.2-3.9	1940-1951
¹ Maximum value equal in two adjacent subsamples.			

Contaminants from the Yerington copper mine site can be delivered to Weber Reservoir by direct fallout of windborne dust, fluvial transport of dust blown from the site to drainages, stormwater runoff from the site into the river, and contaminated ground water discharging into Wabuska Drain and possibly into the Walker River. The National Weather Service cooperative station at Yerington does not collect wind-movement data (www.wrcc.dri.edu/summary/climsmnv.html), and records of stormwater releases from the site are not readily available (Arthur Gravenstein, Nevada Division of Environmental Protection, oral. commun., May 2006).

One analysis of meteorological data collected at the Yerington mine site for calendar year 2003 indicates that the wind direction at this site most frequently is from the southwest (almost 20 percent). However, dust characteristics and analysis of atmospheric transport indicate a threshold wind speed of 20 miles per hour is necessary to redistribute dust from the mine site. In 2003, winds in excess of this threshold were predominantly from the southwest about 5 percent of the time, and from the west and south less frequently (Hamilton and Arno, 2004, p. 10–16), indicating that windborne dust from the mine site can be transported toward WRIR and Weber Reservoir. However, the radiological dose assessment concluded that the potential exposure rate is 200,000 times

less than the radiation that average Nevadans are exposed to from natural background radiation (Hamilton and Arno, 2004, p. 20).

Analysis of precipitation records for 1956–62, the period when maximum values of constituents of concern had the highest frequency, indicates that there were 11 days with more than 0.5 in. of precipitation (Western Regional Climate Center, 2006, accessed April 12, 2006). Seven of those days were during May through September, when precipitation averaged 0.77 in.; a maximum precipitation of 1.1 in. fell on September 17, 1957. During the period of precipitation record at the Yerington station (1914–2006), the probability that 0.01 in. of rain would occur during May through September was less than 10 percent, and the probability that 0.5 in. of rain would occur was less than 1 percent.

During water years (October 1 through September 30) 1943–2005, daily-mean streamflow data for USGS stream-gaging station 10301500, Walker River near Wabuska (Fig. 2, site 6) ranged from less than 1 ft³/s (cubic feet per second) on 14 days in October and November 1977 to 2,740 ft³/s on June 7, 1986. Mean values of daily-mean streamflow for each period representing each core subsample ranged from 358 ft³/s (1979–84) to 37 ft³/s (1933–35), and maximum values ranged from 2,740 ft³/s (1984–90) to 410 ft³/s (1935–40). The mean of daily streamflow values for 1957–62, the period when maximum values for 9 of the 19 constituents of concern had maximum concentrations, was 113 ft³/s, with a maximum streamflow value of 1,900 ft³/s. The period with the largest mean of daily-mean streamflow (1979–84) had the highest concentrations of chromium and nickel, and the period with the largest maximum daily-mean streamflow (1984–90) had the second highest concentrations of copper, iron, and second largest activities of ²²⁶Ra and ²²⁸Ra. The second highest concentration of zinc was measured in this sub-sample, but this concentration also was equaled in four other sub-samples (table 4).

Concentrations and activities of constituents of concern detected in sediment-core samples from the Weber Reservoir indicate varying rates of deposition, but because each sample represents sediment that accumulated over 5–6 years, episodic stormwater releases from the mine, as well as discharge from a contaminated ground water site would be diluted by normal sedimentation. Sediment contaminated at levels that exceed advisory guidelines (table 3) may be responsible for the maximum values shown in figure 5. The samples of river-bottom sediment collected for this study generally had lower contaminant concentrations and activities than the samples of the reservoir-sediment samples (table 5), but the differences are small, largely owing to the geology and mining activities throughout the Walker River Basin.

Mining and mineral exploration have been active in the Walker River Basin since the middle of the 19th century, as evidenced by the elevated mercury concentrations reported in water, sediment and biota (Seiler and others, 2004). All the constituents of concern in the basin are associated with the naturally occurring rocks and mineral deposits that stimulated mineral exploration. More than a century of mining and milling activity has increased the potential for their release into the environment.

SUMMARY

The Walker River Paiute Tribe is concerned that mining operations at the Yerington copper mine site, located in the Singatse Range, near Yerington in Lyon County, Nev., have contaminated the Walker River Indian Reservation. Mining in the Walker River Basin began in the mid to late 1800s; large-scale open-pit mining operations at the site began in 1952 and continued intermittently until closure of the mine in 2000 because of bankruptcy. Investigations authorized by the Comprehensive Environmental Response, Compensation, and Liability Act began in the late 1990s in response to reports that elevated concentrations of trace elements and radionuclides have been measured in ground water, tailings leachate, and leachate-contaminated soil samples.

Consolidated rocks in the Walker River Basin range in age from Triassic to Quaternary and primarily consist of quartz monzonite, granodiorite, basalt, rhyolite, and andesite. Basin-fill deposits consist of unconsolidated alluvial sediments underlying the valley floors and alluvial fan deposits near the base of mountain ranges. Lacustrine clay deposits at least 200-ft thick are exposed near Weber Reservoir.

The East Fork and the West Fork of the Walker River flow into Mason Valley where they converge into the main stem of the river which flows northward into Campbell Valley and ultimately into Walker Lake. The principal use of water in the Walker River Basin is for irrigation of crops and pastures. Extensive networks of canals, ditches, and drains have been constructed to convey water from the river for irrigation. The Wabuska Drain originates at the base of mine tailings and intermittently discharges to the Walker River. Weber Reservoir, the only reservoir on the main stem of the Walker River, was constructed in 1934. Local runoff is ephemeral and occasionally has resulted in flash floods. More than 1 million acre-feet of ground water is in the uppermost 50 feet of saturated alluvial aquifers beneath Mason Valley.

The U.S. Geological Survey, in cooperation with the Walker River Paiute Tribe, began an investigation in 2005 to establish a chronology of the sediment quality of Weber Reservoir. Bottom-sediment samples were collected from seven locations that are tributary to Weber Reservoir and from two sediment cores from the reservoir. Samples were analyzed for selected major and trace elements, and radionuclides. Three sites were selected to characterize the chemical quality of bottom sediment in the river upstream of the Yerington mine site, and four sites, including one on Wabuska Drain, were selected to characterize sediment downstream from the mine site. Two sediment cores were collected from Weber Reservoir: a 2.1-foot core was collected when the reservoir had an ice layer that limited access to the preferred sampling location and a 4.0-foot core was collected later near Weber Dam. Two additional samples were collected from 4.2 to 4.6 feet beneath the sediment surface using a peat borer-type sampler.

Sediment samples were analyzed for cesium-137, which is an anthropogenic isotope that has been used as an age marker for periods of above-ground nuclear weapons testing. Also analyzed were constituents identified as being potentially toxic or carcinogenic or that have been measured in samples from the Yerington copper mine site at levels that are greater than background. Bottom-sediment samples represent sediment that was moving within the river system in 2005. Sediment-core data from Weber Reservoir represent a chronologic history of the sediment quality in the Walker River above Weber Reservoir. Mean concentrations and activities of constituents measured in bottom-sediment samples generally were lower than those measured in reservoir sediment. Advisory concentrations

for iron (21,200 µg/g) and manganese (460 µg/g) were exceeded in all samples, and the advisory concentration for arsenic (33 µg/g) was equaled in one riverbed sample. The concentration of mercury in one reservoir sample (1.00 µg/g) is near the advisory concentration (1.06 µg/g). Concentrations of mercury in all samples, except one bottom-sediment sample from the West Walker River, exceeded the sediment effects threshold concentration that may adversely affect freshwater invertebrates in Ontario, Canada (0.2 µg/g). No other sediment advisory concentration or activity was exceeded. Maximum concentrations of mercury and molybdenum were from the subsample deposited during 1936–40.

Cesium-137 data from the second core collected from Weber Reservoir showed a clearly defined peak that represents the year of maximum above-ground nuclear weapons testing and resulting cesium-137 releases in 1963 in the subsample from a depth 2.2 to 2.5 ft below the sediment surface. The initial detection was in the subsample from a depth 2.8 to 3.2 ft below the sediment surface and represents 1950, when above-ground nuclear weapons testing began. Assuming a linear rate of sedimentation and neglecting density compaction, sediment accumulated in Weber Reservoir at a rate of 0.04 ft/yr during 1950–63, and at a rate of 0.06 ft/yr during 1963–2003 and for the 70-year period 1935–2005. Age estimates are plus or minus 3 years because each subsample was 0.2 to 0.3 ft in length.

Maximum concentrations of aluminum, arsenic, beryllium, cadmium, copper, iron, lead, manganese, thorium, and zinc were in the subsample from 2.6 to 2.9 ft below the sediment surface, which represents sedimentation during 1957–62. Seventeen of the 37 other analytes determined also had maximum concentrations in this subsample. Maximum concentrations of chromium and nickel were in the subsample from the 1.2- to 1.6-ft interval that was deposited during 1979–84, and maximum concentrations of uranium were from two adjacent samples from the 3.5- to 4.2-ft interval that was deposited before the reservoir was constructed until 1944. Both isotopes of radium-226 and radium-228 and gross alpha radioactivity had maximum activities in the samples from the 1.9- to 2.2-ft interval, which was deposited during 1968–73; the maximum gross beta radioactivity was in two adjacent samples from the 3.2- to 3.9-ft interval that was deposited during 1940–51. Maximum concentrations of mercury and molybdenum were from samples from the 3.9- to 4.4-ft interval which represents pre-reservoir sediment.

Contaminants from the Yerington copper mine site can be delivered to Weber Reservoir by direct fallout of windborne dust, fluvial transport of dust blown from the site to drainages, stormwater runoff from the site into Wabuska Drain and the river, and contaminated ground water discharging into Wabuska Drain and possibly into the Walker River. Concentrations and activities of constituents of concern in the sediment-core samples from Weber Reservoir indicate varying rates of deposition; but, because each sample represents sediment that accumulated over a 5- to 6-year period, episodic stormwater releases from the mine site, as well as discharge of contaminated ground water, would be diluted by normal sedimentation. Mining and mineral exploration has been active in the Walker River Basin since the mid-1800s, and all the constituents of concern are associated with naturally occurring rocks and mineral deposits. Samples of river-bottom sediment generally had smaller concentrations and activities than the subsamples from the reservoir core, but the differences were small, probably owing to the geology and mining activities throughout the Walker River Basin.

REFERENCES

- Arbogast, B.F., ed., 1996, Analytical methods manual for the Mineral Resource Surveys Program: U.S. Geological Survey Open-File Report 96-525, 248 p.
- Brown and Caldwell, 2003, Wabuska Drain work plan—Draft final: Carson City, Nev., Brown and Caldwell, prepared for Atlantic Richfield Company, variously paged.
- Hamilton, I.S., and Arno, M.G., 2004, Yerington mine site fugitive dust radiological dose assessment: Bryan, Texas, Foxfire Scientific, Inc., 23 p. and 1 appendix.
- Huxel, C.J., Jr., 1969, Water resources and development in Mason Valley, Lyon and Mineral Counties, Nevada, 1948–65: Nevada Division of Water Resources Bulletin No. 38, 77 p.
- Ingersoll, C.G., MacDonald, D.D., Wang, Ning, Crane, J.L., Field, L.J., Haverland, P.S., Kemble, N.E., Lindskoog, R.A., Severn, Corrine, and Smorong, D.E., 2000, Prediction of sediment toxicity using consensus-based freshwater sediment quality guidelines: U.S. Environmental Protection Agency, Great Lakes National Program Office Chicago, EPA 905/R-00/007, variously paged; accessed March 2006 at <http://www.cerc.usgs.gov/pubs/center/pdfDocs/91126.pdf>
- Knopf, Adolph, 1918, Geology and ore deposits of the Yerington District, Nevada: U.S. Geological Survey Professional Paper 114, 68 p.
- Lemly A.D., and Smith, G.J., 1987, Aquatic cycling of selenium—Implications for fish and wildlife: Washington, D.C., U.S. Fish and Wildlife Service, Fish and Wildlife Leaflet 12, 10 p.
- Ludington, Steve, Moring, B.C., Miller, R.J., Flynn, Kathryn, Hopkins, M.J., Stone, Paul, Bedford, D.R., and Haxel, G.A., 2005, Preliminary integrated geologic map databases for the United States—Western states: California, Nevada, Arizona, and Washington, version 1.0: U.S. Geological Survey Open File Report 2005-1305, unpaginated. [Available on the World Wide Web at <http://pubs.usgs.gov/of/2005/1305/>]
- Moore, J.G., and Archbold, N.L., 1969, Geology and mineral deposits of Lyon, Douglas, and Ormsby Counties, Nevada: Nevada Bureau of Mines Bulletin 75, 42 p.
- Nevada Division of Environmental Protection, 2002, Administrative Order on Consent: accessed March 6, 2006, at <http://ndep.nv.gov/yerington/AR%20Final%20AOC%2010-24-2002.pdf>
- Nevada Division of Environmental Protection, 2003, Yerington Mine update—December 2003: accessed March 6, 2006 at http://ndep.nv.gov/yerington/yerington_site_site_briefing03.pdf
- Nevada State Library and Archives, 2000, [U.S. Census Bureau] Nevada Census 2000: accessed April 18, 2006, at http://dmla.clan.lib.nv.us/docs/nsla/sdc/census_2000.htm
- Persaud, D.R., Jaagumagi, R., and Hayton, A., 1993, Guidelines for the protection and management of aquatic sediments in Ontario: Toronto, Canada, Ontario Ministry of the Environment and Energy, Water Resources Branch, 23 p.
- Price, J.G., 1995, The Nevada mineral industry—1994: Nevada Bureau of Mines and Geology, Special Publication MI-1994, 57 p.
- Reheis, Marith, 1999, Extent of Pleistocene lakes in the western Great Basin: U.S. Geological Survey Miscellaneous Field Studies Map MF-2323.

- Seiler, R.L., Lico, M.S., Wiemeyer, S.N., and Evers, D.C., 2004, Mercury in the Walker River Basin, Nevada and California—Sources distribution, and potential effects on the ecosystem: U.S. Geological Survey Scientific Information Report 2004-5147, 24 p.
- Seitz, H.R., Van Denburgh, A.S., and La Camera, R.J., 1982, Ground-water quality downgradient from copper-ore milling wastes at Weed Heights, Lyon County, Nevada: U.S. Geological Survey Open-File Report 80-1217, 48 p.
- Shelton, L.R., and Capel, P.D., 1994, Guidelines for collecting and processing samples of stream bed sediment for analysis of trace elements and organic contaminants for the National Water-Quality Assessment Program: U.S. Geological Survey Open-File Report 94-458, 20 p.
- Stockton, E.L., Jones, C.Z., Rowland, R.C., and Medina, R.L., 2004, Water Resources Data—Nevada, Water Year 2003: Water-Data Report NV-03-01, 679 p.
- Taggart, Jr., J.E., ed., 2002. Analytical methods for chemical analysis of geologic and other materials, U.S. Geological Survey: U.S. Geological Survey Open-File Report 02-223, 26 chapters, accessed January 2005, at <http://pubs.usgs.gov/of/2002/ofr-02-0223/OFR-02-0223.pdf>
- Thomas, J.M., 1995, Water budget and salinity of Walker Lake, western Nevada: U.S. Geological Survey Fact Sheet FS-115-95, 4 p.
- Tingley, J.V., 1992, Mining districts of Nevada: Nevada Bureau of Mines and Geology Report 47, 124 p.
- University of Reno, 1997, Copper mining in Nevada: accessed March 17, 2006, at <http://www.unr.edu/sb204/geology/minetext.html>
- Van Metre, P.C., Wilson, J.T., Fuller, C.C., Callender, Edward, and Mahler, B.J., 2004, Collection, analysis, and age-dating of sediment cores from 56 U.S. lakes and reservoirs sampled by the U.S. Geological Survey, 1992–2001: U.S. Geological Survey Scientific Investigations Report 2004-5184, 180 p.
- Western Regional Climate Center, 2006, Yerington, Nevada—NCDC 1971–2000 Monthly normals: accessed April 12, 2006, at <http://www.wrcc.dri.edu/cgi-bin/cliNORMNCDC2000.pl?nvyeri>

Acknowledgments - The authors express their appreciation to the Walker River Paiute Tribe for allowing access to sampling sites and to Roy Begay, Non-Point Source Coordinator for the Tribe for his offer to assist retrieving the sample boat from Weber Reservoir should the truck become stranded in soft beach sand. Cesium-137 analyses and age-dating provided by Daniel R. Engstrom, Science Museum of Minnesota, and chemical analyses of soil samples from the Yerington mine site provided by Paul Meyer, Bureau of Land Management, also are appreciated.

Technical Note

New method for calculating activity coefficients of surface ions in concentrated electrolytes

ANPALAKI J RAGAVAN, Department of Civil and Environmental Engineering
University of Nevada, Reno, NV 89557

This technical note was intended to introduce a new method for calculating activity coefficients of surface ions in concentrated 1:1 electrolytes that would benefit geochemical modeling of environmental and industrial processes, which is currently severely hindered due to the unavailability of an equation to calculate the activity coefficients of ions adsorbed onto solid surfaces and/or located near solid surfaces in solution-solid interfaces also known as surface ions. In an electrolyte solution Coulomb forces between ions affect the thermodynamic and physical properties of the system. Hence law of mass action is strictly valid only when activities are used instead of concentrations. The only currently available Debye-Huckel (Onsager, 1933; Onsager and Fuoss, 1932; Wingrave, 2001) equation and its extended forms for calculating activity coefficients in real electrolyte solutions are limited to low electrolyte concentrations less than 0.01 moles (M) due to the use of linearized Poisson-Boltzmann equation in their derivation (Onsager, 1933; Onsager and Fuoss, 1932; Wingrave, 2001). Debye-Huckel equation also assumes that the dielectric constant of solvent molecules is unaffected by the concentration of solute ions in solution which limits its use to homogeneous solutions of concentrations less than 0.001 moles (Onsager, 1933; Onsager and Fuoss, 1932; Wingrave, 2001). It is frequently necessary to work with high concentrations of inert electrolytes present. A theoretically based activity coefficient equation for surface ions was derived in this paper based on rigorous electrostatic and thermodynamic laws and non-linear Poisson-Boltzmann equation, and used to simulate the activity coefficients of ions located at or near solid surfaces in solution-solid interfaces of 1:1 aqueous electrolyte solutions. The dielectric constant (DC) of the solvent molecules near the solid surface was calculated as a continuous function of the solute ion concentration. The mathematical incompleteness of Debye-Huckel equation was corrected in the derived equation with the use of non-linearized Poisson-Boltzmann equation. The derived equation gave reasonable results for ions of all types and valences at all concentrations of 1:1 electrolytes. The derived equation can also be easily extended to other type (1:2 and 2:2) of electrolytes.

INTRODUCTION

First of all I would like to give a brief introduction to the purpose for such an equation and the theory behind its derivation. Solids (e.g: metal oxides and hydroxides) are frequently used to remove toxic ions like lead, cadmium, arsenic, and selenium, from drinking and waste-water systems (Standard Handbook of Hazardous Waste Treatment and Disposal, 1989) through the technique called adsorption. Adsorption, also called surface complexation, onto metal oxide surfaces is the best currently available water treatment technology recommended by the U.S. Environmental Protection Agency (USEPA, 2001) to remove toxic ions from water and waste-water systems. Due to the unavailability of an equation to calculate the activity coefficient of surface ions, activity coefficients of surface complexed ions especially at moderate to high concentrations of the electrolyte solutions are incorrectly ignored or set equal to unity when calculating thermodynamic equilibrium constants for surface complexation reactions. Mass action is strictly valid only when activities are used instead of concentrations in real solutions (Onsager, 1933; Wingrave, 2001). Studying very dilute solutions (total electrolyte concentrations less than 10^{-3} M), in which the combination of activity coefficients, are practically equal to unity, is evidently limited to very stable complexes and high electrolyte concentrations are necessary when working with weak or moderately stable complexes. Therefore, ignoring activities in surface complexation models as done by current researchers and treatment facilities (Wang and others, 1997; Goldberg and Johnston, 2001) can lead to erroneous calculations and reporting of the results of the amount of toxic ions adsorbed onto solid surfaces and removed from drinking and waste water systems.

Ions follow Boltzmann's distribution in solution. Any derivation of the activity coefficient of ions in a real solution should be a solution to the Poisson-Boltzmann equation. Serious discrepancies between the Debye-Huckel predictions and the experimentally calculated activity coefficients even in very dilute solutions necessitate far reaching revision, if not rejection of the Debye-Huckel equation (Onsager, 1933). Several researchers have indicated that the discrepancies are due to the incomplete mathematical derivation of the equation (La Mer and others, 1931). In addition, the Debye-Huckel assumption, that the dielectric constant of the solvent in electrolyte solutions is the same as that of pure solvent makes it unusable for ions near solid surfaces in solution-solid (S-S) interfaces. As a result of counter-ion concentration near charged solid surfaces, an electrostatic diffusion double layer of surface ions, and counter-ions are formed in real S-S interfaces, which can result in electric field strength (EFS) of large magnitudes near solid surfaces (James and Healy, 1972), that can electrically saturate the nearby solvent molecules, reducing the dielectric constant (DC) of the solvent medium near solid surfaces, from the pure solvent value to a fully electrically saturated solvent value especially at high ionic strength of the medium. Interfacial EFS and the DC of solvent molecules are continuous functions of the ionic strength of the medium, electrostatic potential, and the distance from the solid surface. Due to the complex nature of the distribution of ions and the electrostatic potentials in an S-S interface, very few studies have been conducted in this area. No attempt has been made so far to develop an equation to estimate the activity coefficients of surface ions in real S-S interfaces with moderate to high concentrations of inert electrolytes present.

A brief description of what an activity coefficient is and its applicability to surface ions is given below. Thermodynamic properties of ideal solutions are calculable but, of real solutions, in most cases are not calculable, hence must be estimated from ideal solution properties. Activity coefficient (f_Y), describes the relationship between the activity (α_Y) of an ion (Y_Z) of valence Z and its mole fraction (X_Y) in real solutions as: $\alpha_Y = X_Y f_Y$ (Lewis and Randall, 1961). When two phases, where one is a solid and the other is a liquid are allowed to contact, counter-ions (ions of opposite charge) in the solution phase are attracted towards the charges on the solid surface by Coulomb forces, at the same time they tend to move towards the bulk solution because of their thermal motion, establishing an equilibrium distribution of counter-ions near solid surfaces (James and Healy, 1972). As counter-ions accumulate near solid surfaces, ions of the same sign (co-ions) are excluded from near the surface due to electrostatic interaction. Depletion of co-ions and the excess of counter-ions near solid surfaces result in screening of the charge of the surface ions. In real S-S interfaces the role of inert electrolyte concentration on electrostatic free energy of a surface ion is manifest in this screening of the surface charge on the surface ion by the counter-ions that concentrate near solid surfaces (Sen and others, 1975). Due to the counter-ion screening the amount of work required to overcome the electrostatic potential of a surface ion when charging the surface ion, which is the electrostatic contribution of the surface ion to its thermodynamic potential (electrostatic free energy), becomes smaller than the work required in an S-S interface without electrolytes (pure solvent). This can best be understood by a brief explanation of the ion charging process. An increment of work must be expended each time an increment of electrostatic charge is added to the surface of any solute ion. The source of this expenditure of work results from the fact that a surface ion with some amount of electrostatic charge will resist the addition of even more electrostatic charge of like sign. When counter-ions move nearer the surface of a surface ion each time an increment of charge is added to the surface ion addition of charge is favored, and the amount of energy required to make each incremental electrostatic charge addition is lowered (Sen and others, 1975). Absence of screening in ideal S-S interfaces indicates that counter-ions play no role in determining the electrostatic free energy of surface ions in ideal solutions. Therefore, real solution properties can be differentiated from ideal solution properties by deriving an equation for the difference in electrostatic free energy of a surface ion in concentrated real S-S interfaces and in pure S-S interfaces.

METHODS

The electrostatic free energy of any ion, can be computed directly from the work of charging the ion in a given dielectric medium at constant temperature (T) and constant volume (V) of the solution (Sen and others, 1975; Israelachvili, 1992; Wingrave, 2001). During charging an ion (Y_Z) of valence Z , the initial electrostatic charge q of Y_Z is gradually increased from zero by adding an infinitesimal amount of electrostatic charge (dq) to Y_Z , transported from a vacuum at infinite distance from Y_Z , where the electrostatic charge has no interaction energy. Whenever an infinitesimal amount of electrostatic charge (dq) is transferred to Y_Z an infinitesimal amount of work must be done reversibly in T and V to overcome the increasing electrostatic potential on the surface of Y_Z (at

distance r measured radially from the center of Y_Z , where r is the crystallographic radius of Y_Z). The quantity of the reversible work done is equal to the energy created or lost in the work process. Since the system is not thermally isolated but kept at constant temperature (T) the energy created becomes the free energy of the system.

In classical thermodynamics, definition of chemical potential (μ_Y) of a single solute ion (Y_Z) in a real solution phase (gas or liquid) is given as the change in the Gibbs free energy (∂G) of the solution phase with an incremental change in Y_Z (∂n_Y) at T and constant pressure (P). However, the above definition does not describe the dependence of μ_Y on the composition of the solution. The composition dependence of μ_Y requires a different derivation, which was achieved in this technical note by modifying the Gibbs-Duhem equation (Gibbs, 1948; Wingrave, 2001) (eq. 2), which describes the chemical potential of a component gas g (μ_g) in a gaseous system, under the constraints of T , and constant composition of all components except the composition of g (n_g) in the system applicable to liquid solutions.

$$-VdP + SdT + \sum_i^N n_i d\mu_i = 0 \quad . \quad (1)$$

S , and N in eq. 1 are entropy and the total number of all component gases other than g . To make computations easy, eq. 1 can be rearranged into the following integral form between the two hypothetical pressure states p_1 and p_2 :

$$\int_{\mu_g(p_1)}^{\mu_g(p_2)} d\mu_g = \int_{p_1}^{p_2} V_g dp \quad \text{iff, } dT = dn_{i \neq g} = 0 \quad . \quad (2)$$

Eq. 2 when combined with the equation of state for a hypothetical ideal gas (g) yields:

$$\mu_g^{ID}(p_2) - \mu_g^{ID}(p_1) = RT \ln \left[\frac{p_2}{p_1} \right]_{dT=dn_{i \neq g}=0} \quad , \quad (3)$$

where R is the gas constant, and $\mu_g^{ID}(p_2) - \mu_g^{ID}(p_1)$ is the chemical potential change of g between the pressure states p_1 and p_2 . If the pressure variables p_2 and p_1 in eq. 3 are taken to equal the ideal and the reference states of g , the following equation for the chemical potential difference of g between its ideal (μ_g^{ID}) and reference (μ_g^*) states can be derived:

$$\mu_g^{ID} = \mu_g^* + RT \ln X_g^{ID} \quad , \quad (4)$$

where $X_g^{ID} (= p_2/p_1)$ is the partial pressure variable for g in an ideal gas phase, which provides a convenient correspondence to the mole fraction of Y_Z (X_Y^{ID} : the ratio between the ideal molar concentration of Y_Z ($[Y_Z^{ID}]$), and its standard state molar concentration ($[Y_Z^*]$) in an ideal liquid solution. Therefore, an equation of state for an ideal liquid solution can be written in terms of μ_Y^{ID} and X_Y^{ID} as:

$$\mu_Y^{ID} = \mu_Y^* + R_B T \ln X_Y^{ID} \quad . \quad (5)$$

The gas constant ($R=8.3144$ Joule (J) M^{-1} Kelvin (K) $^{-1}$) in eq. 4 needs to be replaced by the Boltzmann's constant ($R_B = 1.381*10^{-23}$ J K^{-1}) for liquid solutions (Lewis and Randall, 1961). Eq. 5 describes the chemical potential of ions in ideal liquid solutions and does not take into account of the non-ideality in real liquid solutions.

The non-ideality in real liquid solutions was taken into account by incorporating the activity of Y_Z (f_Y) in eq. 5 in place of the mole fraction and writing an equivalent expression for the chemical potential (μ_Y) of Y_Z in real liquid solutions (Israelachvili, 1992) as:

$$\mu_Y = \mu_Y^* + R_B T \ln X_Y + R_B T \ln f_Y \quad , \quad (6)$$

where X_Y (ratio between the molar concentration of Y_Z in real liquid solutions [Y_Z] and its standard molar concentration ($[Y_Z^*]$)) is the mole fraction of Y_Z in real liquid solutions. From here onwards the term solutions will be used for liquid solutions. By restricting eq. 5 and eq. 6 to apply to ideal and real equimolar solution phases of Y_Z ($[Y_Z] = [Y_Z^{ID}]$) and subtracting the ideal solution equation (eq. 5) from the real solution equation (eq. 6), the chemical potential difference of Y_Z in real and ideal solutions in terms of f_Y was obtained as:

$$\mu_Y - \mu_Y^{ID} = -R_B T \ln f_Y \quad . \quad (7)$$

Eq. 7 is not an explicit equation for predicting f_Y in real solutions, since μ_Y and μ_Y^{ID} are not directly measurable experimentally. An explicit equation for f_Y requires the estimation of $\mu_Y - \mu_Y^{ID}$ in directly measurable parameters.

For the next step in the derivation, which involves obtaining an explicit expression for $\mu_Y - \mu_Y^{ID}$ ion charging was used. As discussed earlier, the electrostatic free energy of an ion anywhere in a solution (ideal or real) or in an S-S interface, which is also its chemical potential can be computed directly from the reversible work of charging the ion. The reversible infinitesimal work of charging Y_Z was computed separately in ideal (dW_Y^{ID}) and in real (dW_Y) solutions (Israelachvili, 1992) as:

$$dW_Y = \left\{ \frac{q.dq}{4.\pi.\varepsilon_o.\varepsilon_r.r} \right\} \quad , \quad (8)$$

$$dW_Y^{ID} = \left\{ \frac{q.dq}{4.\pi.\varepsilon_o.\varepsilon_r^{ID}.r} \right\} \quad , \quad (9)$$

where ε_o is the electrical permittivity of the vacuum ($= 8.854*10^{-12}$ coulomb 2 (c 2) $v^{-1}m^{-1}$), r is the crystallographic radius of Y_Z in m, and, ε_r is the DC of the solvent molecules near Y_Z located at or near solid surfaces in a concentrated real S-S interface, which is a

continuous function of the electrostatic field strength $\left(\left\{ \frac{d\psi_Y(r)}{dr} \right\}_r \right)$ of the interfacial

solution near Y_Z in $v m^{-1}$, and ε_r^{ID} is that in a pure solvent medium. The total reversible work done in charging Y_Z , which is the chemical potential of Y_Z in real and in ideal inert electrolyte solutions in T and in V were obtained by integrating eq. 8 and eq. 9 respectively from zero up to the final charge of Y_Z (Q) as:

$$\mu_Y = \int_0^{W_Y} dW_Y = \frac{Q^2}{8.\pi.\varepsilon_o.\varepsilon_r.r} \quad . \quad (10)$$

$$\mu_Y^{ID} = \int_0^{W_Y^{ID}} dW_Y^{ID} = \frac{Q^2}{8.\pi.\varepsilon_o.\varepsilon_r^{ID}.r} \quad . \quad (11)$$

An equation for $\mu_Y - \mu_Y^{ID}$ was made possible in terms of the DC of the solvent molecules near Y_Z by subtracting eq. 11 from eq. 10 as:

$$\mu_Y - \mu_Y^{ID} = \left\{ \frac{Q^2}{8.\pi.\varepsilon_o.r} \right\} \left\{ \left\{ \frac{1}{\varepsilon_r} \right\} - \left\{ \frac{1}{\varepsilon_r^{ID}} \right\} \right\} \quad . \quad (12)$$

Eq. 12 was substituted into eq. 7 for $\mu_Y - \mu_Y^{ID}$ to obtain a simplified expression for f_Y in terms of ε_r as:

$$\ln f_Y = - \left\{ \frac{1.15(10^{-28}).Z^2}{r.R_B.T} \right\} \left\{ \frac{\varepsilon_r^{ID} - \varepsilon_r}{\varepsilon_r.\varepsilon_r^{ID}} \right\} \quad . \quad (13)$$

In eq. 13, ε_r is the only parameter that is unknown. An explicit equation to calculate f_Y of surface ions in real solutions requires an explicit expression for ε_r .

The final step in the derivation involves estimating ε_r at the solution-solid interface. Several equations are available in the literature that allows the calculation of ε_r in terms of $\left\{ \frac{d\psi_Y(r)}{dr} \right\}_r$ in an S-S interface. The equation by Sacher and Laidler (James and Healy, 1972; Sen and others, 1975) was chosen after replacing the high field limits of n_α^2 (where n_α is the optical refractive index) with the DC of the fully electrically saturated solvent molecules (ε_S) for calculating ε_r in real S-S interfaces in this technical note. The modified form of the equation is shown below:

$$\varepsilon_r = \left\{ \frac{(\varepsilon_B - \varepsilon_S)}{\left(1 + B \left\{ \frac{d\psi_Y(r)}{dr} \right\}_r^2 \right)} \right\} + \varepsilon_S \quad , \quad (14)$$

where B is a dimensional constant (James and Healy, 1975) equal to $1.2 * 10^{-17} \text{ m}^2 \text{ v}^{-2}$. The above equation (eq. 14) calculates ε_r as a continuous function of

$\left\{ \frac{d\psi_Y(r)}{dr} \right\}_r$ between its high (ε_S) and low (ε_B) field limits. Gouy-Chapman equation (Israelachvili, 1992) for 1:1 electrolyte solutions (eq. 15) was chosen to estimate $\left\{ \frac{d\psi_Y(r)}{dr} \right\}_r$ near Y_Z . For surface ions distance from the solid surface was replaced by their ionic radii (r).

$$\left\{ \frac{d\psi_Y(r)}{dr} \right\}_r = - \left\{ \frac{2.k.R_B.T}{e} \right\} . \sinh \left\{ \frac{e.\psi_Y(r)}{2.R_B.T} \right\} \quad , \quad \text{vm}^{-1} \quad . \quad (15)$$

In eq. 15 e is the charge of an electron ($=1.6022 \times 10^{-19}$) in c, and T is the absolute temperature of the medium in K, $\psi_Y(r)$ is the electrostatic potential on the surface of Y_Z in real S-S interfaces, and k is the reciprocal length of the diffusion ion atmosphere in m^{-1} also known as the reciprocal Debye length (Wingrave, 2001). In eq. 15 $\psi_Y(r)$ is the only unknown. If charging of Y_Z was independent of solution composition or ideal $\psi_Y(r)$ would simply be the coulomb electrostatic potential (Sen and others, 1975; Wingrave, 2001) for Y_Z , which would describe the ideal electrostatic potential of Y_Z in pure dielectric medium, which is a function of ϵ_r^{ID} making $\psi_Y(r)$ a constant equal to $\psi_Y(r)^{ID}$. Due to counter-ion concentration near Y_Z the electrostatic charge on the surface of Y_Z (initially ideal) will be partially offset by the proximity of ions of opposite charge. The screened electrostatic charge of the initially ideal surface potential which is the electrostatic potential of Y_Z in real solutions should be a function of ϵ_r . Since there are no other concentration dependent variables in the ideal electrostatic potential equation (Sen and others, 1975) the screening of the diffusion ion atmosphere on $\psi_Y(r)$ due to counter-ion concentration in real S-S interfaces is manifest in ϵ_r where ϵ_r is a continuous function of the solution ion concentration through $\left\{ \frac{d\psi_Y(r)}{dr} \right\}_r$ as shown is eq. 14. The coulomb electrostatic potential in ideal S-S interfaces was modified to compute $\psi_Y(r)$ in real S-S interfaces as follows:

$$\psi_Y(r) = \left\{ \frac{Q}{4\pi\epsilon_o\epsilon_r r} \right\}, \text{ v} \quad (16)$$

Eq. 16 was substituted for $\psi_Y(r)$ into eq. 15 along with values for the constants (R_B, T , and e) to obtain the following simplified equation for $\left\{ \frac{d\psi_Y(r)}{dr} \right\}_r$ in real solutions at 25°C:

$$\left\{ \frac{d\psi(r)}{dr} \right\}_r = \{-0.0514 k\} \sinh \left\{ \frac{280.2(10^{-10})Z}{\epsilon_r \cdot r} \right\}, \text{ vm}^{-1} \quad (17)$$

In eq. 17 k and ϵ_r are the concentration dependent variables. At 25°C values of k in m^{-1} for 1:1 electrolyte solutions (Israelachvili, 1992) can be calculated as:

$$k = \frac{[I]^{0.5}}{0.304 * 10^{-9}}, \quad (18)$$

where I is the ionic strength of the medium in M. As k increases with increasing electrolyte concentration in real solution interfaces $\left\{ \frac{d\psi_Y(r)}{dr} \right\}_r$ will increase in agreement with eq. 17. This increase in $\left\{ \frac{d\psi_Y(r)}{dr} \right\}_r$ is due to the decrease in $\psi_Y(r)$ of the nearby solute ions due to screening by the diffusion ion atmosphere of counter-ions around and near the solute ions. In real solution interfaces ϵ_r is inversely related to $\left\{ \frac{d\psi_Y(r)}{dr} \right\}_r$ as

shown in eq. 14. Increase in $\left\{\frac{d\psi_Y(r)}{dr}\right\}_r$ due to increase in k is very much larger (Wingrave, 2001) compared to that due to decrease in ε_r . For example in 1:1 aqueous electrolyte solutions of 1 M, k (from eq. 18) is equal to $3.29 * 10^9 \text{ m}^{-1}$, $\left\{\frac{d\psi_Y(r)}{dr}\right\}_r$ (from eq. 17) is equal to $1.22 * 10^{8.5} \text{ vm}^{-1}$, and ε_r (from eq. 14) is equal to 35.45. The influence of ε_r on the value of $\left\{\frac{d\psi_Y(r)}{dr}\right\}_r$ is much less than $2.7 * 10^{0.5}$, which is almost negligible compared to the influence of k on the value of $\left\{\frac{d\psi_Y(r)}{dr}\right\}_r$, which is in the order of $1.22 * 10^{8.5}$. The influence of k on the value of $\left\{\frac{d\psi_Y(r)}{dr}\right\}_r$ further increases as values of I increase. In aqueous S-S interfaces at very high I values equal to infinity k becomes equal to infinity (according to eq. 18) leading $\left\{\frac{d\psi_Y(r)}{dr}\right\}_r$ to approach infinity, but the value of ε_r approaches 6. In aqueous S-S interfaces at very low values of I close to zero, k as well as $\left\{\frac{d\psi_Y(r)}{dr}\right\}_r$ approaches zero, but values of ε_r remains close to 78.46. Therefore, k can be considered as the only significant concentration dependent (screening) variable in eq. 17. Therefore, the argument inside the sinh() in eq. 17 can be considered independent of I and the variations in ε_r with I especially in aqueous electrolyte solutions can be ignored. For the same reason and since the argument inside the sinh() term is in the order of 10^{-10} , the sinh() term in eq. 17 was replaced by the argument itself according to the following hyperbolic identity:

$$\sinh(x) = x + \frac{x^3}{3!} + \frac{x^5}{5!} + \frac{x^7}{7!} + \dots + \dots, \quad (19)$$

where ! stands for factorial notation. When the argument inside the sinh() term is small enough the higher order terms after x in eq. 19 were ignored and the following

simplified equation was obtained for $\left\{\frac{d\psi_Y(r)}{dr}\right\}_r^2$ after substituting x for sinh(x) in eq. 17:

17:

$$\left\{\frac{d\psi(r)}{dr}\right\}_r^2 = \left\{\frac{14.4(10^{-10})k.Z}{\varepsilon_r.r}\right\}^2, \text{ v}^2\text{m}^{-2}. \quad (20)$$

The maximum and the average percent error associated with the above substitution of x for sinh(x) in eq. 17 in aqueous electrolyte solutions at I values between 10^{-10} M and 250 M were calculated and found to be equal to 0.02 percent and 0.005 percent

respectively which are negligible. Eq. 20 was substituted for $\left\{\frac{d\psi(r)}{dr}\right\}_r^2$ into eq. 14 and

the resulting cubic equation was solved for ε_r in 1:1 electrolyte solutions in MATLAB

(version 7.0). Ignoring the negative roots (since ε_r cannot be negative) the following solution for ε_r in 1:1 electrolytes was obtained:

$$\varepsilon_r = \left\{ \frac{(\varepsilon_B \cdot A \cdot r^2) + (\varepsilon_S \cdot C \cdot k^2 \cdot Z^2)}{(A \cdot r^2) + (C \cdot k^2 \cdot Z^2)} \right\}, \quad (21)$$

Using eq. 21 ε_r of water molecules near solid surfaces in 1:1 aqueous electrolyte solutions at 25°C at a wide range of k values were calculated varying Z and r . In addition interfacial $\left\{ \frac{d\psi_Y(r)}{dr} \right\}_r$ using eq. 20 and eq. 21 as a function of I and the distance from the solid surface in 1:1 aqueous electrolyte solutions at 25°C was calculated.

Eq. 13 along with eq. 21 provides an explicit solution to calculate f_Y of surface ions in S-S interfaces of 1:1 electrolyte solutions. Eq. 13 was simplified to obtain an explicit expression for f_Y of surface ions in 1:1 electrolyte solutions at 25°C (eq. 23). Eq. 23 was used to calculate f_Y of surface ions in 1:1 aqueous electrolyte solutions (i.e., NaCl) at 25°C at a wide range of I values (10^{-20} M to 250 M). Surface ions of two different valences (± 1 , ± 3) and two different radii (0.5, and 5.0 nm (nanometers)) were used in the calculations.

As ions move from the bulk solution towards the solid surfaces due to Coulomb attraction they loose all or part of their hydration sphere before they reach the solid surface for adsorption. The ions that loose part of their hydration sphere form hydrated complexes (outer-sphere complexes) with the solid surfaces while the ions that loose their hydration sphere completely form non-hydrated complexes (inner-sphere complexes) with the solid surfaces. Thus ions that form outer-sphere complexes are considered to be at distance r_e from the solid surface and the ions that form inner-sphere complexes are at distance r from the solid surface where r_e is the radius (effective radius) of the partially hydrated ion and r is the radius (crystallographic radius) of non-hydrated ion. The effective radii of partially hydrated surface ions (Sverjensky and Molling, 1992) at the S-S interface were obtained as:

$$r_e = r + Z * (0.94) \quad , \quad (22)$$

where Z is the valence of the ion. The final form of the derived AC equation is shown below.

$$f_Y = \exp \left\{ - \frac{2.8 * 10^{-8} (\varepsilon_B - \varepsilon_r) Z^2}{\varepsilon_B \cdot \varepsilon_r \cdot r} \right\} \quad , \quad (23)$$

$$\text{where } \varepsilon_r = \left\{ \frac{(\varepsilon_B \cdot A \cdot r^2) + (\varepsilon_S \cdot C \cdot k^2 \cdot Z^2)}{(A \cdot r^2) + (C \cdot k^2 \cdot Z^2)} \right\} \quad ,$$

where A ($= 6.16 * 10^3$) and C ($= 2.5 * 10^{-35}$) are constants without units.

Eq. 23 is explicit since all the terms in the equation can be either calculated or measured in the laboratory and also does not restrict its application to any concentration of the inert electrolyte present, since its derivation involves rigorous electrostatic and thermodynamic laws that are applicable at all concentrations of real solutions. The

Gouy-Chapman equation used to obtain interfacial $\left\{ \frac{d\psi_Y(r)}{dr} \right\}_r$ is based on non-linear

Poisson-Boltzmann equation (La Mer and others, 1931) and leads to reasonable values for the variables at a wide range of inert electrolyte concentrations. Extensions of eq. 23 to other electrolyte types (1:2, 2:2) are possible with careful reconstruction of the Gouy-Chapman equation (Israelachvili, 1992). The magnitude of all parameters including k depends solely on the properties of the solution and not on any property of the solid.

The above derived equation was applied to a simulated 1:1 electrolyte S-S interfacial system (i.e., NaCl) with selected system parameters to a) calculate activity coefficients of cations (i.e., M^+ , M^{2+} , M^{3+}) and anions (i.e., A^- , A^{2-} , A^{3-}) as a function of ionic radii (5 to 50 Angstroms) and valences, b) to validate the existence of values of $\left\{ \frac{d\psi_Y(r)}{dr} \right\}_r$ greater than 10^8 vm^{-1} near (0.9 nm from solid) solid surfaces in 1:1 aqueous electrolyte solutions at I values greater than 0.01M (Figure 1) which can electrically saturate the solvent molecules near solid surfaces and, c) to study the relationships among $\left\{ \frac{d\psi_Y(r)}{dr} \right\}_r$, I and ϵ_r . The I values were varied between 250 M and 10^{-20} M, and the distance from the solid surface was varied between 0.1 Angstroms and 1000 Angstroms. ϵ_r was calculated using eq. 21, $\left\{ \frac{d\psi_Y(r)}{dr} \right\}_r$ using eq. 20 and f_Y using eq. 23. The calculations were performed in Microsoft EXCEL 2003.

RESULTS

According to the results, interfacial $\left\{ \frac{d\psi_Y(r)}{dr} \right\}_r$ were strongly and positively correlated with I at all I values as I was increased from 10^{-20} to 250 M ($R^2=0.99$) (Figure 1), and decayed exponentially away from the solid surface (Figure 2). $\left\{ \frac{d\psi_Y(r)}{dr} \right\}_r$ values above 10^8 vm^{-1} were found to exist near solid surfaces (0.9 nm from solid) which can cause significant electric saturation of solvent molecules (Figure 1). As $\left\{ \frac{d\psi_Y(r)}{dr} \right\}_r$ increased ϵ_r of the solvent (water) molecules decreased continuously from the pure solvent value ($=78.46$ at 25°C), towards the fully electrically saturated solvent value ($=6$ at 25°C) (Figure 3). Solvent ϵ_r increased continuously from the fully electrically saturated value ($=6$ at 25°C) towards the pure solvent value ($=78.46$ at 25°C) as the distance from the solid surface was increased (Figure 4) indicating a decay in electric saturation of the solvent molecules away from solid surfaces.

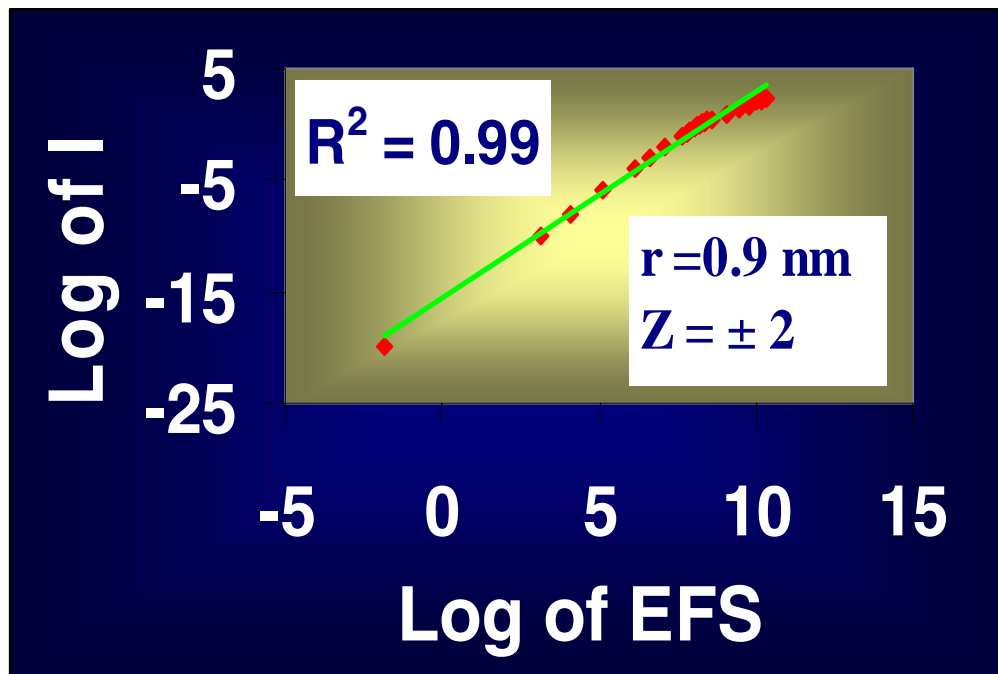


Figure 1. Log of interfacial electric field strength (EFS) as a function of the log of medium ionic strength (I) near divalent ions at 0.9 nanometers (nm) from the solid surface. Unit of EFS is volts per meter and that of I is moles.

At very low I ($\leq 10^{-10}$ M), ϵ_r near solid surfaces remained equal to that of pure solvent value indicating very low or no electric saturation of the solvent molecules at these low I values. Higher the I values higher were the deviations of ϵ_r near solid surfaces (0.9 nm from solid) from that of the pure solvent value ($=78.46$ at 25°C) (Figure 5). The difference in ϵ_r near monovalent and trivalent ions at 0.9 nm from the solid surface were not statistically significant at the 5% level (Figure 5).

According to the activity coefficient (f_γ) of the surface cations and anions calculated from eq. 23, f_γ of surface ions vary inversely with I at I values greater than 0.01 M indicating significantly decreased activities of surface ions at electrolyte concentrations greater than 0.01 M, and approached unity at lower I values leading activities to approach concentrations at these lower I values (Figure 6 and Figure 7). In addition higher the valence of the ion higher were the deviations of f_γ from unity at I values greater than 0.01M and vice versa. The differences in f_γ of the surface ions of the two valences (± 1 , ± 3) were significant at the 5% level ($P > |t| = 0.004$). Differences in f_γ of the surface ions of two radii (5.0 and 0.5 nm) were not statistically significant at the 5% level.

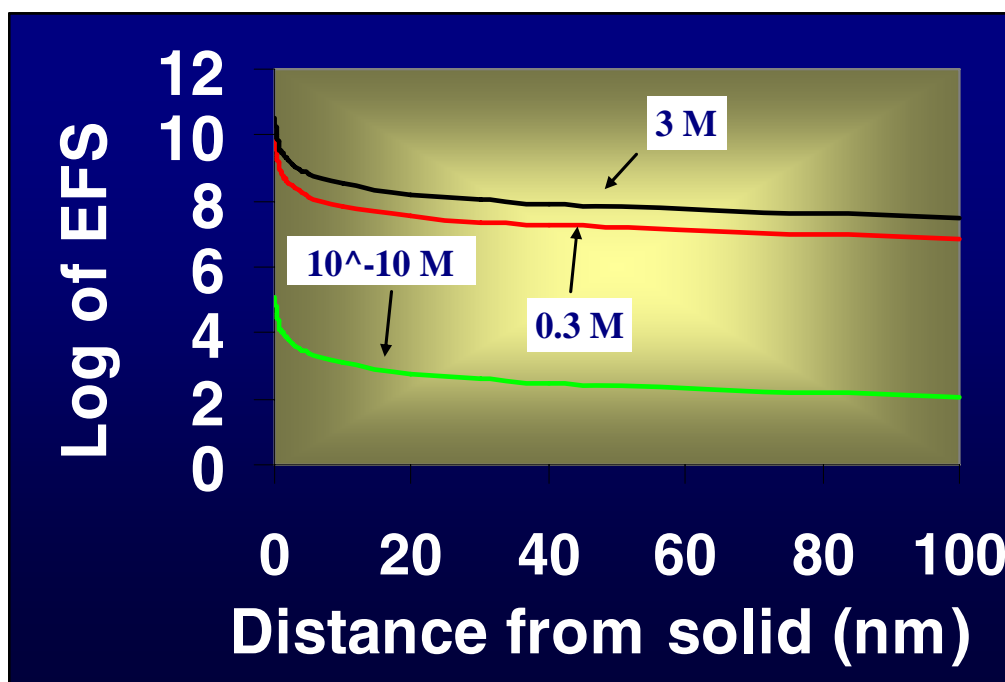


Figure 2. Log of interfacial electric field strength (EFS) as a function of the distance from the solid surface at three selected medium ionic strength (I) values. Unit of EFS is volts per meter, and that of I is moles (M).

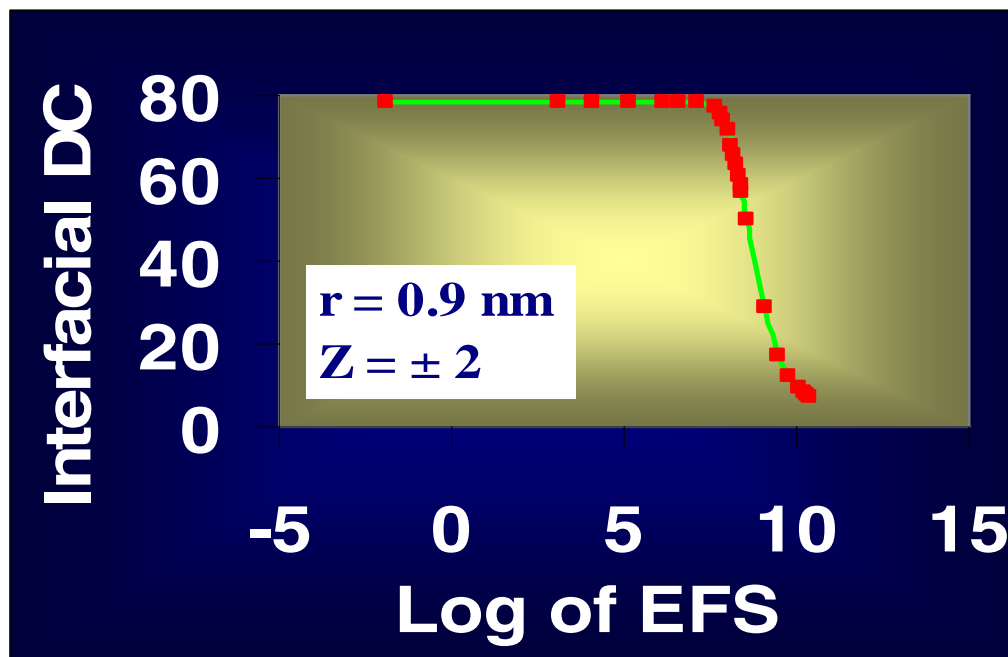


Figure 3. Interfacial solvent dielectric constant (DC) as a function of log of electric field strength (EFS) near divalent ions at 0.9 nm from the solid surface. Unit of EFS is volts per meter.

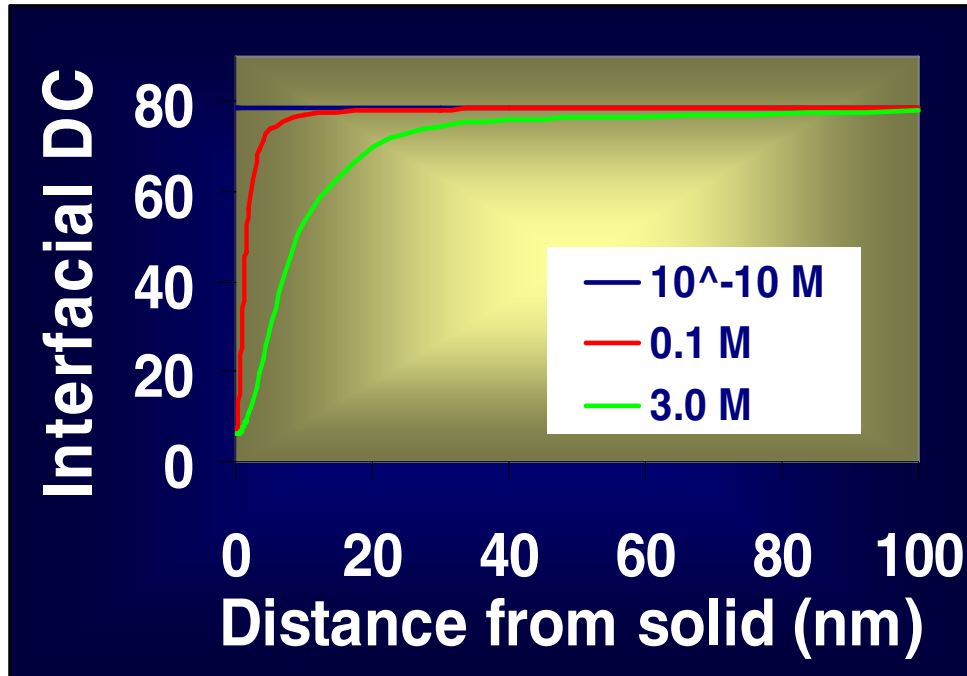


Figure 4. Interfacial solvent dielectric constant (DC) as a function of the distance from the solid surface at three selected medium ionic strength (I) values. Unit of I is moles (M).

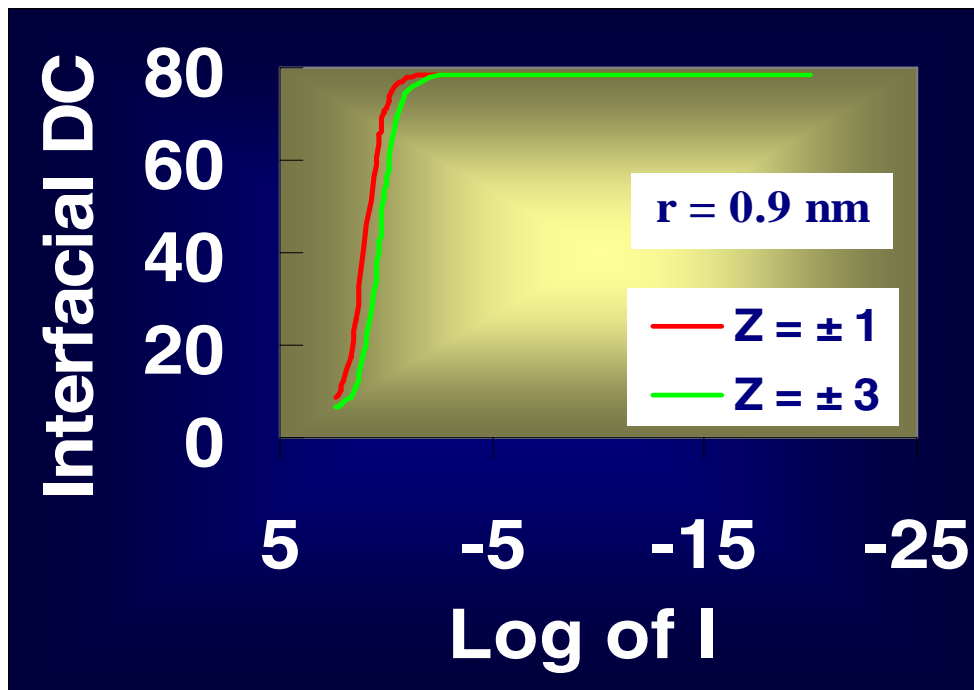


Figure 5. Interfacial solvent dielectric constant (DC) as a function of the log of medium ionic strength (I) near monovalent, and trivalent cations and anions at 0.9 nm from the solid surface. Unit of I is moles.

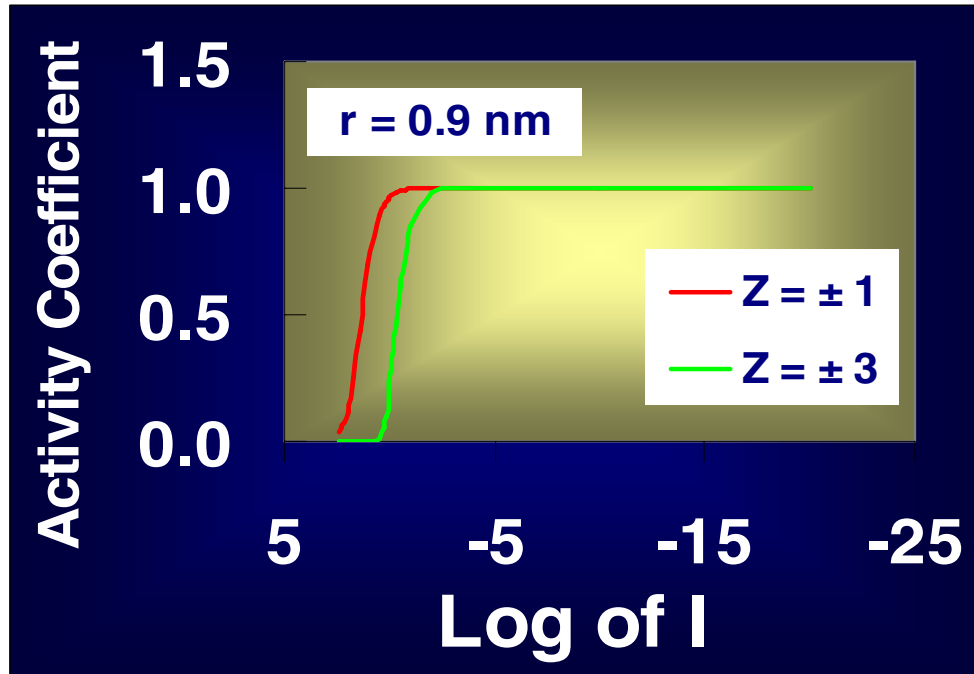


Figure 6. Activity coefficients as a function of the log of medium ionic strength (I) for monovalent and trivalent ions at 0.9 nm from the solid surface. Unit of I is moles.

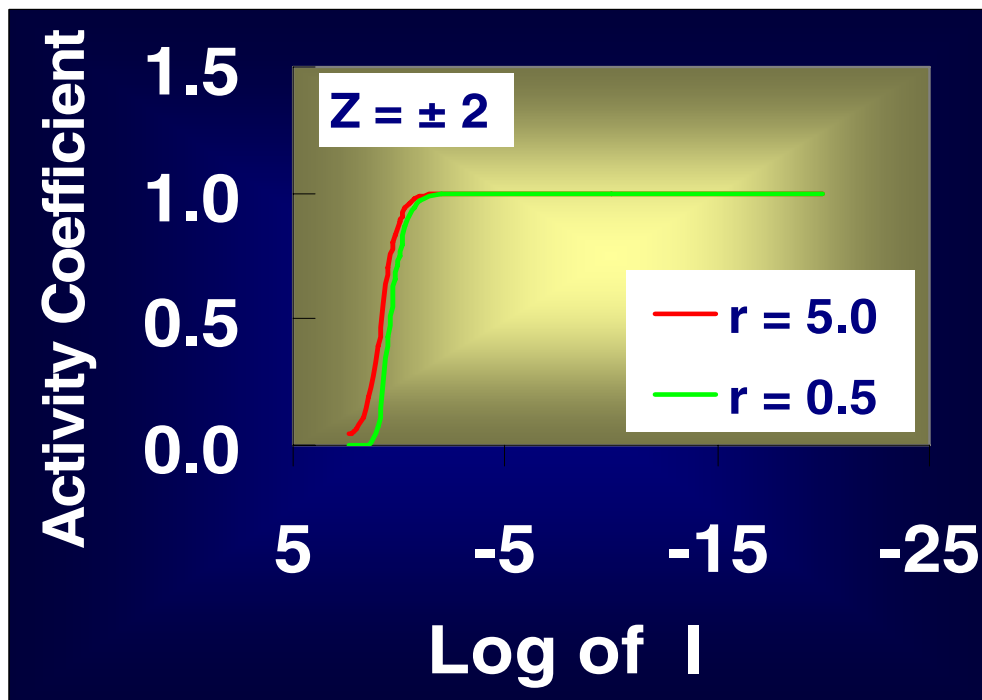


Figure 7. Activity coefficients as a function of the log of medium ionic strength (I) for two divalent ions of 0.5 nm, and 5 nm radii. Unit of I is moles.

CONCLUSIONS

According to the results, electrostatic field strength of large magnitudes ($>10^8$) exist near charged solid surfaces in real solution solid interfaces especially at high concentrations of inert electrolytes, and vary positively and linearly with the concentration of electrolytes. The screening of the electrostatic potential of a surface ion located at or near charged solid surfaces is manifest on the dielectric constant of nearby solvent molecules as well on the reciprocal length of the diffuse ion layer through this electric field strength. The dielectric constant of the solvent molecules near charged solid surface and the reciprocal length of the diffuse ion layer can be used to describe real solution properties almost completely in solid solution interfaces. The electrostatic free energy of an ion located at or near charged solid surfaces, which is a function of the dielectric constant of the solvent molecules near the ion can be used explicitly to calculate the activity coefficients of surface ions in real solution solid interfaces. Equation 23 computes f_γ reasonably accurately for surface ions at all valences and sizes, at all concentrations of 1:1 inert electrolyte solid-water interfaces at 25°C. In addition setting f_γ of the surface ions equal to unity or ignoring f_γ of surface ions in surface complexation models can lead to significant errors in the calculation of equilibrium constants of surface complexation reactions especially at electrolyte concentrations greater than 0.01 M. The results are general hence can be applied to other types of solvents and temperatures with very little modification.

REFERENCES

- Gibbs, J.W., 1948, The Collected Works of J. Willard Gibbs: Yale University Press, New Haven, CT.
- Goldberg, S., and Johnston, C.T., 2001, Mechanisms of arsenic adsorption on amorphous oxides evaluated using macroscopic measurements, vibrational spectroscopy, and surface complexation modeling: *Journal of Colloid and Interface Science*, v. 234, p. 204-216.
- Israelachvili, J.N., 1992, *Intermolecular and Surface Forces*, (2nd ed.): Academic Press, London.
- James, R.O., and Healy, T., 1972, Adsorption of hydrolysable metal ions at the oxide-water interface III, A thermodynamic model of adsorption: *Journal of Colloid and Interface Science*, v. 40, no. 1, p. 65-81.
- La Mer, V.K., Gronwall, T.H., and Greiff, L.J., 1931, The influence of higher terms of Debye-Huckel theory in the case of unsymmetric valence type electrolytes: *Journal of Physical Chemistry*, v. 35, p. 2245-2288.
- Lewis, G.N., and Randall, M., 1961, *Thermodynamics*, (3rd ed.): McGraw-Hill Higher Education, New York.
- Onsager, L., 1933, Theory of concentrated electrolytes: *Chemical Reviews*, v. 13, p. 73-89.
- Onsager, L., and Fuoss, R.M., 1932, Irreversible processes in electrolyte, diffusion, conductance, and viscous flow in arbitrary mixtures of strong electrolytes: *Journal of Physical Chemistry*, v. 36, p. 2689-2778.

- Sen, R.K., Yeager, E., and O'Grady, W.E., 1975, Theory of charge transfer at electrochemical interfaces: *Annual Review of Physical Chemistry*, v. 26, p. 287-314.
- Standard Handbook of Hazardous Waste Treatment and Disposal, 1989: McGraw-Hill Higher Education, New York.
- Sverjensky, D.A., and Molling, P.A., 1992, A linear free energy relationship for crystalline solids and aqueous ions: *Nature*, v. 356, p. 231-234.
- U.S. Environmental Protection Agency, 2001, EPA to implement 10 ppb standard for arsenic in drinking water-EPA 815-F-01-010: U.S. Government Printing Office, Washington DC.
- Wang, F., Chin, J., and Forsling, W., 1997, Modeling sorption of trace metals on natural sediments by surface complexation model: *Environmental Science and Technology*, v. 31, p. 448-453.
- Wingrave, J.A., 2001, Activity coefficient and electrostatics at S-MO interface: *Surfactant Science Series*, v. 103, p. 201-254.